DESIGN, SYNTHESIS AND EVALUATION OF PYRIDINE-STRETCHED OLIGONUCLEOTIDES

MICHAEL LESLIE DAVIS

Doctor of Philosophy

ASTON UNIVERSITY

September 2005

Aston University

Design, Synthesis and Evaluation of Pyridine-Stretched Oligonucleotides

A thesis submitted by Michael Leslie Davis for the degree of Doctor of Philosophy

September 2005

Summary

Design, synthesis and evaluation of oligonucleotides containing pyridine-stretched bases (PSBs) targeted to DNA are described. PSBs are linear, tricyclic analogues of purine bases, where a central ring of pyridine connects the familiar six-membered pyrimidine and five-membered imidazole rings. A series of pyridine-stretched bases with potentially improved DNA binding properties was considered and of these, strI, the pyridine-stretched analogue of the purine nucleoside inosine (I), was chosen as a synthetic target.

Although glycosylation of 1-chloro-2-deoxy-3,5-di-*O*-toluoyl-α-D-ribofuranose with different metal salts of 4(5)-nitroimidazole was heavily dependent upon the reaction conditions, giving mixtures of up to four isomeric products, reaction conditions were optimized to ensure formation of the required, pure 5β isomer in 65% yield. NOESY experiments provided conclusive proof of structure. Reduction of the nitro group proceeded smoothly but gave the rather unstable amine product, which was reacted immediately with ethoxymethylene malononitrile to give a stable, isolable dinitrile product. Despite much chemical effort to improve the outcome, this step was invariably low yielding (23 to 37%). Cyclisation of the dinitrile compound and concomitant deprotection of the sugar gave a key intermediate nucleoside (89%) that was converted to strI. Dimethoxytritylation at O5' followed by phosphitylation at O3' gave the necessary strI phosphoramidite. Oligonucleotides were prepared from this material by automated solid phase synthesis, and their DNA molecular recognition properties were evaluated by UV thermal melting studies. Incorporation of strI into self-complementary 10-mers caused duplex stabilization, attributable to enhanced base stacking. Participation of strI in triplex formation was aluded to but not established conclusively.

In parallel, solid phase synthesis and characterisation of a metronidazole oligonucleotide conjugate for possible DNA targeting was achieved. Preliminary studies on the formation of a planned pyridinone base for inclusion in peptidic nucleic acid structures were also undertaken.

Keywords: Nucleoside, pyridine-stretched inosine, strI, DNA synthesis, duplex, triplex.

To the memory of my mom

Acknowledgements

I wish express my profound thanks and gratitude to my supervisor Dr. William Fraser for all his help, advice, assistance, support and more throughout the extended time of this project. His supported was particularly appreciated when deadlines came and went on a number of occasions. I apologise to Lorraine for taking up so much of his time.

I would like to thank all the people within the Medicinal Chemistry Labs for their understanding while this work was undertaken. A special thanks to Karen Farrow, Dr. Dan Rathbone and Dr. Qinguo Zheng.

I am very grateful to Dr. Andrew Walsh, Dr. Russell Clayton and Prof. Chris Ramsden for assistance and collaborative work.

Thanks to Prof. David Billington for his positive encouragement to undertake this work many years ago.

A special thanks to Alison Birch for her assistance in coping with missed deadlines.

Thanks to all people at Aston University for directly or indirectly enabling this work.

Thanks to Dad, Sue, Sal and Lloyd for understanding this was a bit of a mission.

Finally, a special thanks to my friends Ivan Barnes and his wife Valerie for being good listeners over the years.

Contents

List of Figures

List of Schemes

List of Tables

Chapter 1

Triplex-Forming Oligonucleotides (TFOs)

1.1 The structure of DNA

Watson and Crick elucidated the double helical structure of 2'-deoxyribonucleic acid (DNA) in 1953. They demonstrated that it existed as a double helical structure formed from two complementary strands held together by selective inter-strand hydrogen bonds (Watson & Crick 1953a,b). The main evidence for such a structure was derived from X-ray diffraction data acquired by Rosalind Franklin (Franklin & Gosling 1953a,b) and Maurice Wilkins (Wilkins et al. 1953) and also Chargaff's rule (Chargaff 1948; Vischer & Chargaff 1949). By 1952 Chargaff had published data relating to the base composition of DNA from a variety of sources (**Table 1.1**). The data indicated that, irrespective of which organism the DNA came from, for the four bases found in DNA the molar amount of adenine (A) **1.1** was always near equivalent to that of thymine (T) **1.2**. Similarly, the number of moles of guanine (G) **1.3** and cytosine (C) **1.4** were near equivalent (**Figure 1.1, Table 1.1**). With these discoveries the mechanism of DNA replication and the fact that genetic information is stored and coded for by the complementary, sequence-specific matching of the two strands of DNA became apparent. The four DNA bases, A, G, C and T, are connected to a 2-deoxyribose sugar through a glycosidic bond to the anomeric carbon, in the β

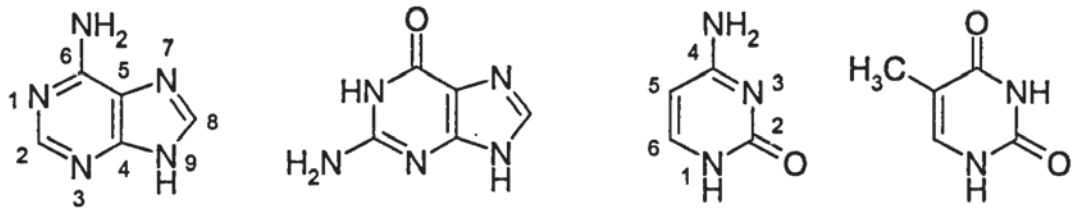

Adenine (A) **1.1** Guanine (G) **1.2** Cytosine (C) **1.3** Thymine (T) **1.4**

Figure 1.1 Structure and numbering of DNA bases; purines A and G, pyrimidines C and T.

Table 1.1 A sample of some of Chargaff's data in part, giving the base composition of DNA from various organisms. Deviation from Chargaff's rule implies that the DNA is single stranded as for microorganism *f*X174.

Source	Mol % of bases				Ratios		% GC
	A	G	C	T	A/T	G/C	
*f*X174	24.0	23.3	21.5	31.2	0.77	1.08	44.8
Maize	26.8	22.8	23.2	27.2	0.99	0.98	46.1
Octopus	33.2	17.6	17.6	31.6	1.05	1.00	35.2
Chicken	28.0	22.0	21.6	28.4	0.99	1.02	43.7
Rat	28.6	21.4	20.5	28.4	1.01	1.00	42.9
Human	29.3	20.7	20.0	30.0	0.98	1.04	40.7

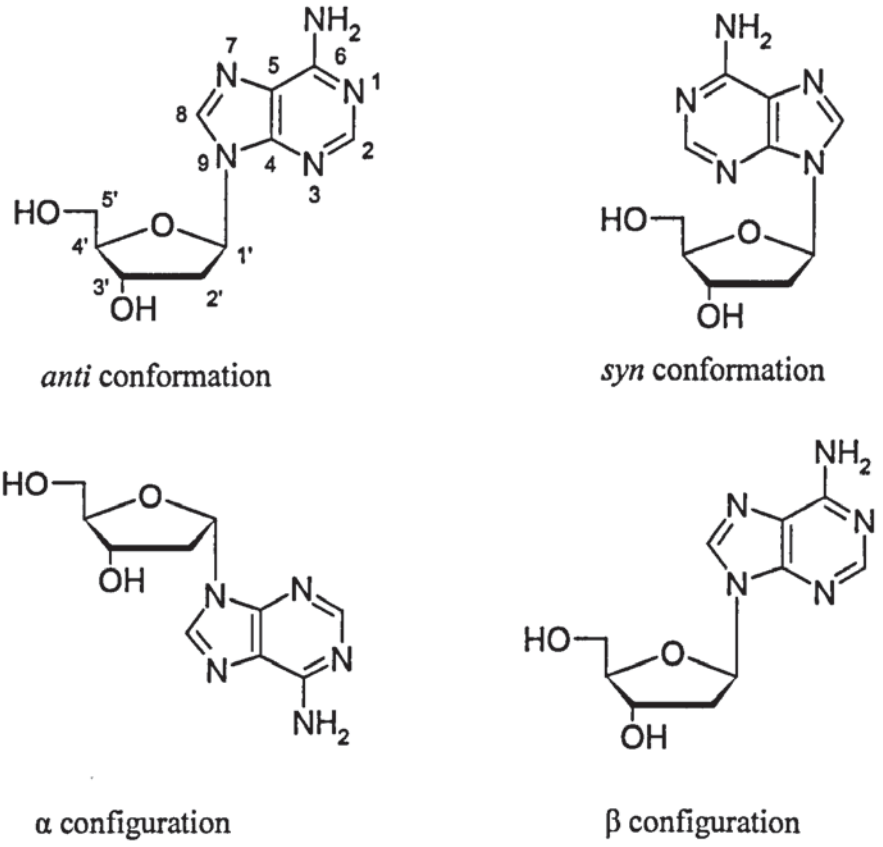

Figure 1.2 2'-Deoxyadenosine nucleosides.

configuration, in nucleosides. Rotation about this bond gives rise to *anti* or *syn* conformations. With restricted rotation the *anti* conformation is generally preferred due to steric constraints. It is the comformation that is generally adopted in DNA. However, rotation about this bond enables a high degree of flexibility to the DNA structure (**Figure 1.2**) (Bansal 2003; Baxter 2005; Bowater 2003). The two complementary DNA sequences consist of linear polymeric nucleotides; i.e. each nucleoside has a 5' phosphate group. Of the four natural bases that are found in DNA, adenine, (A) and guanine, (G) are purine

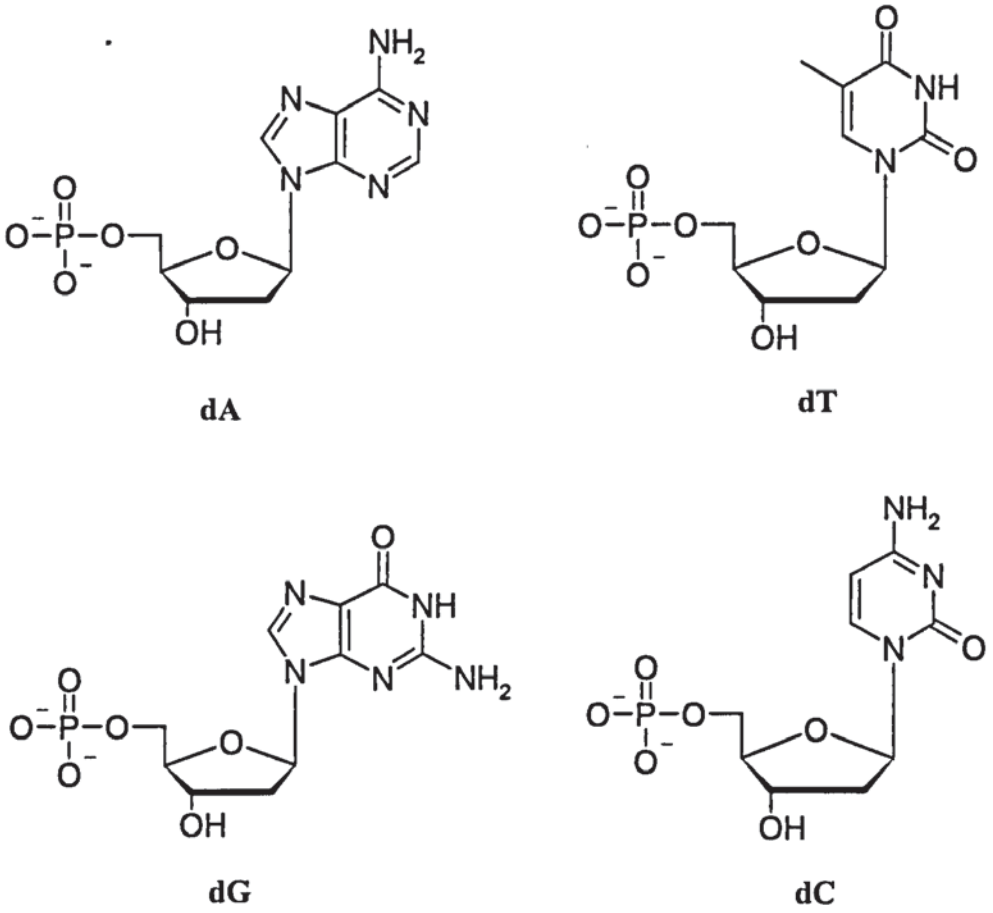

Figure 1.3 2'-Deoxyadenosine 5'-phosphate, (dA), 2'-deoxycytosine 5'-phosphate, (dC), 2'-deoxyguanosine 5'-phosphate, (dG), and 2'-deoxythymidine 5'-phosphate, (dT), nucleotides.

derivatives and cytosine, (C) and thymine, (T) are pyrimidines (**Figure 1.3**). The numbering of the purine and pyrimidine rings is given in **Figure 1.1**. The numbering in nucleosides is given in **Figure 1.2** where prime numbers are used to differentiate atoms in the sugar ring from those of the base. Thus, in the *anti* conformation, the H1'-C1'-N9-C8 torsion angle is at or near 180°, whereas in the *syn* conformation this torsion angle is at or near 0°. Covalent attachment of these monomeric nucleotides to form long linear oligonucleotide chains is through formation of internucleotide phosphodiester bonds that

Figure 1.4 Structure of DNA and base pairing (Bowater 2003).

link the primary 5'-phosphate group of one nucleotide to the secondary 3'-hydroxyl group of its neighbour (**Figure 1.4**).

The encoding of the required genetic information is achieved through specific base paired sequences of the four possible combinations of the two sets of base pairs (A.T), (T.A), (G.C) and (C.G). With the selectivity, specificity and preference of the base pairs, the

Figure 1.5 Chemical structure of DNA: (a) base pairs (b) sugar phosphate backbone (c) major and minor grooves.

sequence of one strand of DNA defines the sequence of the complementary stand, precisely. The two strands of a DNA duplex align antiparallel with the 5'-end of one stand being positioned at the 3'-end of its complementry strand (**Figure 1.5**). By convention, the base sequence of a given oligonucleotide is written from 5' to 3' end. The selectivity of the A.T and G.C base pairing in the DNA duplex can be attributed to Watson-Crick hydrogen bonding within the steric constraints of the double helix that is achieved with these matching base pairs.

The G.C base pair imparts a greater degree of stability to the double helix through having three hydrogen bonds as opposed to the two for the A.T pairing. The symmetry of preferred base pairs in DNA is such that if an A.T base pair is overlaid on the other base pairs (T.A, G.C or C.G) the phosphodiester backbones overlap each other. Thus the natural base pairs are readily accommodated within the double helix structure and are interchangeable without causing any distortion. At the physiological pH of 7.2 each phosphodiester group ($pK_a = 1$) exists as an anion giving rise to the term nucleic acid. Thus, *in vivo* they are long chain highly charged hydrated polyanionic molecules with the double helix structure accommodating the hydrophobic bases towards its centre with the sugar rings and negatively charged phosphates forming an external backbone that is hydrophilic. Separation of adjacent base pairs is about 0.34 nm and one 360° rotation of the helix is repeated every 10 to 11 base pairs. Within each of these turns there are over half a million possible combinations of base pairs. For a 15 base pair sequence, the possible cominations rise to over five hundred million.

The overall stability of the standard double helix conformation can be attributed to a combination of inter-related factors. The molecular dimensions of the interlocking helical

structure of the B form of DNA, favored at physiological pH (*in vivo)*, enables selective and targeted Watson-Crick hydrogen bonding between the complementary duplex strands. The twist of the right handed double helix enables the planar heterocyclic bases to stack on top of each other resulting in a net favorable interaction within the central scaffold of overlapping π systems. Mismatching of the base pairs results in destabilization of the helices due the disruption of this stacking arrangement (**Figures 1.4, 1.5**).

Having the hydrophobic base pairs orientated towards the centre of the duplex results in extensive hydration of the outer hydrophilic sugar-phosphate backbone with a significant enhancement of entropy. The term right-handed indicates that the double helix twist is

Figure 1.6 Representations of; A-DNA, B-DNA and Z-DNA. Three of the ever increasing number of DNA conformations that have been characterized (Bansal 2003).

clockwise when viewed from above or below; when viewed from the front the sugar-phosphate backbone slopes down from top right to bottom left. In this principal B-DNA form of the duplex, the double helical structure has a wider "major groove" and a narrower "minor groove" tracing the entire length of the molecule (**Figures 1.4, 1.5, 1.6**).

Chemical interactions with DNA can occur within these grooves. Proteins principally target the major groove. However the mode of action of some naturally occurring antibiotics which act by targeting DNA directly has been shown to be through binding within the minor groove. Some natural products which bind site-specifically to DNA have been isolated and characterized. The mode of action of chromomycin, calicheamicin and distamycin has been demonstrated to be though minor groove interaction (**Figure 1.7**) (Arcamone et al. 1964).

1.2 Variations in the structure of DNA

Whilst under standard physiological conditions of high humidity, it is the B-DNA structure that is favored. In the same year that the double helix was proposed Franklin showed that B-DNA could interconvert to another well defined conformation at low humidity. This was subsequently assigned A-DNA (Franklin & Gosling 1953). Like B-DNA, the A-DNA form is a right handed double helix but with 11 base pairs per turn and separation of 0.256 nm (2.56 Å) as opposed to 0.34 nm (3.4 Å) for B-DNA (**Figure 1.6**). It is this form that is preferred by RNA. The structures designated C- and D-DNA are also right handed double helical forms that have been characterized. In C-DNA there are 9.3 base pairs per full rotation of the duplex and in D-DNA there are 8 (Bansal 2003). Subsequently it has been shown that DNA has an enormous capacity to adopt a wide variety of tertiary structures

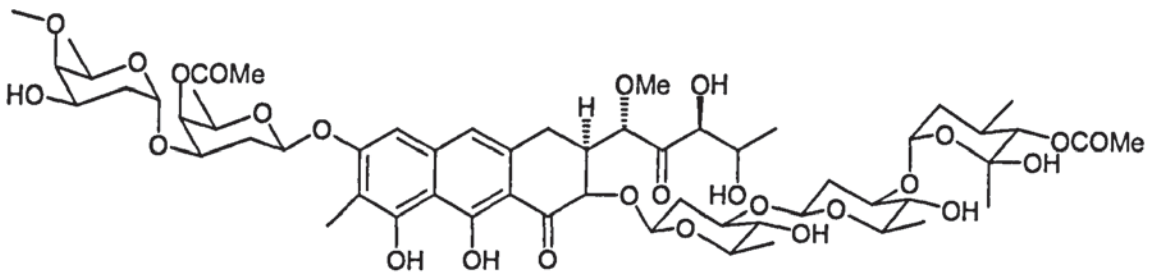

Chromomycin, target 5'-GGCT-3'

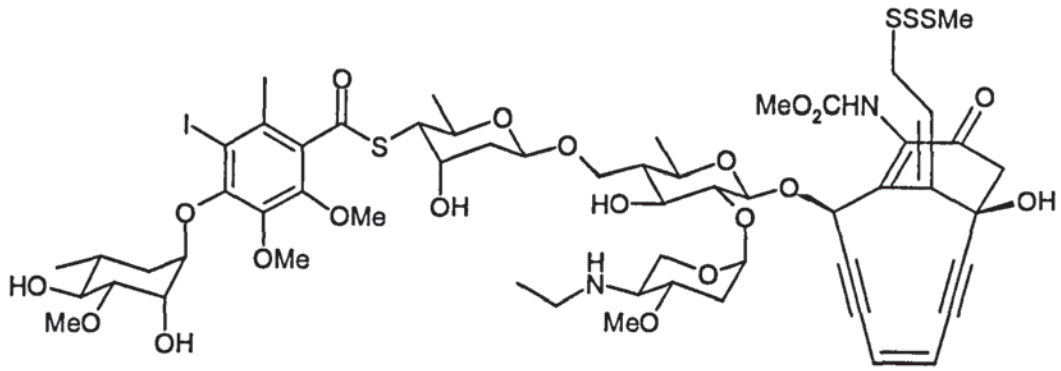

Calicheamicin oligosaccharide, target 5'-TCCT-3'

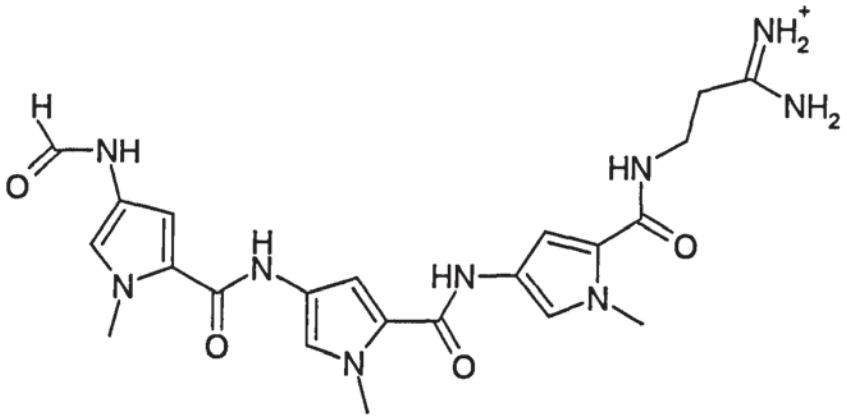

Distamycin, target 5'-(A,T)-3'

Figure 1.7 Natural products that bind to DNA.

depending on its environment (Ghosh & Bansal 2003). One form that can occur at high salt concentration, Z-DNA, has a left handed helical orientation. It is termed Z-DNA because the sugar phosphate backbone traces a zigzag pattern (**Figure 1.6**).

Considering the exceptional nature of DNA and its capacity to perform such a wide range of tasks at a molecular level, flexibility of conformation must be an important property. DNA has the ability to undergo controlled structural reorganization by hydrogen bond transfer and modification. Together with its molecular flexibility, these features must make an important contribution to DNA in its ability to carry out all of its structural and biological functions. The B-DNA form itself is far from rigid. Extensive bending of the structure is required to allow it to physically "fit" within its cellular environment. There is some structural data analysis to suggest that differing conformations can occur at contiguous regions along the length of the same DNA molecule (Bansal 2003).

1.3 Triplex-forming oligonucleotides (TFOs)

It was recognized very soon after the DNA double helix was proposed by Watson and Crick that it might be targeted by a third strand oligonucleotide. Theoretical DNA triplexes were suggested by Pauling and Corey (1953) and probed experimentally by Felsenfield, Davies and Rich (1957) four years later. The work initially demonstrated that a poly A and two poly U (uracil) would align to form a triple helical structure. With the resources available at the time the scope of the work was limited but the triplex helix structure had been described. With no apparent biological relevance at the time there was limited interest in such a triple helical structure. Considering the practical constraints at the time these structures would probably have been regarded as no more than a curiosity. Over thirty years

later the publication of three independent reports relating to these structures initiated a tremendous growth in the interest and investigation of triple helical structures (Doronina & Behr 1997).

As far back as 1963, X-ray crystal structure studies by Hoogsteen revealed that the DNA bases A and T can form base pairs with a different hydrogen bonding arrangement to that found in the DNA double helix. This type of hydrogen bonding, Hoogsteen (H) and reversed Hoogsteen (RH) can be achieved with purine targets within the major groove of DNA (**Figure 1.8**) (Hoogsteen 1963; James et al. 2003). In 1987, Moser and Hélène both published work showing that oligonucleotides could bind to DNA in a sequence specific way by forming a third helical strand in the major groove (Le Doan et al. 1987; Moser & Dervan 1987). This demonstration and Mirkin and Frank-Kamenetskii's characterisation of an intramolecular triple helix, termed H-DNA that could form in natural DNA, resulted in renewed and continued interest in triple helical structures (Mirkin et al. 1987). Extensive collaboration between these particular research groups has resulted in much progress being made in the area of triplex-forming oligonucleotides (TFOs).

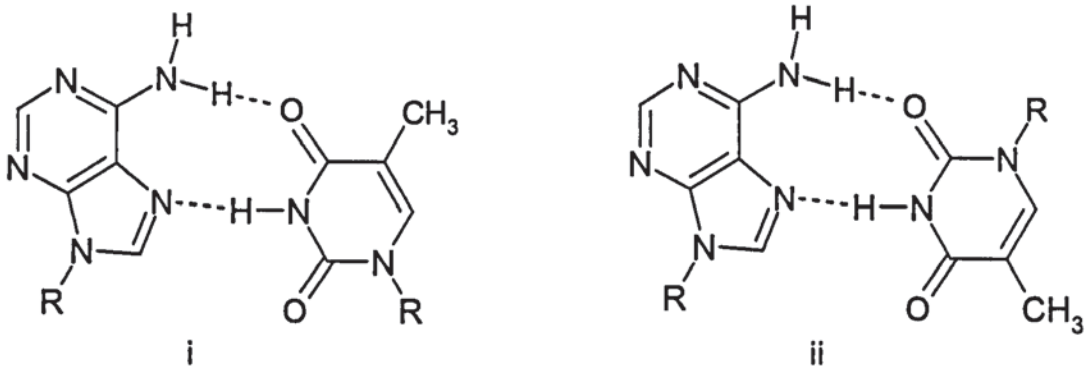

Figure 1.8 A.T i, Hoogsteen (H) pairing ii, reversed Hoogsteen (RH) pairing.

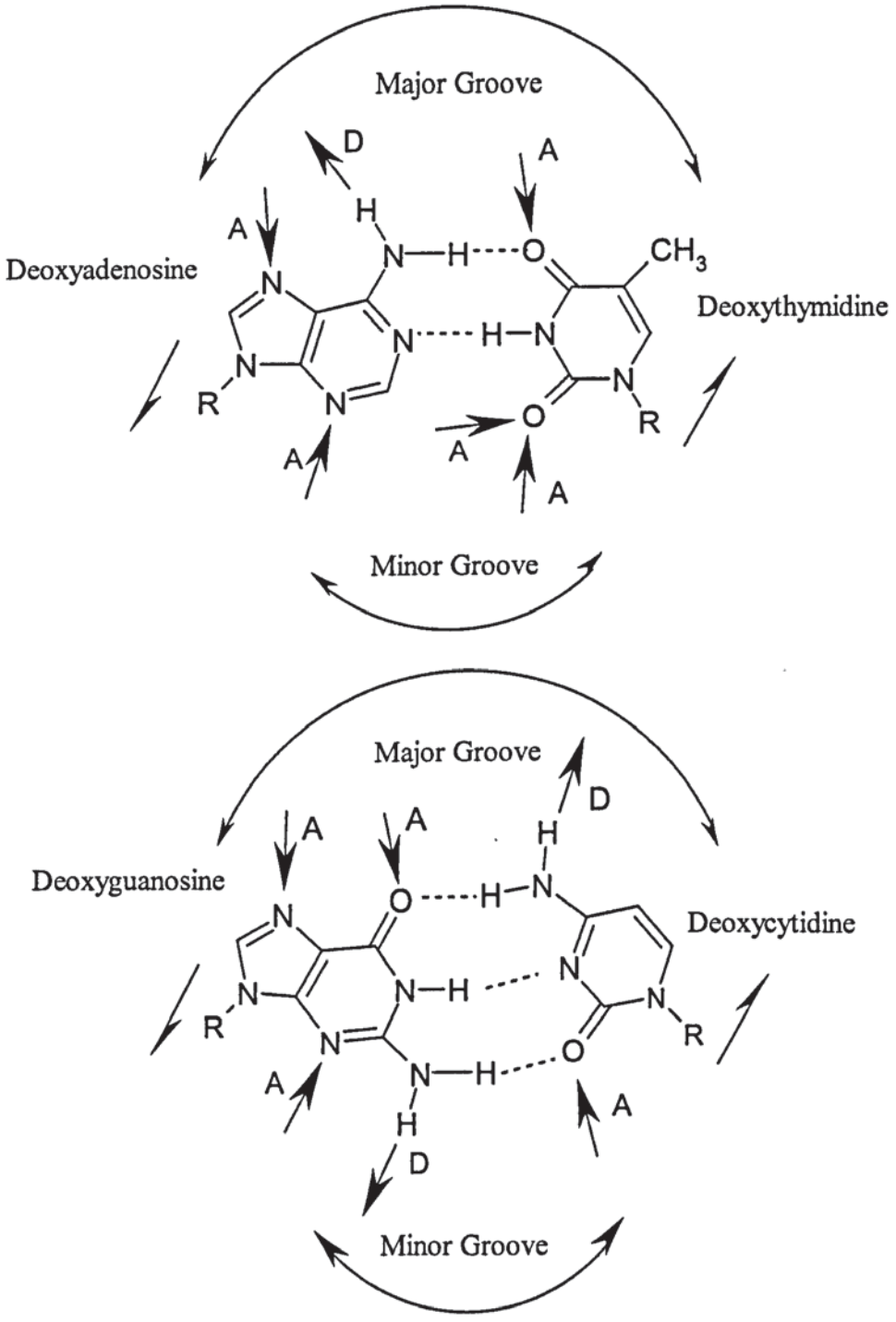

Figure 1.9 Possible available donor, D, and acceptor, A, hydrogen bond sites within the major and minor grooves of DNA for triplex formation.

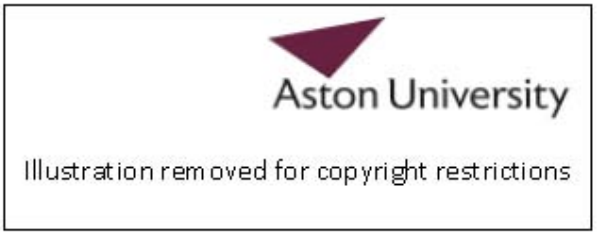

Figure 1.10 Base triplets that can be formed by nucleic acid bases with Watson and Crick A.T and C.G base pairs. The left column is Hoogsteen hydrogen bonding interactions and the right column to reversed Hoogsteen interaction. Oxygen and nitrogen atoms have been omitted for clarity (Hélène 1994).

1.3.1 Structural requirements and limitations for TFOs

With the double helical structure of DNA, both the major and minor groove give access to potential hydrogen bonding sites within the central base-paired scaffold (**Figures 1.9, 1.10**). Besides the Watson and Crick hydrogen-bonded base pairing of the four constituent bases of DNA (A, G, C, T), there are a further twenty-seven possible combinations that could result in the formation of two hydrogen bonds between any two of these bases.

The major groove can be targeted by triplex-forming oligonucleotides containing natural bases and structural analogues. Hydrogen bonding between the third strand and the duplex target is through the two available hydrogen bonding sites of each purine within the DNA duplex target. Depending on the target base sequence, selectivity can be achieved through either Hoogsteen or reversed Hoogsteen hydrogen bonding. Sequence specificity with TFOs is achieved due to T on the TFO recognizing the A.T pair of the duplex target to form a triplex (T*A.T). Similarly, C^+ recognizes G.C (C^+*G.C), G recognizes G.T (G*G.T) and A recognizes A.T (A*A.T) (**Figure 1.10, 1.11**).

For triplex formation to be structurally viable there is the requirement for purines to be located on the same DNA strand, and contiguous, so that the sugar phosphate backbone of the TFO can align with the major groove.

Recognition and differentiation of the double helix base pair sequences by the TFOs is through the matching of donor and acceptor hydrogen bonding sites with the targeted polypurine strand. Stability is achieved by the accomodation of the sugar-phosphate backbone and base interactions within the major grove.

Figure 1.11 Representation of DNA triple helix structures with G*G.C triplet on the left and a T*A.T, G*G.C triplet on the right. The Watson-Crick duplex is in cyan and the triplex-forming third strand is in yellow (Radhakrishnan & Patel 1993; Vlieghe et al. 1996).

Figure 1.12 Triplex formation (Baxter 2005).

There is the necessity for cytosine to be protonated (C^+) first in order to form the two required hydrogen bonds (**Chapter 6**). This results in the formation of cytosine-containing TFOs being pH dependant. While the pK_a of cytosine is 4.5 this can rise to well above the physiological pH of 7.2 for an isolated cytosine in a TFO. This imparts stability to a triplex disproportionate to that expected from the formation of an additional hydrogen bond, and is attributed to possible favourable electrostatic or base stacking interactions (James et al. 2003). With increasing cytosine content, pH dependency increases, and thus the stability at physiological pH is significantly reduced. To overcome this, a number of potential pH-independent cytosine analogue have been prepared (Asensio et al. 1998; Keppler & Fox 1997; Lee et al. 1984). These structures are considered in more detail in **Chapter 6.**

The alignment of the TFO with the homopurine containing strand of the target DNA is dependant on the base sequence and hydrogen bonding pattern and type. In relation to the targeted homopurine tract of the duplex DNA, C,T-containing TFOs can be orientated parallel though Hoogsteen bonding or antiparallel through a reversed Hoogsteen bonding conformation. TFOs containing G.A adopt an antiparallel orientation, again through reversed Hoogsteen bonding. In the case of G,T-containing TFOs parallel base triads are energetically favoured because the base triplet T*G.C and T*A.T are not isomorphous in either the Hoogsteen or reversed Hoogsteen modes. However, increasing the number of GT or TG transitions results in triplex backbone distortion and a preference for reversed Hoogsteen, antiparallel orientation (**Figure 1.11, 1.12, 1.13**).

GA-containing TFOs with a high G to A ratio have been shown to be capable of forming stable triplexes (Debin et al. 1999). However, G-rich oligonucleotides have the capacity to

self-associate. The G content of a TFO is an important factor in the design of TFOs and should be limited because of this tendency to form G quadruplexes that compete with triplex formation. These quadruplex structures are stabilized by potassium ions. Under physiological conditions, quadruplex formation, stabilised by potassium ions, can thus inhibit triplex formation (**Figure 1.13**) (Haider et al. 2002; Mohanty & Basal 1993; Risitano & Fox 2003).

1.3.2 H-DNA

In 1985 regions of eukaryotic genes were identified, which exhibited anomalous behavior by being hypersensitive to nucleases and reagents specific to single stranded DNA. These regions were designated H-DNA. The transition to this form of DNA was found to be favored by acidic conditions and the transition resulted in a drop of topoisomer mobility equivalent to what would have been expected by a duplex to single strand DNA transformation (Lyamichev 1986). Unambiguous structure elucidation of H-DNA was accomplished in 1988 using DNA probing techniques involving base-specific and single strand DNA-specific reagents The significant structural feature of H-DNA was shown to be the formation of an intramolecular triple helix from an entire pyrimidine strand and half of the purine complement (**Figure 1.14**) (Mirkin et al. 1987).

Figure 1.13 Multiple stranded DNA G-quartet and folded G-quadraplex structures (Darby et al. 2002).

Figure 1.14 Representation of DNA strands in the intramolecular triplex of H-DNA. Black ribbon indicates homopurine strand, light ribbon indicates homopyrimidine and the grey ribbons indicates adjacent double helical DNA (Mirkin 1999).

The resultant triplex is stabilized by isomorphous C^+*G.C and T*A.T base triads and thus allows efficient stacking in the triplex structure. The pH dependence arises from the pre-requisite of cytosine to be protonated, mentioned earlier, in order to form the required hydrogen bonds. In general, the lower the ratio of C^+*G.C within the triplex structure, the less pH dependant it is. With duplex and triplex strands being derived from a folded homopyrimidine tract, all the purines are required to be located on the same strand. The presence of an extraneous single stranded homopurine loop accounts for the susceptibility to nuclease and single strand-specific reagents.

Similarly the presence of a homopyrimidine loop in the intramolecular triplex results in the specific demand for the two arms of the folded segment to have mirror symmetry and thus a palindromic sequence with respect to the location of dCs and dTs. By default, the homopurine sequence must comply with this limitation. In theory both 5' and 3' oriented triplexes can be formed depending on which sections are involved in duplexation. In practice there might be additional factors, steric constraints, pH and hydration might combine to favor a particular orientation. Subsequent investigations that followed on from the discovery of the conformation of the triple helical structures.of H-DNA have revealed an extended family of related triple helical structures (**Figure 1.15**) (Mirkin 1999; Mirkin & Frank-Kamenetskii 1995).

The homopyrimidine, homopurine structure described above is designated H-y-DNA. In H-r-DNA, by comparison, the intramolecular triplex is essentially a Pu*Py.Pu construct. However, T residues are tolerated and accommodated within the third strand by forming reversed Hoogsteen hydrogen bonds with A (**Figure 1.12**). H-r-DNA is pH-independent and can form at neutral pH in the presence of a suitable divalent cation. H-yr-DNA

incorporates both an H-y and an H-r type intramolecular triplex (**Figure 1.15**). In any system with junctions where major structural reorganizations are necessary, there can be an accumulated "stability penalty" due to the adjustments required. For stability the H-yr form requires extended sequences to mitigate the change from the H-y to the H-r form. An H-dr DNA has been described where a strand from one section of the DNA's double helix can migrate and form a triple helix equivalent to another section aligned alongside (**Figure 1.15**) (Mirkin 1999). Although the existence of H-DNA triplexes in nature has been clearly demonstrated the exact biological significance of these structures remains unclear. Translating the observations from *in vitro* studies to the situation *in vivo* is inherently problematic due to the vast increase in complexity of cellular systems. There is an indication that natural triplexes could act as molecular switches. Some proteins for example preferentially bind to the available single-stranded segment. Mutations, which disrupt the ability to form H-DNA, have been shown to inhibit viral replication (Portes-Sentis 1997). It has been recently suggested that triplexes might be involved in promoting genetic instability by causing the elongation of repeater units within DNA during replication. Formation of an H-y-type structure during replication could expose a section for repeat expansion (Gacy 1998).

1.3.3 Minor groove targeting TFO analogues

The minor groove can be targeted sequence specifically by compounds consisting of heterocyclic five membered rings attached to a modified amide backbone. Their mechanism of action differs from major groove TFOs in that it can be considered to be strand invasion with hydrogen bonding being directed inter-strand within the DNA

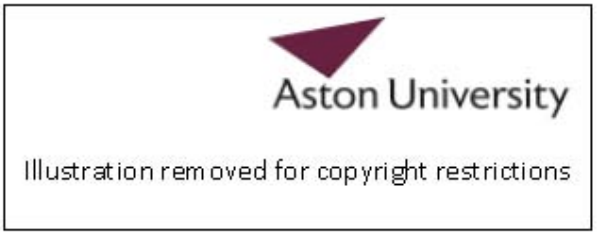

Figure 1.15 Known structural variations of H-DNA. Column A, different types of H-DNA known; Column B, corresponding intramolecular triplexes. Black rectangles for homopurine sequences; white rectangles, homopyrimidine sequences; thin lines, continuation of DNA strands (Mirkin 1999).

duplex (Lyamichev et al. 1986). The formation of 2:1 complexes within the minor groove were identified and characterized with naturally occurring DNA binding molecules (Mirkin & Frank-Kamenetskii 1995). The minor groove can be targeted with high site- and sequence-specificity by designed complimentary sequences tethered by a suitable linker to

form a hairpin 2:1 structure within the minor groove. Dervan and co-workers have studied targeting of the minor groove of DNA using oligopyrrole and oligoimidazole structures and a viable set of pairing rules have been established (Dervan 2001). Recently, conjugates of TFOs attached to minor groove binding molecules have been described (Ghosh et al. 2004). The purpose of these structures is to exploit the sequence specifity of a TFO and the extra stability from minor groove binding.

1.3.4 Potential applications of TFOs

The apparent potential of being able to suppress and inhibit gene expression by targeting duplex DNA site specifically through triplex formation is termed the antigene approach as opposed to the antisense approach, where RNA is the target. With a limited number of potential targets, the benefits of antigene therapy include the use of minimal dosage since disabling the targeted DNA site has the prospect of suppression of possible malignant effects within the body. The limited dosage that would be required and the fact that the mode of action would be through physicochemical binding to a specific target site has the potential to mitigate and minimize any possible toxicological effects and undesired side effects due to unforeseen secondary interaction. Thus optimized delivery and efficient uptake could ensure a very low local and regional concentration away from the target within the groove of the duplex DNA target. Any secondary interactions and effects from eventual break down products should be very low especially when compared to therapeutics that requires a significant local concentration to be effective. The current and ongoing developments in delivery technology, especially those devoted to improving

Figure 1.16. Possible pathways for TFO alteration of gene expression. (A) Blocking of transcription by competition with transcription factors or by interference with elongation. (B) TFO directed site-specific mutagenesis. (C) Gene correction via homologous recombination (Knauert & Glazer 2001).

current antisense therapy, could prove invaluable in the success any future antigene therapy.

1.3.5 Oligonucleotides with modified structural features

Perhaps the most dramatic alteration to the structure of DNA, that preserves all of the molecular recognition properties of DNA and introduces some new ones, is the complete

change of phosphodiester backbone to give peptidic nucleic acids (PNA) (Petersson et al. 2005). The PNA structure is condidered in more detail in **Chapter 6**. Many other changes to the sugar-phosphate backbone and to the heterocyclic bases, through chemical modification and synthesis of analogues, have been documented (Buchini & Leumann 2003). The phosphate group has been replaced by; phosphorothioate, phosphorodithioate, methylphosphonate, formacetal, 5'- and 3'-thioformacetal, guanidino (Linkletter 2001), N3' -P5' phosphoramidate (Obike et al. 2003) amongst many others (Rojanasakul 1996). Of the many structural changes that have been made to the sugar ring (Leumann 2002), the C4-O2 methylene bridge features in the commercially available building blocks (Link technologies 2005) for locked nucleic acid (LNA) structures that have interesting molecular recognition properties (**Figure 1.17**b) (Sørensen et al. 2004). Attachment of cationic groups (Ranasinghe et al. 2005) to the sugar and heterocyclic base improves the stability of

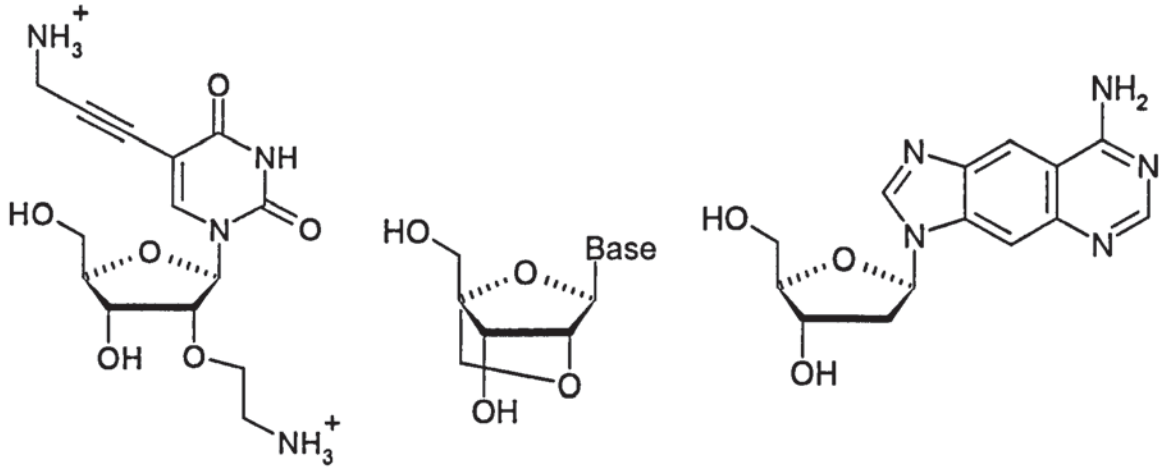

a b c

Figure 1.17 Representative structural formulae showing three of the vast number of reported modifications to the DNA sugar and heterocyclic bases.

DNA triplexes (**Figure 1.17**a) while increasing the size of the heterocyclic base (Liu et al. 2003) can improve base stacking (**Figure 1.17**c).

1.4 Aims and objectives

The aim of the project work was to design, synthesise and evaluate pyridine-stretched oligonucleotides for targeting to DNA. Towards this aim a series of pyridine-stretched analogues of the purine bases with potentially improved DNA binding properties were considered. Of these, the nucleoside strI, the pyridine-stretched analogue of the purine nucleoside inosine, was chosen as a synthetic target. Chemical synthesis of the nucleoside followed by its incorporation into triplex-forming oligonucleotides (TFOs) by solid phase synthesis methods was concluded with evaluation of the duplex- and triplex-forming properties of the new pyridine-stretched structure. On the theme of DNA targeting, the feasibility of solid-supported synthesis and characterisation of a metronidazole oligonucleotide conjugate with preliminary studies on the formation of a pyridinone base for inclusion in peptidic nucleic acid structures were also considered. With the aim of the project and, targeting of duplex DNA in mind, the chemical and structural features of nucleic acids were considered in the introductory **Chapter 1**. The design and chemical synthesis of nucleosides will now be discussed.

Chapter 2

Design and Chemical Synthesis of Pyridine-Stretched Nucleosides (PSNs)

2.1 Introduction

Interest in all potential chemical modifications of each structural aspect of nucleosides and nucleotides, base, sugar and phosphate linkage along with potential analogues, has expanded rapidly over the last two decades. This is due to a number of contributing factors. Nucleosides and their phosphorylated analogues are central to metabolic (ATP) and cell signaling processes (cGMP). Ribose nucleosides provide the building blocks for natural and synthetic RNA structures that are antisense oligonucleotides capable of influencing mRNA translation and antigene oligonucleotides able to interfere with transcription by forming triple helical structures with duplex DNA. The rate of growth in applications that cross over the traditional chemical areas and into biotechnology, gene therapy and nanotechnology is bound to increase.

It has been recognized from the 1950s and 1960s, when nucleoside chemistry was emerging from its infancy, that modified nucleosides can possess valuable therapeutic properties. A range of anticancer agents such as 5-fluoro-2'-deoxyuridine **2.1**, toyocamyin **2.2** and 8-azainosine **2.3** has since been developed (Montgomery 1982). With the emergence of Human Immunodeficiency Virus (HIV), which causes Acquired Immunodeficiency Syndrome (AIDS), the first effective drugs were nucleoside

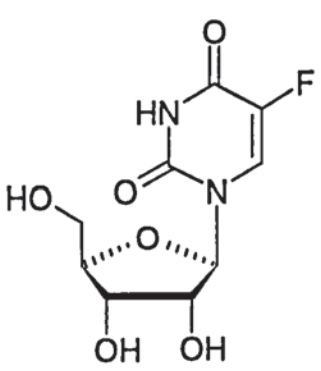

2.1

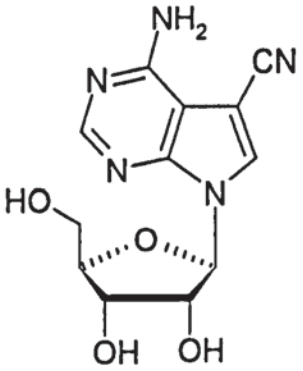

2.2

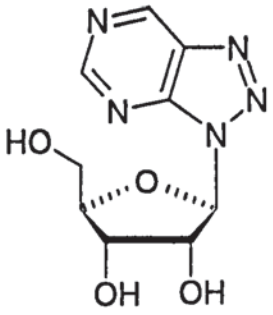

2.3

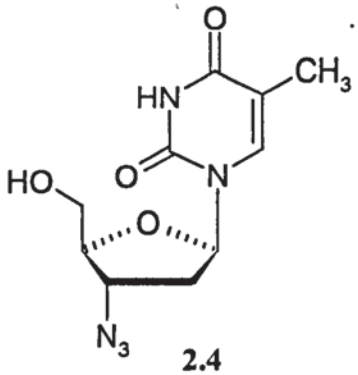

2.4

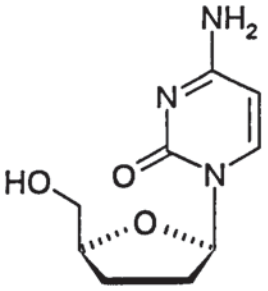

2.5

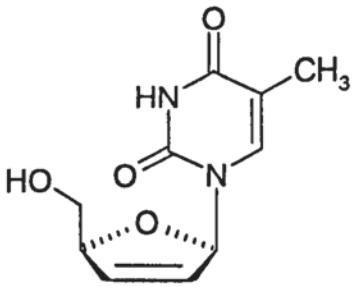

2.6

derivatives; zidovudine **2.4**, zalcitabine **2.5** and stavudine **2.6**, each capable of inhibiting HIV-1 reverse transcriptase. The common feature of these and later analogues is the lack of a 3′-OH group to support chain elongation during DNA replication (Balzarini et al. 1989; Barresinoussi et al. 1993; Horwitz et al. 1964; Simons 2001a).

Work on nucleoside analogues containing extended base ring systems dates back to the 1970s, before the development of the automated DNA synthesis methods that are used today and which are continually being developed and improved upon. A range of nucleosides containing benzene-stretched ring systems as dimensional, biochemical probes

was synthesized by Leonard and co-workers. These were used to investigate the size of the space available or that required by the purine moiety in enzyme-coenzyme binding sites. In these studies the requirement was for a well defined structural expansion of the base with minimal alteration of potential hydrogen bonding characteristics. Accordingly the work was concerned with the benzene-stretched analogues of adenine **2.7, 2.8** and **2.9**. In the case of the linear **2.7** an increase of 2.4 Å in the lateral dimension is achieved. Pyridine-stretched analogues are mentioned briefly in this work by Leonard but were not considered suitable for the study because of the possibility of undesired, modified hydrogen bonding due to the "extra" pyridine nitrogen (Leonard 1982; Leonard & Shivayogi 1986; Leonard et al. 1976; Lessor & Leonard 1981).

More recently, with possible applications in nanotechnology and as fluorescent probes for DNA and RNA assays, the benzene stretched analogues deoxythymine, **xT**, and deoxyadenosine, **xA**, have been synthesized and incorporated into oligonucleotides (xDNA) and their binding properties have been investigated (**Figure 2.1**) (Gao et al. 2004; Liu et al. 2003; Liu et al. 2004a; Liu et al. 2005b; Marx & Summerer 2004).

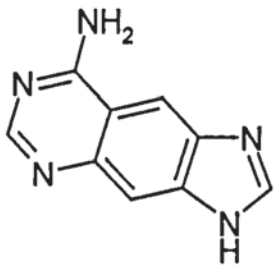

2.7

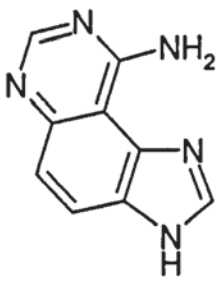

2.8

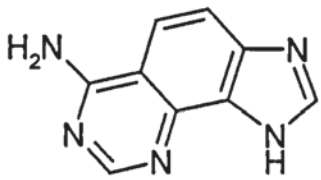

2.9

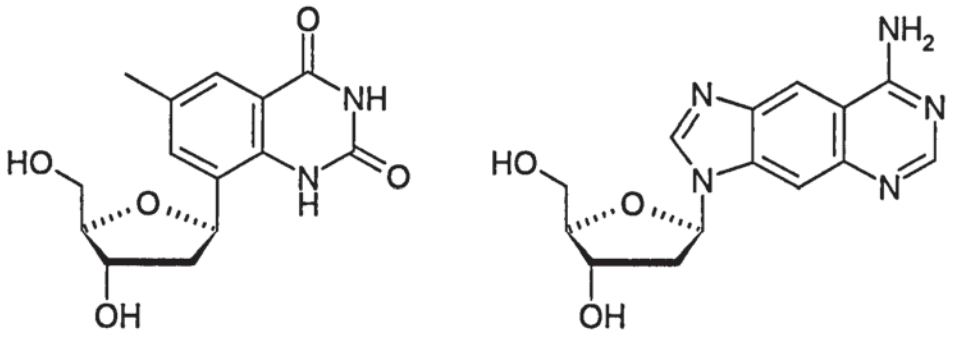

xT **xA**

The xDNA structures were compared with corresponding unmodified DNA structures containing exclusively the natural bases. The constructs **a** and **b**, where an extended base was singularly incorporated near the middle of a 12-base-pair sequence and paired with its

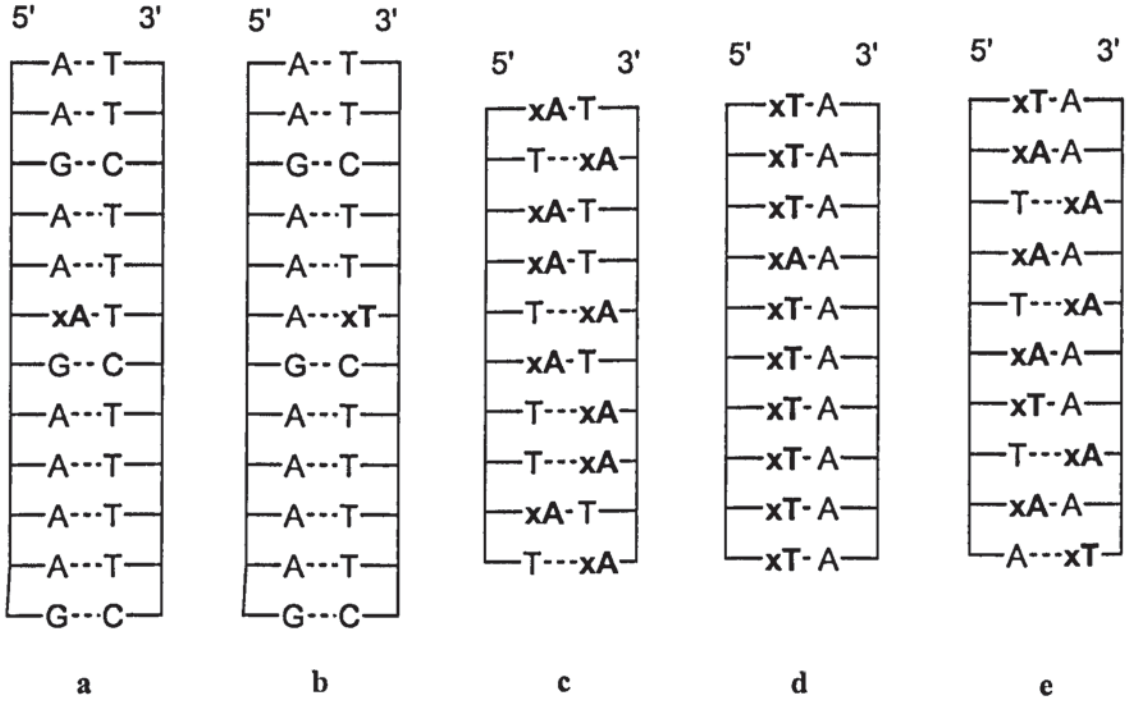

Figure 2.1 Selected DNA and extended DNA (xDNA) constructs.

unmodified partner, showed a decrease in stability compared to the natural A.T base pairing. However, when incorporated throughout the sequence as in constructs **c-d**, a helix structure was formed with an increased stability over the equivalent duplexes containing the natural bases. Construct **c** showed an increase of 5.8 kcal mol^{-1}, this increased stability being attributed to enhanced stacking of the aromatic ring systems. The **xA** was found to have a preference, although slight, for pairing with T over C, G or A. The **xT** base was found to be less selective. Structural and thermodynamic investigations indicated only small conformational changes in the DNA sugar-phosphate backbone and indicate that the larger diameter of the xDNA is due to more bases per turn than natural DNA. More recently the complementary analogues **xC** and **xG** and regioisomers termed **yC** and **yT** have been synthesized (Lee & Kool 2005; Lee et al. 2005; Liu et al. 2004b; Liu et al. 2005a).

The fluorescent properties of these extended nucleoside analogues suggest that they could be used as selective DNA probes. Coupled with natural nucleosides they also offer the prospect of an expanded genetic coding system to eight base-pairs although any biological significance of this prospect remains to be evaluated (Piccirilli et al. 1990).

Implications from this work are that while these and related, extended base systems might cause destabilization within a natural DNA double helix they could contribute favourably to triple helix formation due to improved base stacking and possible lowering of entropy. Comparative studies of an analogous family of pyridine-stretched bases could provide a

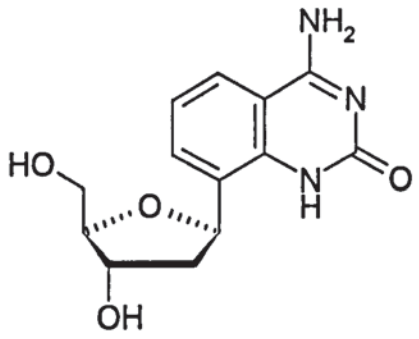

xC

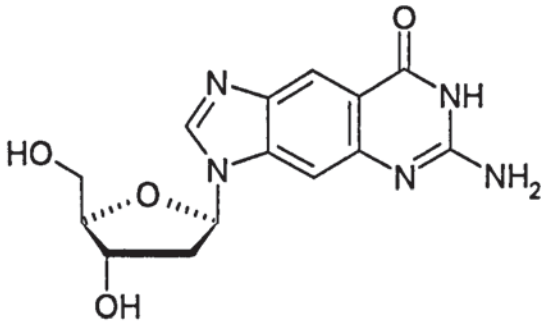

xG

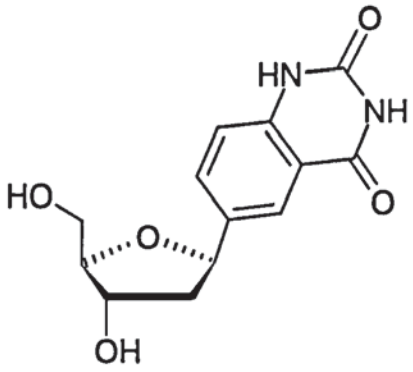

yT

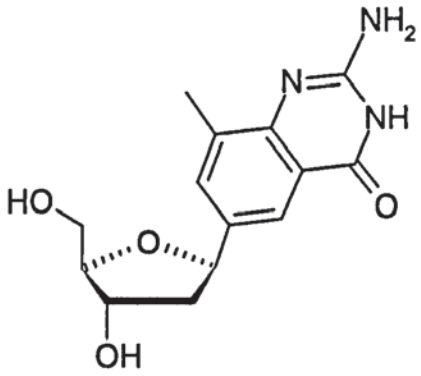

yC

valuable insight into stabilizing factors for the formation of duplex structures in environments with varying pH and salt concentration. The formation and stability of triplex structures have been shown to be dependant on a range of factors including base stacking and hydration. Incorporation of the pyridine ring system could potentially enhance stability by improving base stacking and making a positive contribution to hydration (**Chapter 4**).

A benzene-stretched version of antiviral drug 5'-noraristeromycin **2.10** has been prepared but antiviral activity was lost with this structural modification (Rajappan & Schneller 2001). Thiene-stretched nucleoside base analogues **2.11** and **2.12** have been synthesized

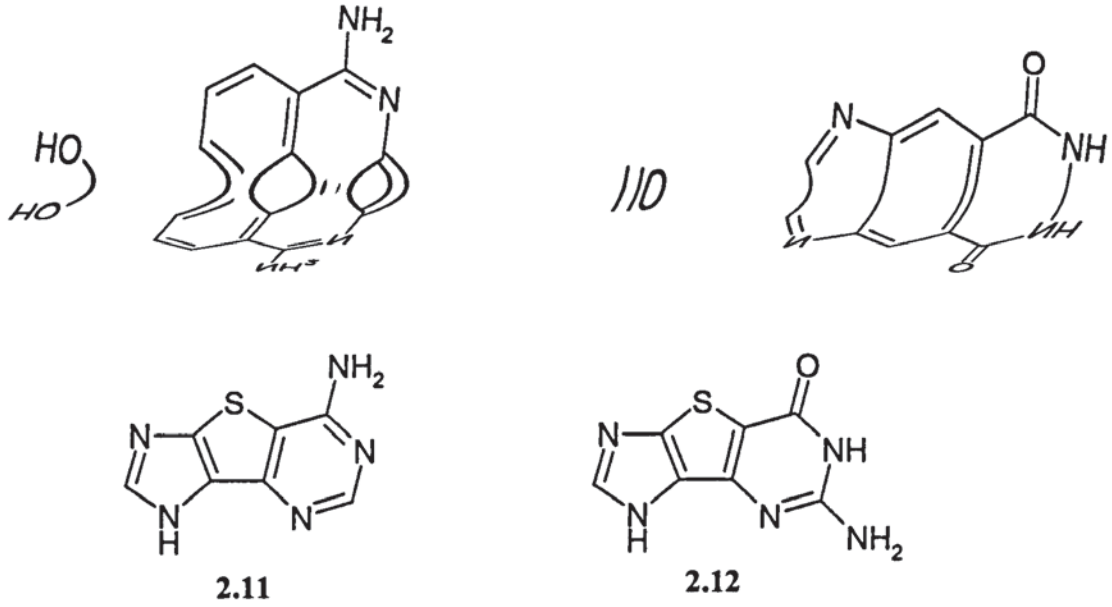

2.11 **2.12**

and their growth inhibitory effects on HCT116 corectal cancer cells studied (Seley et al. 2000).

A wide and varied range of pyrimidine and purine nucleoside analogues has been prepared using a number of synthetic strategies, and these have been extensively reviewed (Hoffer 1960; Simons 2001b). Work on the synthesis of nucleosides containing extended bases is limited by comparison. Synthesis of extended bases and their nucleoside and nucleotide derivatives has generally entailed lengthy procedures to construct the required ring system due to the lack of suitable, commercially available starting materials. Their multi-step synthesis typically results in low overall yields (Leonard & Shivayogi 1986; Liu et al. 2003; Liu et al. 2004a). The aim of this thesis work has been to develop a synthetic strategy for the efficient preparation of the stable key intermediate **2.29.** From past and present work it is envisaged that this compound would give ready access to a whole range of pyridine-

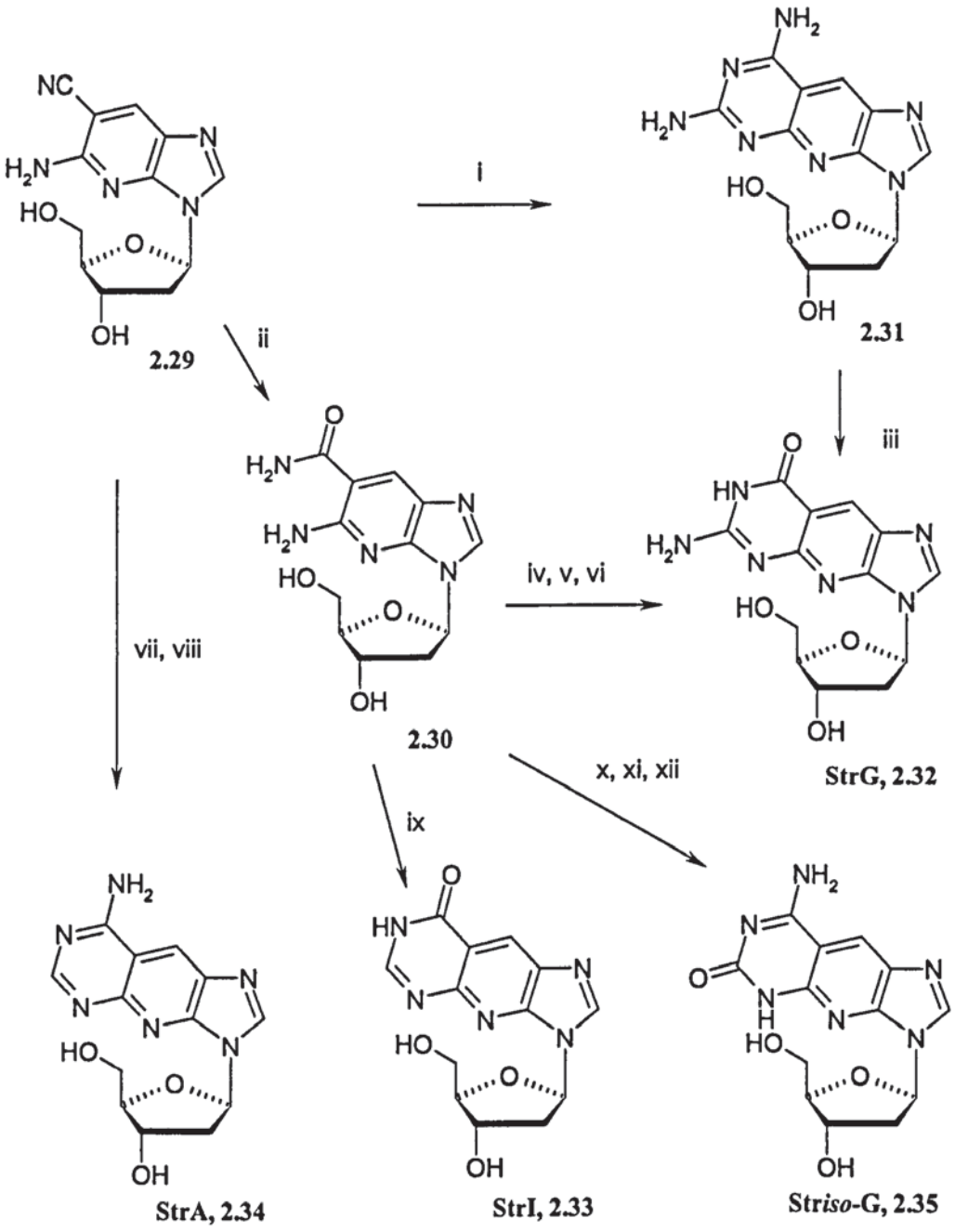

Scheme 2.1 Proposed routes to PSBs from key intermediate **2.29.** Reagents and conditions, i, $HN{=}C(NH_2)_2$, MeONa, MeOH, 140 °C; ii, H_2O_2, conc. NH_3 (aq), rt; iii, HCl, $NaNO_2$; iv, NaOH, CS_2, MeOH; v, H_2O_2; vi, NH_3, vii, $MeCO_2CH(OEt)_2$, reflux; viii, MeOH, Et_3N, H_2O; ix, HCOOEt, NaOEt; x, PhCONCS; xi, MeI; xii, NaOH, H_2O.

stretched nucleoside analogues for a comprehensive study. Possible synthetic routes towards the desired PSNs from **2.29** are summarized and typical conditions for such types of reactions are suggested in **Scheme 2.1.**

Work by Ramsden et al has demonstrated the efficient reduction of 5-nitroimidazoles to 5-aminoimidazoles and the potential synthetic use of the relatively unstable 5-aminoimidazole under suitable conditions (Al-Shaar et al. 1992; Humphries & Ramsden 1999). For this work the two readily and commercially available starting materials 2-deoxyribose **2.13** and 4-nitroimidazole **2.17** were chosen and an efficient glycosylation procedure was thus developed. The proposed synthetic pathway to the desired key nitrile intermediate **2.29** is outlined in **Scheme 2.2** and the proposed conditions are given.

2.2 Preparation of 2-deoxychlorosugar 2.16

The 2-deoxychlorosugar, 1-chloro-2-deoxy-3,5-di-*O*-toluoyl-α-D-ribofuranose **2.16**, has been demonstrated to be a useful reagent for the synthesis of a wide range of 2'-deoxynucleoside analogues since its efficient synthesis from 2-deoxyribose **2.13** was first published by Hoffer (1960). This work was subsequently reviewed by Bhat (1968) (**Scheme 2.3**). The chlorosugar **2.16** readily undergoes coupling reactions, notably glycosylation, with the sodium **2.20** and mercury salts of 4(5)-nitroimidazole. The silver salt of 4(5)-nitroimidazole **2.18** has also been used in related reactions (Dhimitruka & SantaLucia 2004; Hubbard et al. 1984).

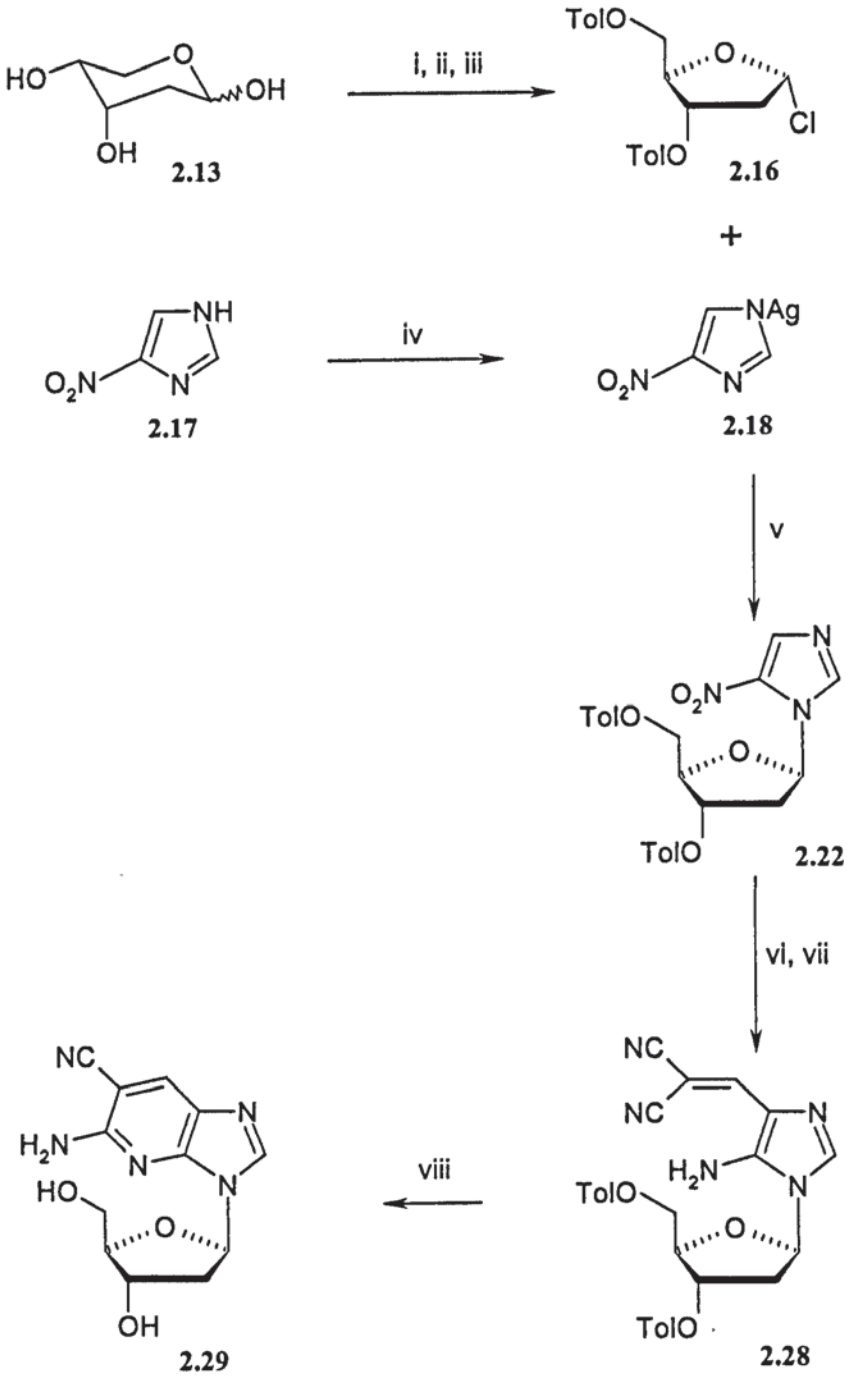

Scheme 2.2 Proposed route to the key intermediate **2.29.** Reagents and conditions, i, MeOH, CH_3COCl, Ag_2CO_3, rt; ii, *p*-toluoyl chloride, pyridine, 0 °C to rt; iii, HCl, AcOH, 15 °C; iv, $AgNO_3$, conc. NH_3 (aq), rt; v, xylene, reflux; vi, H_2, Pd on C, THF; vii, EMMN **2.41,** THF, rt; viii, NaOH, MeOH, reflux.

Methylation of 2-D-deoxyribose **2.13** gave a mixture of anomeric isomers of 2-deoxy-1-*O*-methyl-α/β-D-ribofuranose **2.14** as a colourless oil in near quantitative yield (**Scheme 2.3**). In the standard published procedure, a methanolic solution of HCl (g) is used. A low concentration of HCl is required to favour the formation of a furanose rather that a pyranose ring. Rather than having to prepare such a solution, a more convenient procedure is to generate the required amount of dry HCl *in situ* using acetyl chloride (Hubbard et al. 1984) or by using the commercially available dioxane solution containing 4 M HCl (Chin et al. 1997).

The α and β isomers were clearly seen as two spots on TLC analysis and as two sets of peaks in the ^{1}H NMR spectrum. The anomeric proton signals appear as a doublet and triplet

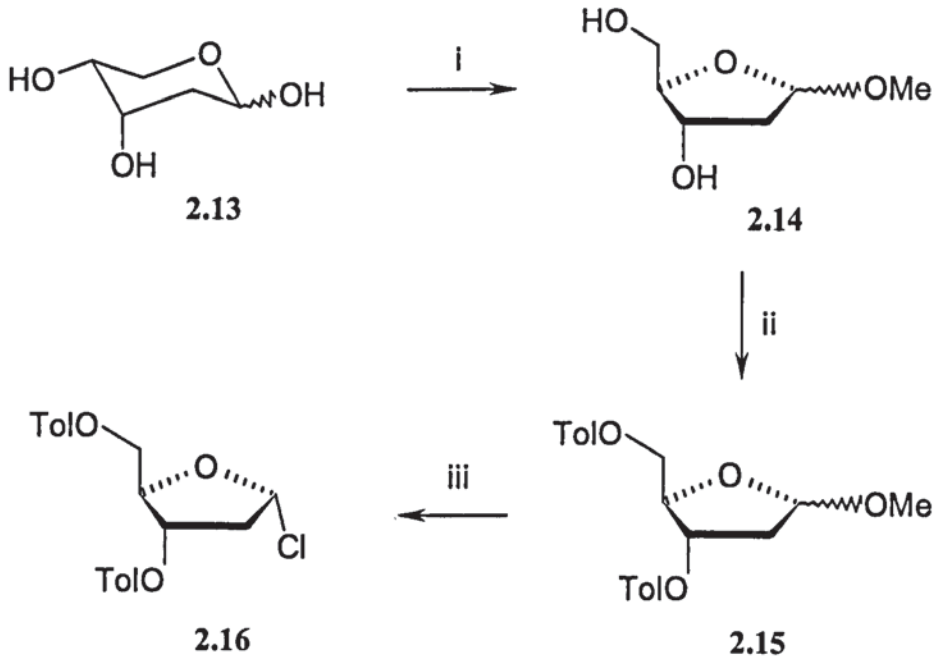

2.13 **2.14** **2.15** **2.16**

Scheme 2.3 Preparation of 2-deoxychlorosugar **2.16**. Reagent and conditions, i, MeOH, CH_3COCl, Ag_2CO_3, rt; ii, *p*-toluoyl chloride, pyridine, 0 °C to rt; iii, HCl, AcOH, 15 °C.

for the α and the β isomers respectively. The difference in multiplicity of these protons results from the difference in coupling pattern. In the β isomer, the anomeric proton couples to just one of the neighbouring protons attached at C2 due to a Karplus angle of 90° in the preferred conformation of the β isomer.

Subsequent reaction with *p*-toluoyl chloride in dry pyridine gave the protected sugar, 2-deoxy-3,5-di-*O*-toluoyl-1-*O*-methyl-α/β-D-ribofuranose **2.15** as a clear orange oil, initially. On extended drying under high vacuum on a slow turning rotary evaporator the oil slowly crystallized to a pale, buff-coloured solid in near quantitative yield.

Initially, the literature procedure was followed for the preparation of the chlorosugar **2.16.** Reaction of **2.15** with cold glacial acetic acid, saturated with HCl (g) gave a white precipitate consisting of the single α isomer, 1-chloro-2-deoxy-3,5-di-*O*-toluoyl-α-D-ribofuranose **2.16.** During the course of this reaction it is essential to keep the time to a minimum following the precipitation of the product. Filtration of the product soon after it has precipitated is crucial otherwise the reaction mixture darkens rapidly due to decomposition. A reaction mixture that was allowed to stand for 2 h resulted in a significantly reduced yield (35%). The filter cake was packed down during filtration and re-slurried with cold ether and re-packed twice before being dried under high vacuum over several days to remove any residual HCl that may be present. This procedure gave the chlorosugar **2.16,** in 73% yield, as a white solid. To avoid the use of a cylinder of HCl (g), a far more convenient method was to use the commercially available 4 M HCl in dioxane (Chin et al. 1997). The benefits of using this reagent include ease of handling, ease of limiting the amount of HCl used. Further, following addition the dioxane prevents the

acetic acid from freezing when cooled with an ice/water bath. It was observed that using these conditions greatly reduced the rate at which the reaction filtrate darkened and degraded. ^{1}H NMR indicated the product was of comparable quality although the yield (67%) was slightly lower. It was found that if stirring is continued during the precipitation of **2.16,** a thick slurry is obtained which is slow to filter and gave a powdery product. However, if the stirring is stopped when precipitation starts or the reaction mixture is seeded, the particle size is increased and the product filters rapidly and becomes easier to handle.

^{1}H NMR and TLC analyses were used to measure the purity and to confirm the quality of the product **2.16**. The required α anomeric purity was shown by the presence of a doublet due to the anomeric proton signal. Only a very minor side peak attributable to the β isomer was observed in freshly prepared **2.16.** This is in contrast to the two methoxysugar precursors **2.14** and **2.15** that are prepared and reacted as a 50:50 mixture of α and β anomers.

The reaction of the α/β methoxysugar **2.15,** to give only the required α isomer of the chlorosugar **2.16,** is due to the anomeric effect. This anomeric effect results from the donation of the non-bonding lone pair of electrons by the sugar ring oxygen for interaction with the σ* antibonding orbital of the carbon-chlorine bond. Thus the chlorine atom is directed axial **(Figure 2.2).** To a lesser extent, the fact that the α-anomer has a smaller overall dipole moment relative to the β-anomer also contributes to the axial preference of the chlorine.

The chlorosugar **2.16** has been reported to be unstable, decomposing in weeks even when

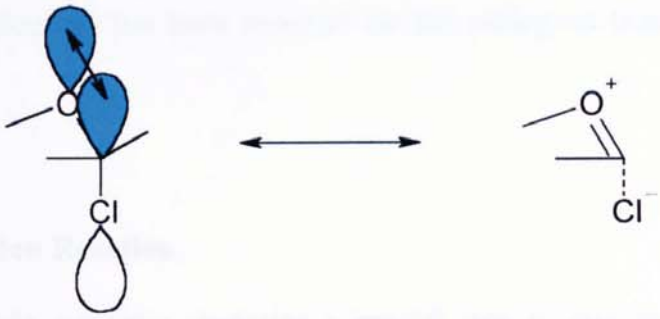

Figure 2.2 ***nOsp3*** $\rightarrow \sigma^{*}$***C-X*** anomeric effect which stabilises the α-anomer (no-bond, double-bond resonance)

stored under vacuum in a dessicator. Various modifications to the procedure have been proposed including purification of the intermediates, and using *p*-toluic anhydride instead of the chloride in an attempt to improve the stability (Dhimitruka & SantaLucia 2004).

The initial procedure followed here using the AcOH/HCl (g) method without specific purification stages gave a product that has been demonstrated to be relatively stable on extended storage provided that it is thoroughly dried under vacuum and stored at -20 °C in a well-sealed container, purged with argon. ^{1}H NMR analysis of a sample which had been stored for over two years under these conditions indicated 7% isomerization to the β isomer with no other significant deterioration. Subsequent use of this stored sample for the glycosylation reaction resulted in reduced yields of the desired β isomer and ^{1}H NMR analysis showed a significant increase in the percentage of both the 4α and 5α isomers (**Scheme 2.7**). However, the β isomer **2.24** was still isolated in 50% yield. Any residual HCl in the product or its generation by hydrolysis in the presence of moisture, or photochemically by light, could possibly initiate isomerisation and degradation of the

product. The chlorosugar can be recrystallized from dry toluene and an effective purification procedure has been reported for the analogous bromosugar (Hadd & Kokosa 2003).

2.3 Glycosylation Reaction

In all nucleoside synthetic strategies a crucial step is ensuring the correct stereo- and regiochemistry at the glycosidic bond formed between the sugar and the base. In typical purine analogues it is the β orientation that is required with the N9 rather than the N7 position of the base attached to the sugar ring. Standard glycosylation reactions involve the coupling of a heterocyclic base in the form of a salt or other derivative to a halo sugar that is protected, for example as acetate, benzoyl or toluoyl esters. When ribose sugar derivatives are employed, the required β configuration in the nucleoside product is readily achieved irrespective of the initial C1 configuration due to operation of the *trans* rule and neighbouring group participation (NPG). NGP promotes formation of the required β-configured nucleoside product by stabilizing the oxonium ion intermediate formed in the S_N1 process illustrated in **Scheme 2.4.** Alternatively, if the leaving group at C1 adopts the α configuration a S_N2 mechanism will also favour the β isomer since the approach of the nucleophile is directed *trans* to ester group attached at C2 due to steric hindrance. (Humphries & Ramsden 1995; Humphries & Ramsden 1999) **(Scheme 2.4).**

In the proposed route to the pyridine-stretched deoxynucleosides, that are the focus of this current research, the absence of the hydroxyl group at C2 precludes NGP as a directing influence in the stereochemical outcome of the glycosylation reaction proposed in **Scheme**

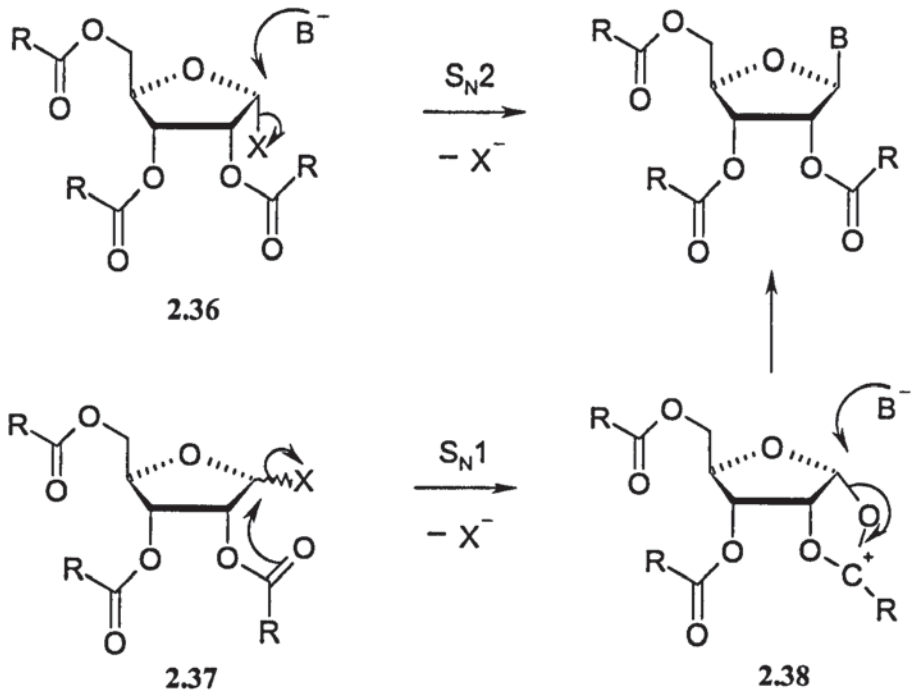

Scheme 2.4 Nucleophilic substitution at C1 of protected ribose derivatives, R = alkyl, X = halide and B = heterocyclic base.

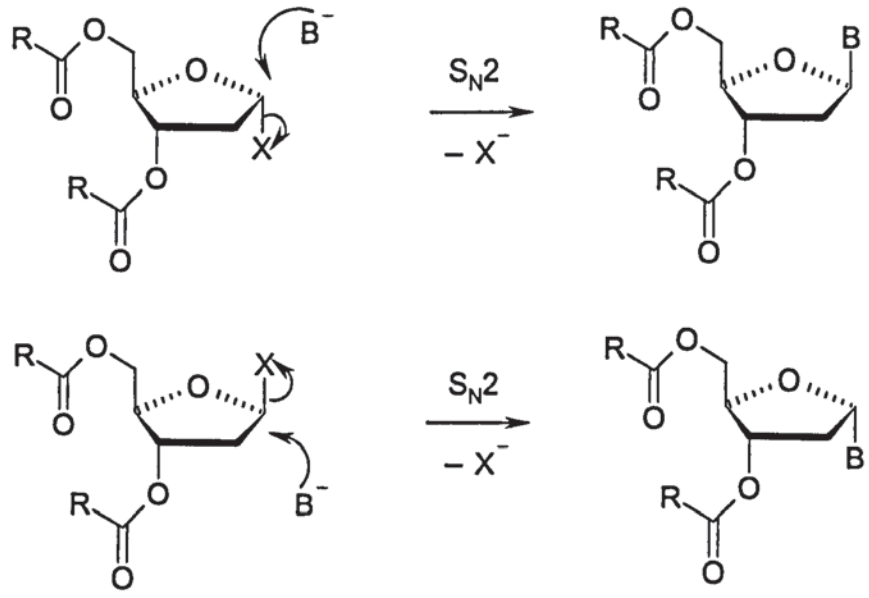

Scheme 2.5 Nucleophilic substitution at C1 of protected 2-deoxyribose derivatives, R = alkyl, X = halide and B = heterocyclic base.

2.2. Use of a 2-deoxyribose sugar starting material would rely on a S_N2 Walden inversion process at C1 to give the required β-configured product. The α-stereochemistry at C1 of the sugar reagent is therefore crucial to the success of the proposed glycosylation process (**Scheme 2.5**). Because the stereochemistry at C1 is exclusively α not β, this makes chlorosugar **2.16** the starting material of choice.

In practice, such reactions using α-deoxyhalosugars rarely give the target β isomer as the sole product. The presence of varying amounts of the α configuration in the glycosylation reactions carried out using this α-chlorosugar **2.16** can be explained by considering a S_N1 mechanism but with inversion of the halosugar at C1 prior to glycosylation or the formation of a planar intermediate oxonium ion (**Scheme 2.6**).

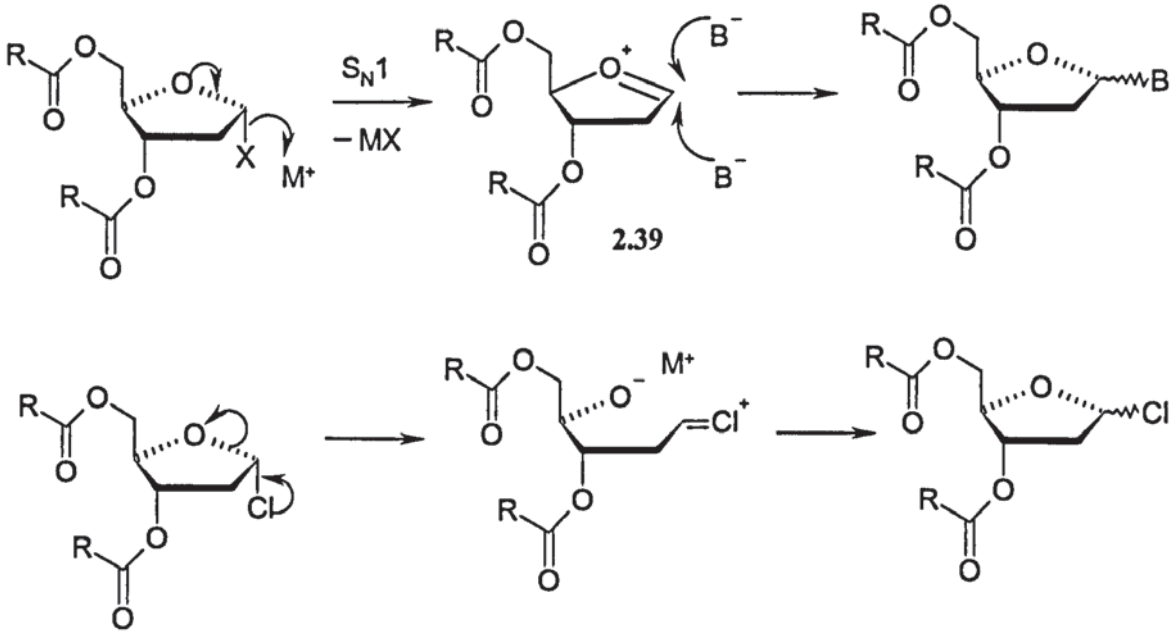

Scheme 2.6 Possible sugar ring opening, ring closing pathways responsible for anomerisation, R = alkyl, M = metal and B = heterocyclic base.

Both processes would be influenced by the ability of the solvent and metal ion to stabilize the likely intermediate cations. The α-chlorosugar **2.16** has indeed been previously shown to isomerise in solution where the rate of isomerisation correlates with the polarity of the solvent (Hubbard. et al. 1984). This was investigated by monitoring solutions of the chlorosugar **2.16** in deuteriated acetonitrile (d_3-CH_3CN), deuteriated THF (d_8-THF) and deuteriated chloroform (d-$CHCl_3$), over time by ^1H NMR analysis. The two anomeric proton signals were readily distinguished and quantified by integration. The rate of isomerization was shown to be in the order $CHCl_3$ < THF << CH_3CN, and mirrored by the respective dielectric constants, 4.8, 7.6 and 37.5. After 3 h, ^1H NMR indicated 8%, 15% and 35% isomerisation respectively.

The coupling reaction of the chlorosugar **2.16** to 4(5)-nitroimidazole **2.17** can yield not only the α- and β-configurational isomers but also, as mentioned above, the 4- and 5-nitroimidazole regioisomers to give the total of four possible isomeric products. Only the 5β regioisomer is required for the proposed synthesis (**Scheme 2.7**). Subsequent work demonstrated that a mixture of all four possible isomers are obtained, the isomeric ratios being influenced by a range of factors including the quality of reactants, reaction conditions, concentration, solvent and the 4(5)-nitroimidazole salt.

In the literature the silver salt **2.18**, soduim salt **2.20** and the mercury salts of 4(5)-nitromidazole have been used for similar glycosylation reactions. Because of its inherent toxicity and potential risk, the mercury salt was not considered further for use in this thesis work.

The glycosylation reaction was initially attempted using sodium hydride in acetonitrile to form the sodium salt **2.20** *in situ*, and using the preformed silver salt in refluxing xylene. In

both cases two products were isolated in limited quantity from the reaction product mixtures following workup and flash chromatography. These were characterized as the 4α

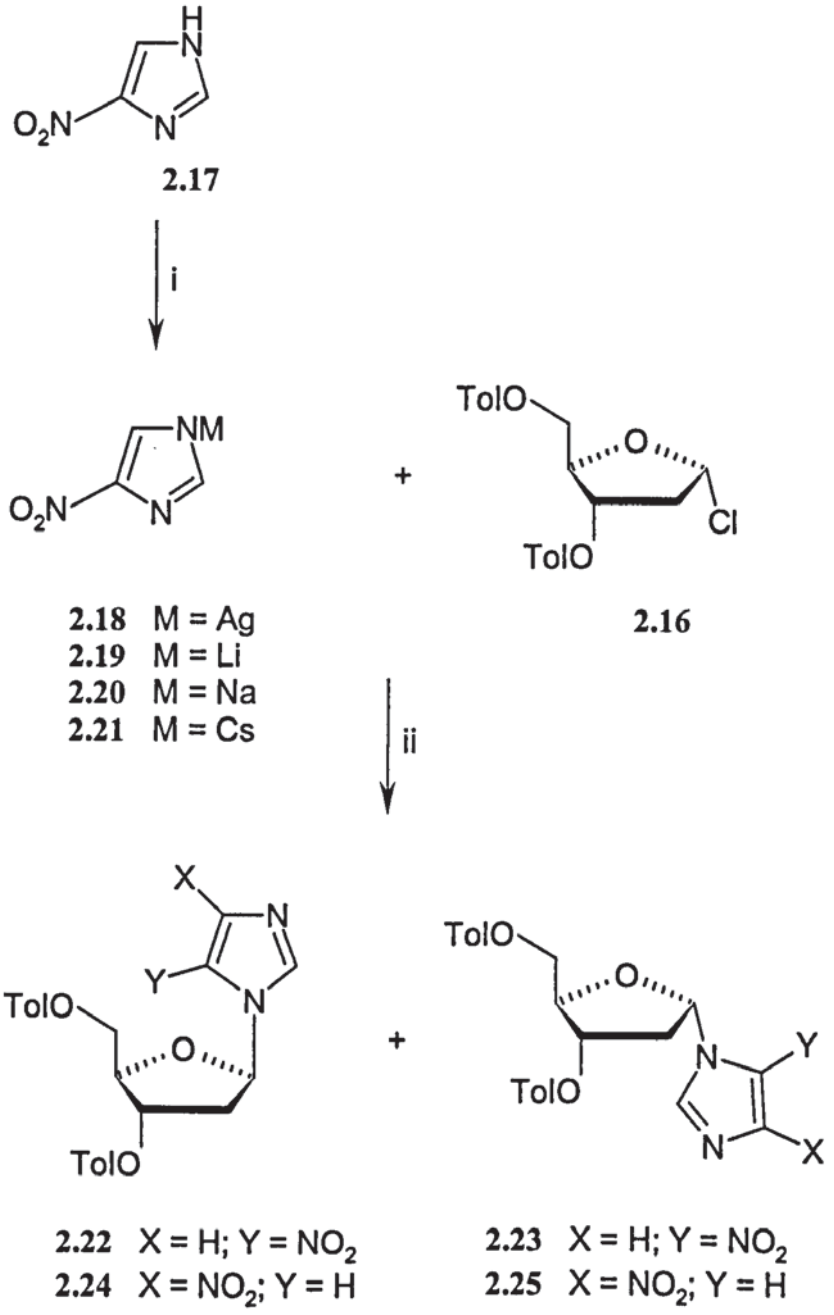

Scheme 2.7 Chemical synthesis of the target nucleoside **2.22**. Reagents and conditions, i, MOH, MeOH; ii, THF, 62 °C, 3 h.

and 4β isomers **2.23** and **2.24**. In the case of sodium hydride it was concluded that the quality of the sodium hydride was suspect resulting in isomerisation and hydrolysis of the chlorosugar. TLC analysis indicated that the reaction was slow and incomplete when using the silver salt **2.18** in xylene. For subsequent work the metal salts of 4(5)-nitroimidazole were preformed rather that formed *in situ*.

Confirmation of the structure of the two isomeric products was by ^{1}H NMR, NOESY, COSY and ^{13}C NMR analysis following deprotection with CH_3NH_2. Comparison tables of the observed chemical shifts for the unsubstituted carbon and the carbon bearing the nitro group in the imidazole ring in a wide range of 4- and 5-nitroimidazoles have been published, enabling them to be distinguished by comparing their ^{13}C-NMR spectra (M^{c}Killop 1983). While substitution at the C2 can result in a significant downfield shift of the C2 signal, there is limited effect on the chemical shifts of the C4 and C5 signals. More significantly, the 4(5)-substitution pattern of the imidazole ring, results in a consistent and predictable shift of the ^{13}C-NMR signals in question. For 1-substituted-4-nitroimidazole the respective chemical shifts were reported to be around 120 and 146 ppm whereas for 1-substituted-5-nitroimidazole, these are reported to be around 132 and 138 ppm. There is very good agreement between the recorded values and those given in the literature ensuring a high level of confidence in the structural assignments of the nucleoside products formed from these glycosylation reactions (**Table 2.1**). Moreover, the α and β isomers were readily identified from NOESY NMR experiments (**Figure 2.3**). From this spectroscopic analysis,

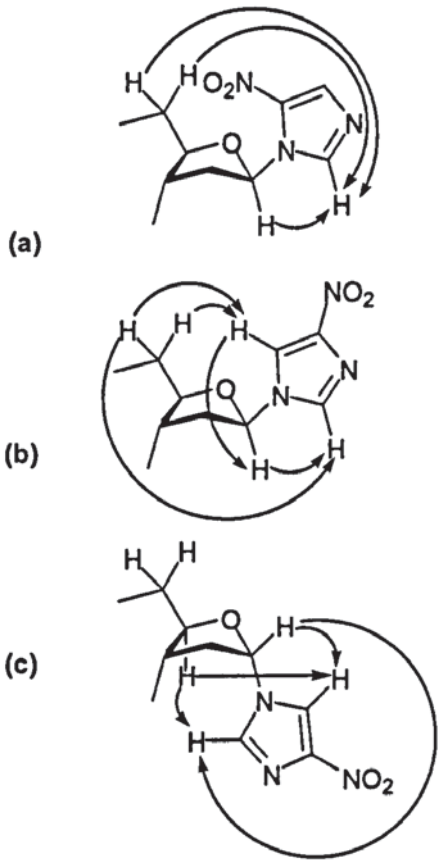

Figure 2.3 Strong nOe enhancements from NOESY spectra, (a) compound **2.22** (b) compound **2.24** (c) compound **2.37.**

Table 2.1 ^{13}C NMR chemical shifts of 4(5)-nitroimidazole.

Compound	R_1	R_2	R_3	Chemical shift (δ) values ppm		
				C2	C4	C5
2.22	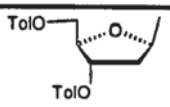	H	NO_2	138.13	134.33	Not observed
2.24	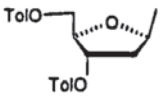	NO_2	H	135.71	147.47	119.53
2.46	CH_2Ph	NO_2	H	136.03	Not observed	119.42

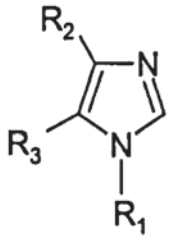

the reaction product of higher R_f was identified as the 4β isomer, 1-(2'-deoxy-3',5'-di-*O*-toluoyl-β-D-ribofuranosyl)-4-nitroimidazole **2.25**, and that of lower R_f as the 4α isomer, 1-(2'-deoxy-3',5'-di-*O*-toluoyl-α-D-ribofuranosyl)-4-nitroimidazole **2.23**. Using the same spectral analysis, the structure of the subsequently prepared target 5β isomer **2.22** was assigned. The NOESY spectra are given in the **Appendix 1.**

With the reversal of the ratios of the 4α and 4β isomers formed in the glycosylation reactions performed using different metal ions, the nature of the metal ion on the outcome of the product distribution was examined in detail. In view of the influence of the solvent choice on the rate of isomerization of the β-chlorosugar, a thorough investigation was undertaken to determine the exact conditions to favour the formation of the required 5β-isomer; 1-(2'-deoxy-3',5'-di-*O*-toluoyl-β-D-ribofuranosyl)-5-nitroimidazole **2.22.** The cation size and co-ordinating power of the metal cation, and the actual reacting species, 4- or 5-nitroimidazole tautomer, were considered. Lithium and the cesium salts, in addition to the sodium and silver salts, were therefore prepared for comparison purposes. The Li, Na and Cs 4(5)-nitroimidazole salts were readily prepared from the respective metal hydroxide and 4-nitroimidazole **2.17** in methanol. To minimize isomerisation, the chlorosugar was added as a solution or solid to a stirred mixture of the 4(5)-nitroimidazole salt in the selected solvent. The reactions were monitored by TLC analysis during the addition and subsequent reaction of the chlorosugar, and the isomeric ratio of the crude product was determined from the integration of the anomeric proton.

The nature of the metal cation was found to have a significant effect on the product isomer

Table 2.2 Ratio of isomers from glycosylation of chlorosugar **2.16** using different metal salts of 4(5)-nitroimidazole in acetonitrile at rt.

4-Nitroimidazole salt	Reaction time (min)	Ratio of isomers (%)			
		4 α	4 β	5 α	5 β
2.18 (Ag)	180	25	29	14	32
2.19 (Li)	90	48	22	20	10
2.20 (Na)	135	8	54	6	32
2.21 (Cs)	40	2	51	2	45

ratio under comparable conditions reaction conditions **Table 2.2.** Of the different metal used, the cesium salt was shown to consistently give the highest yields of the desired 5β isomer **2.22** with generally the lowest yields of the unwanted α inversion products. The use of the lithium salt gave the poorest yield of the desired 5β isomer favouring formation of the α anomers. The rationalization was that the large cesium cation is the least co-ordinating of the metal ions used and least able to cause inversion of the sugar starting material. It may further stabilise the 5-nitroimidazole anion to direct the attack and attachment of the required nitrogen of the imidazole to the sugar ring.

From these initial results the subsequent work was focused on the cesium salt and the effects of the reaction conditions. The reaction was rapid, less than 30 min, in CH_3CN with small amounts of the α isomers formed. However, the unwanted 4β isomer predominated over the 5β product. With THF as the solvent and a reaction temperature of 60 °C the reaction was complete after 2 h with the 5β isomer being the major product (54%).

Attempts to scale this reaction up to access gram quantities of the 5β isomer **2.22**, using these conditions gave disappointing results with lower than expected yields. In the scale-up process, the concentration of reagents was increased and this to resulted in a lower than expected yield of the target 5β isomer. The reaction was repeated using the conditions optimized for the smaller scale reactions but the dilution of the reagents was significantly increased. Reducing the concentration of the reaction mixture had a dramatic effect on the isomeric ratio of the products. Under these circumstances the yield of the desired 1-(2'-deoxy-3',5'-di-*O*-toluoyl-β-D-ribofuranosyl)-5-nitroimidazole **2.22** was increased to over 60%.

While ether is an effective solvent for TLC analysis, the use of ether for separation and purification of 5g or greater batches of product by flash chromatography proved unsatisfactory due the low solubility of the 5β and 4β isomers **2.22** and **2.25**. This invariably resulted in poor separation due to tailing and precipitation in the column tap unless a very low but impractical column loading was used. Although appreciably soluble in chloroform, when used as a mobile phase for TLC, there was negligible migration of the reaction products from the base line. From these observations a practical separation and purification was achieved by loading the crude reaction product onto the flash chromatography column as a solution in chloroform followed by elution with ether-chloroform (1:1). Greater than 5 g batches of the 5β isomer have been readily isolated using a medium sized chromatography column (70 mm).

This optimized reaction, work up and separation procedure was carried out several times to give 65% yields of isolated product. NMR and TLC analysis was used to confirm the purity.

2.4 Reduction of 5-nitroimidazole derivative 2.22

5-Aminoimidazole derivatives with an unsubstituted C4 position have been shown to be highly unstable compounds whose use as synthetic intermediates have only recently been realised by carrying out the reaction *in situ*, otherwise rapid decomposition occurs. The isomeric 4-amino derivatives, however, are stable by comparison and can be readily isolated (Al-Shaar et al. 1992).

Initially, catalytic reduction of the nitroimidazole nucleoside **2.22** over palladium on carbon (Pd on C), using catalyst loadings of up to 20% by weight at 1 atm., was attempted (**Scheme 2.8**). TLC analysis indicated slow reduction and the formation of a complex reaction mixture. However, work by Al-Shaar et al. (1992) demonstrated that if a high loading of catalyst is used, then efficient, rapid reduction to the required 5-aminoimidazole can be achieved and the product could be used promptly in the next synthetic step without isolation.

With the use of between 50 and 100% by weight of 5% Pd on C and vigorous shaking, reduction the 5-nitroimidazole nucleoside **2.22** to the 5-amino derivative **2.40** was achieved in 2 to 3 h with minimal degradation of the product. While TLC analysis of the reduction mixture indicated a complex mixture, this was demonstrated to be due to degradation on the TLC plate and not in the reaction mixture itself.

The efficiency of the reduction was confirmed by carrying out a small scale reduction in ^{8}d-THF. Filtration of the reduction mixture under Ar directly into a dry NMR tube and immediate ^{1}H NMR analysis gave a spectrum that was in agreement with the structure of **2.40** with no other detectable by-products. Because of its instability, the 5-aminoimidazole

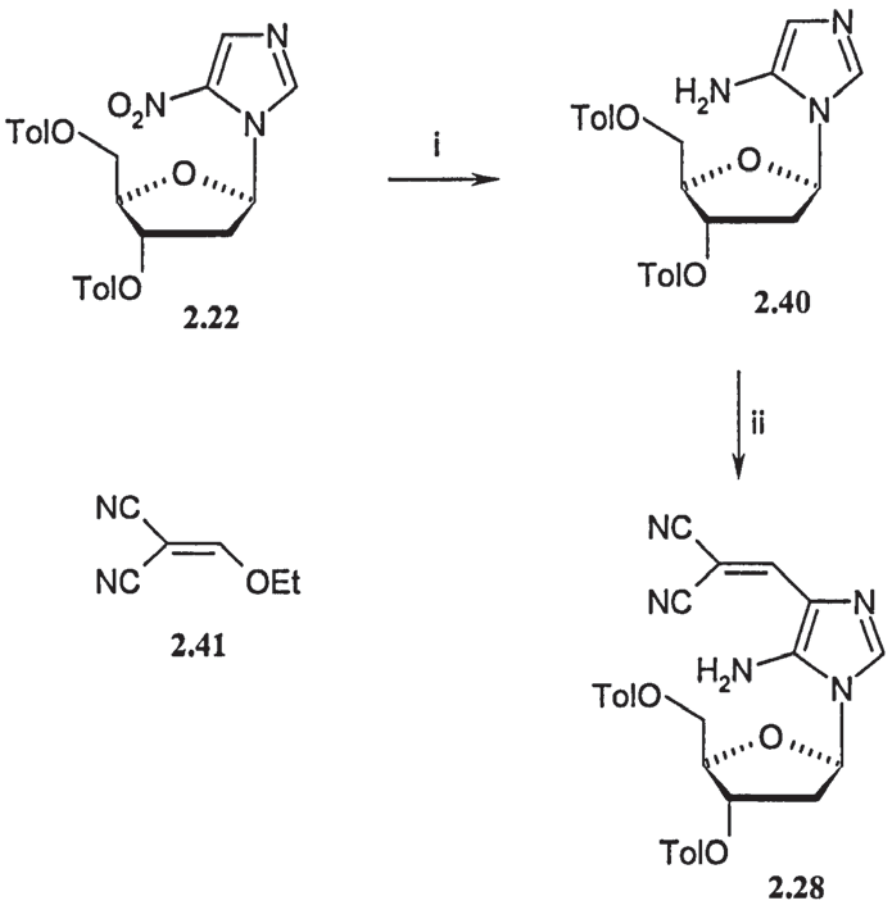

Scheme 2.8 Reduction of **2.22** and reaction with EMMN **2.41**. Reagents and conditions, i, H_2, 5% Pd on C, THF, rt; ii, EMMN , THF, rt.

2.40 was not isolated but reacted immediately following its preparation.

2.5 Preparation of 5-amino-4-(2,2-dicyanovinyl)-1-(2'-deoxy-3',5'-di-*O*-*p*-toluoyl-β-D-ribofuranosyl)-imidazole 2.28

An extensive study of the reactions of 4- and 5-aminoimidazoles with a range of electrophilic reagents showed that, in the case of 4-aminoimidazoles, reaction was exclusively at the amino nitrogen. However, in the case of 5-aminoimidazoles, reaction with ethoxymalononitrile (EMMN) was found to yield the C adduct (**Scheme 2.8**). In an

analogous reaction with the ribose derivative of **2.40**, the C adduct was readily obtained in over 50% yield. Initial attempts at reacting EMMN with the 2'-deoxyribose aminoimidazole **2.40** gave low yields and poor reproducibility. The typical procedure was to filter off the catalyst from the reduction mixture through a filter aid using argon pressure and then react immediately with EMMN. With failure of the initial reactions to give satisfactory results, the EMMN being used, as purchased, was analysed by ^{1}H NMR and thought to be suspect. Attempts at purification by recrystallization were unsuccessful due to its high solubility. Passing the ether solution of the EMMN through a bed of silica gel followed by evaporation and drying under high vacuum gave a pale yellow crystalline solid. ^{1}H NMR confirmed the purity. The reaction of amino nucleoside **2.40** with the purified EMMN reagent was then attempted at a range of temperatures from -78 °C to 50 °C. When the reaction was carried at 5 °C, rt and 50 °C the yields were comparable at 30%. At lower temperatures, -50 °C and -78 °C the reaction was slow and the yield reduced to 20%. A significant by-product was indicated by TLC analysis of the reaction mixture but this rapidly degraded during work up and to date has not been characterized. Only dark brown intractable residues were obtained. If the by-product is a C-unsubstituted 5-aminoimidazole then this would account for its instability. The yield of the desired product was improved to 37% by adding the EMMN directly to the reduction mixture and, after briefly mixing, allowing it to stand over night. Because of high loading of the catalyst, the possibility that a significant amount of the desired product **2.28** might be lost due to adsorption onto the catalyst was considered. The catalysis was recovered from one reduction by centrifuging under argon and re-used. Complete reduction of **2.22** was achieved in 3 h, however, the yield of **2.28** was comparable to that from reductions where fresh catalyst was used. The

pure product **2.28** was readily isolated by filtration followed by washing because of its low general solubility in organic solvents.

2.6 Reaction of 5-Amino-4-(2,2-dicyanovinyl)-1-(2'-deoxy-3',5'-di-*O*-*p*-toluoyl-β-D-ribofuranosyl)-imidazole 2.28 to 5-Amino-6 cyano-3-(2'-deoxy-β-D-ribofuranosyl)-imidazo[4,5-*b*]pyridine 2.29 and 5-Amino-3-(2'-deoxy-β-D-ribofuranosyl)-imidazo[4,5-*b*]pyridine-6-carboxamide 2.30

In previous work with ribose analogues, deprotection of the sugar ring was carried out before the reduction of the nitroimidazole group and reaction with EMMN. Work by Clayton et al. (2005) demonstrated that the protected deoxyribose derivative could be reduced and reacted with EMMN. Treatment of **2.28** with NaOH in methanol and heating for 15 min effected both deprotection and cyclisation. Following work up, purification by flash chromatography and recrystallization from water, the nucleoside **2.29** was obtained in a yield of 84% (**Scheme 2.9**).

The nucleoside products from the cyclisation of **2.28** containing the imidazo[4,5-*b*]pyridine ring system were readily identified by TLC analysis due to their strong fluorescence under long wave (363 nm) UV. Following prolonged heating of **2.28** with NaOH in methanol, TLC analysis showed the formation of a UV fluorescent product of lower R_f than **2.29** and after 5 h heating this was shown to be the main product. Workup of the reaction mixture gave the amide **2.30** in 67% yield from the hydrolysis of the nitrile group (**Scheme 2.9**).

Cationic ion exchange resins have been used to hydrate nitrile groups to give the amide and the possibility of using an ion exchange resin to convert **2.28** directly to the required amide **2.30** was investigated (Bobbitt & Doolittle 1960, Bobbitt & Scola 1964). While no

hydration to the amide was detected, the ion exchange resin proved to be effective for the cyclisation and deprotection of **2.28** to **2.29**. The reaction required stirring the resin and **2.28** in MeOH overnight at rt. After warming to 50 °C, the resin was filtered off and

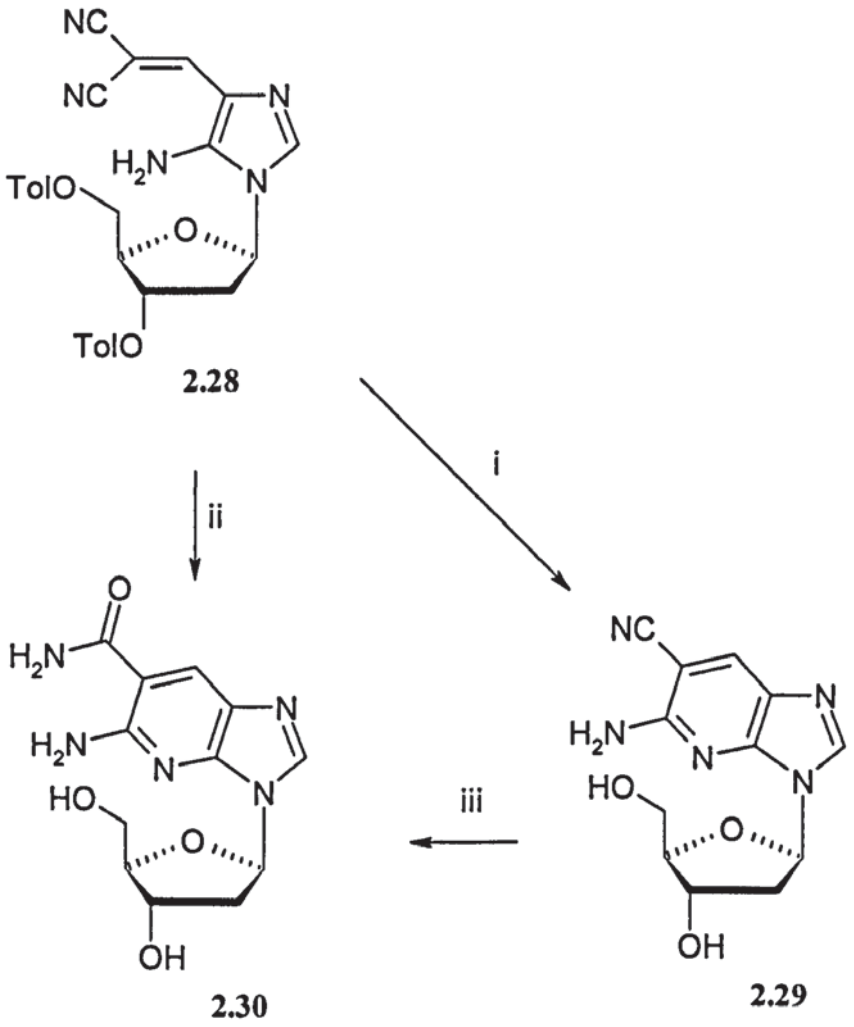

Scheme 2.9 Preparation of key nitrile nucleoside **2.29** and oxidation to amide **2.30**, i, NaOH, MeOH, reflux, 15 min or ion exchange resin, MeOH, rt, 12 h; ii, NaOH, MeOH, reflux.5 h; iii, H_2O_2, conc. NH_3 (aq).

washed well with warm MeOH. Evaporation of the solvent gave a mixture of the methyl toluate ester and nucleoside **2.29**. The ester was readily removed by washing with ether to yield 5-amino-6-cyano-3-(2'-deoxy-β-D-ribofuranosyl)-imidazo[4,5-*b*]pyridine **2.29** in 89% yield. NMR and TLC analysis showed that no further purification was required.

Conversion of **2.29** to the amide **2.30** was readily achieved using the reagent H_2O_2, conc. NH_3 (aq). Oxidation of nitriles using this reagent has been demonstrated to proceed via a hydroperoxyimine intermediate, which subsequently oxidizes excess H_2O_2 and reduces to the amide with no further reaction to the carboxylic acid (**Scheme 2.10**).

Addition of H_2O_2 (35% by weight) to a stirred mixture of nucleoside **2.29** and NH_4OH resulted in the evolution of O_2. After 2 h of stirring at rt, TLC analysis showed only one

Scheme 2.10 Hydrogen peroxide oxidation of nitrile to amide (Wiberg 1953).

spot, which was shown to correspond to the desired nucleoside product **2.30**. Work up of the reaction mixture was straight forward since the only residues were NH_4OH and H_2O. The very slightly cloudy solution was filtered through celite. The filtrate plus methanol washings were concentrated under reduced pressure and the product dried under high vacuum to yield the amide nucleoside **2.30** as a light solid in 79% yield. TLC and NMR analysis confirmed that the product was of acceptable purity and thus required no further purification.

2.7 Preparation the target pyridine-stretched nucleoside strI 2.33

3-(2-Deoxy-β-D-ribofuranosyl)-8*H*-imidazo[4',5':5,6]pyrido[2,3-*d*]pyrimidin-8-one **2.33** was successfully prepared by ring closure of amide **2.30** **(Scheme 2.11)**. The reaction of was carried out by heating **2.30** with a large excess of sodium ethoxide, prepared from sodium plus ethanol, and ethyl formate. Heating at reflux temperature for 2 h and allowing

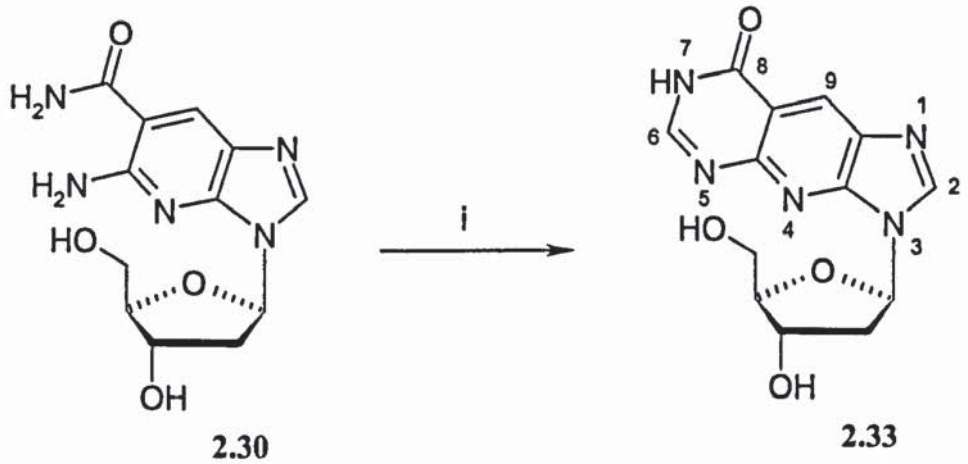

2.30 **2.33**

Scheme 2.11 Preparation of strI. Reagents and conditions, i, HCOOEt, NaOMe, EtOH, 60 °C.

the reaction mixture to stand overnight was concluded by work up, filtration, neutralisation with HCl (aq), and storage overnight at -20 °C. The insoluble material was collected by filtration and washed with water to yield strI (**2.33**) as a light solid in 80% yield. The identity and purity of the target nucleoside strI was confirmed by NMR, TLC and MS.

2.8 Conformational analysis of strI and analogues

Initial attempts to attach the DMT group to strI were unsuccessful using similar conditions that work satisfactorily to derivatise inosine (I) (Matulic-Adamic & Beigelman 2000) and 2',3'-dideoxyinosine (Groebke et al. 1998) (**Figure 2.4**). Even after prolonged treatment of strI with dimethoxytrityl chloride and DIPEA in pyridine, only a trace amount of the desired product was evidenced by TLC analysis. Addition of DMF to the reaction mixture improved the solubility of strI but did not influence the outcome of the reaction. In the benzene-stretched series, dimethoxytritylation of benzene-stretched analogues of 2'-deoxyadenosine (dxA) and 2'-deoxyguanosine (dxG) proceeds smoothly in good yield demonstrating that the presence of tricyclic base is not enough in itself to sterically hinder the primary hydroxyl group at C5' (Liu et al. 2004a; Lui et al. 2005a) (**Figure 2.4**). The possibility that strI, unlike the other nucleoside analogues, could adopt a particular conformation in solution to hamper the dimethoxytritylation reaction, was considered. StrI contains a nitrogen atom, that is part of the central pyridine ring, to which the O5' could possibly form an intramolecular hydrogen bond. To test whether strI might adopt a particular conformation to lessen the reactivity of O5', conformational analysis of inosine, strI and its benzene-stretched analogue was carried out by molecular dynamics simulation. Each nucleoside structure was subjected to CONFLEX™ minimization (Fujitsu

Corporation 2005). Torsion angles encompassing the two rotatable bonds C4'-C5' and the glycosidic C1'-N bond were defined and stepped through –120 to +180 degrees in 20 steps of 15 degrees. The geometry of each defined structure was optimised using MOPAC with PM3 parameters (Stewart 1989) and contour maps constructed by plotting the two torsional angles against energy representing heat of formation (**Figures 2.6, 2.7, 2.8**).

The results presented are those of calculations carried out in the gas phase. However, pyridine as solvent could be taken into account by specifying molecular radius and dielectric constant. In representative calculations where pyridine was specified, no significant conformational differences were observed between the gas phase calculations compared to those mimicking the solution phase used in the actual dimethoxytritylation reaction.

The nucleoside inosine exhibits several low energy conformations, each within 1 kcal mol^{-1} with the lowest exhibiting an anticlinal base orientation in which OH-5' is sterically unhindered (**Figure 2.5**). The difference between the lowest and highest energy conformations is 8.80 kcal mol^{-1}, suggesting a high degree of conformational freedom in this nucleoside structure. The benzene-stretched analogue of inosine (**Figure 2.6**) also exhibits several low energy conformations where, in its anticlinal orientation, the O5' is sterically unhindered. The difference between lowest and highest energy conformations is 7.67 kcal mol^{-1}. This again suggests a conformationally flexible nucleoside structure. Like inosine and its benzene-stretched analogue, strI exhibits several low energy conformations (**Figure 2.7, 2.8**). Even though the lowest energy conformation calculated for strI shows the base orientation to be synclinal with respect to the sugar ring, there is no evidence to support intramolecular hydrogen bond formation between O5' and the pyridine ring

nitrogen atom. The hydroxyl group points away from the area above the plane of the sugar ring occupied by the pyridine-stretched base. Indeed, in the second lowest energy conformation (**Figure 2.8**), which is less than 0.2 kcal mol^{-1} higher in energy, the O5' appears to be completely unhindered sterically. The difference between lowest and highest energy conformations is 9.09 kcal mol^{-1}, suggesting a conformational flexibility similar to inosine and its benzene-stretched analogue. The molecular modeling studies do not provide evidence for a realistic explanation of the reduced reactivity of strI compared to inosine and its benzene-stretched analogue; all three structures are conformationally flexible giving the O5' position accessibility.

Parallel to these modeling studies, more strI starting material was prepared by an improved procedure. Analysis showed this product to be of higher purity that the material used in the initial, failed attempts at dimethoxytritylation. When this fresh batch of strI was used, dimethoxytritylation proceeded smoothly in satisfactory yield. The strI material used in the failed attempts at tritylation was isolated by a work-up procedure involving filtration through celite and then by contact with sand during column chromatography. This could have resulted in unintentional contamination by metal ions, particularly iron, which is known to catalyse detritylation.

The synthesis of the necessary phosphoramidite **2.44**, for use in the automated, solid-supported synthesis of TFOs containing strI (**Chapter 3**) was concluded as shown below. StrI was successfully mono DMT-protected to give derivative **2.43** in 61% yield which was then converted to **2.44** using standard conditions in 79% in crude form after dry column vacuum chromatography. Removal of the H-phosphonate contaminant by repeated (seven

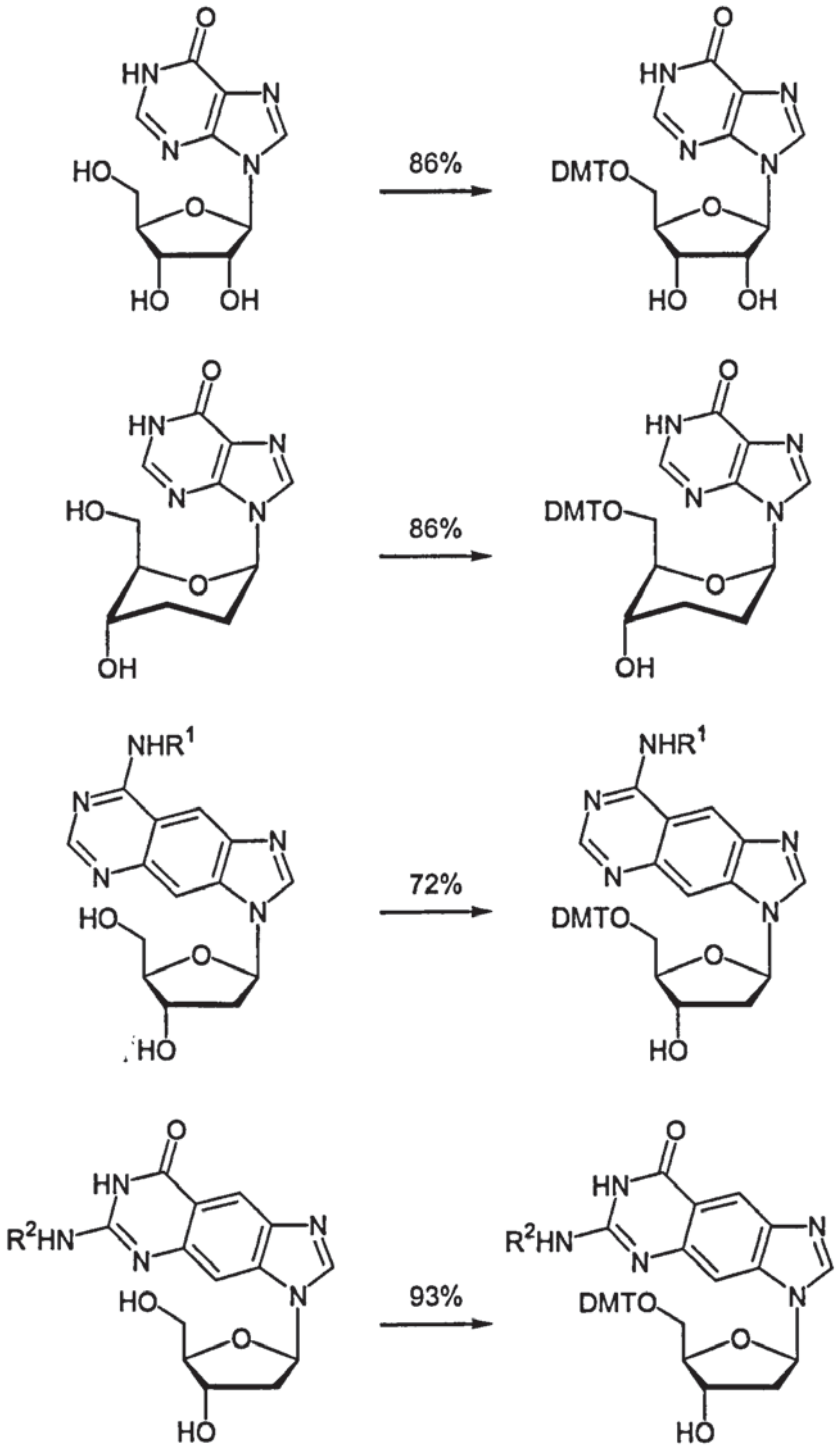

Figure 2.4 Dimethoxyritylation of nucleosides inosine, 2',3'-dideoxyinosine and benzene-stretched analogues of 2'-deoxyadeosine and 2'-deoxyguanosine. R^1 = dimethyl-formamidine, R^2 = isobutyryl.

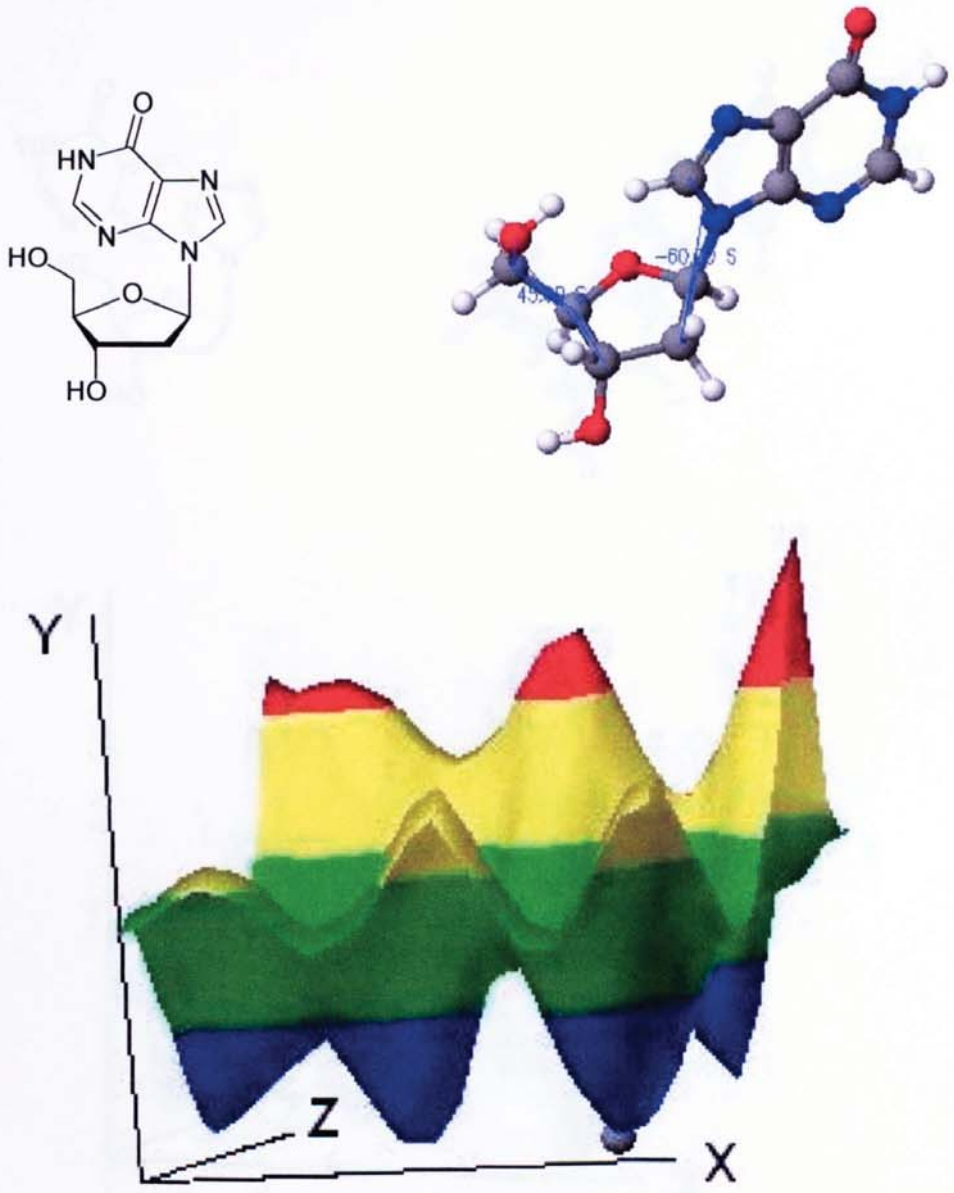

Figure 2.5 Three dimensional contour plot and lowest energy conformation from conformational analysis of inosine. The X-axis represents rotation (-180 to 120°) about the C1'-N bond and the Z-axis represents rotation (-180 to 120°) about the glycosidic C5'-C4' bond. The calculated energy (-118.21 to -109.20 kcal mol^{-1}) for all conformations is given on the Y-axis axis. Blue, yellow and red represent conformations that are lowest, intermediate and highest in energy, respectively. The ball and stick structure represents the conformation at the point indicated by the grey sphere on the contour plot.

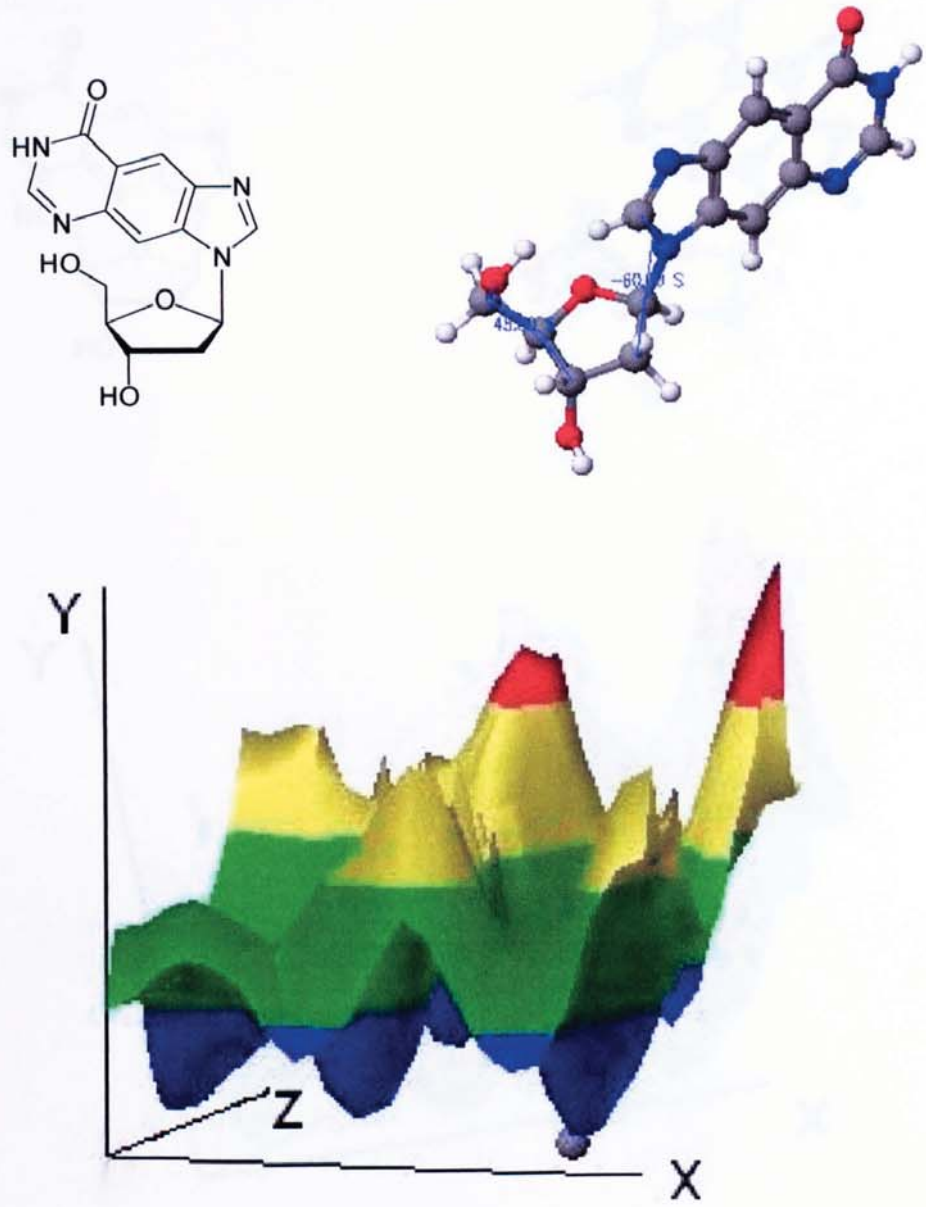

Figure 2.6 Three dimensional contour plot and lowest energy conformation from conformational analysis of bstrI. The X-axis represents rotation (-180 to 120°) about the C1'-N bond and the Z-axis represents rotation (-180 to 120°) about the glycosidic C5'-C4' bond. The calculated energy (-104.46 to -96.89 kcal mol^{-1}) for all conformations is given on the Y-axis axis. Blue, yellow and red represent conformations that are lowest, intermediate and highest in energy, respectively. The ball and stick structure represents the conformation at the point indicated by the grey sphere on the contour plot.

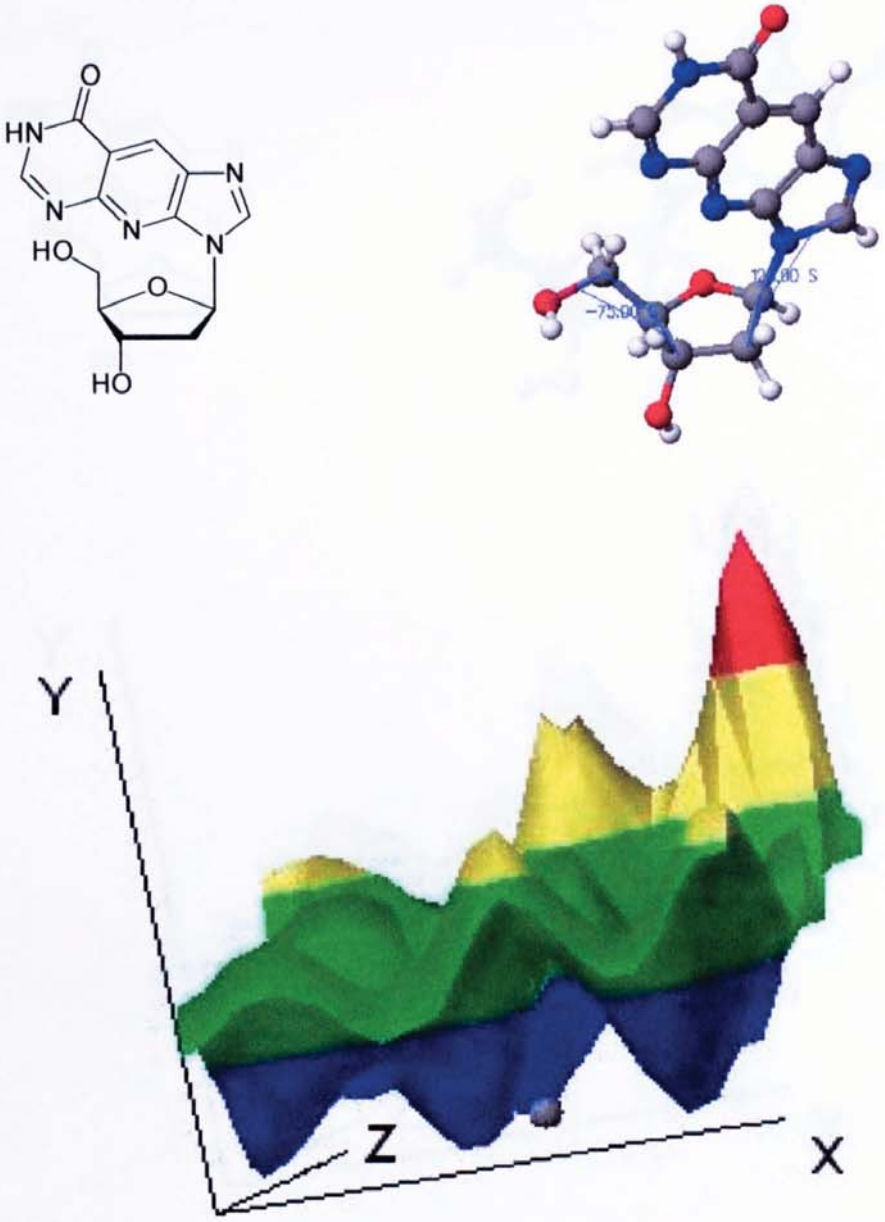

Figure 2.7 Three dimensional contour plot and second lowest energy conformation from conformational analysis of strI. The X-axis represents rotation (-180 to 120°) about the C1'-N bond and the Z-axis represents rotation (-180 to 120°) about the glycosidic C5'-C4' bond. The calculated energy (-95.64 to -85.88 kcal mol^{-1}) for all conformations is given on the Y-axis axis. Blue, yellow and red represent conformations that are lowest, intermediate and highest in energy, respectively. The ball and stick structure represents the conformation at the point indicated by the grey sphere on the contour plot.

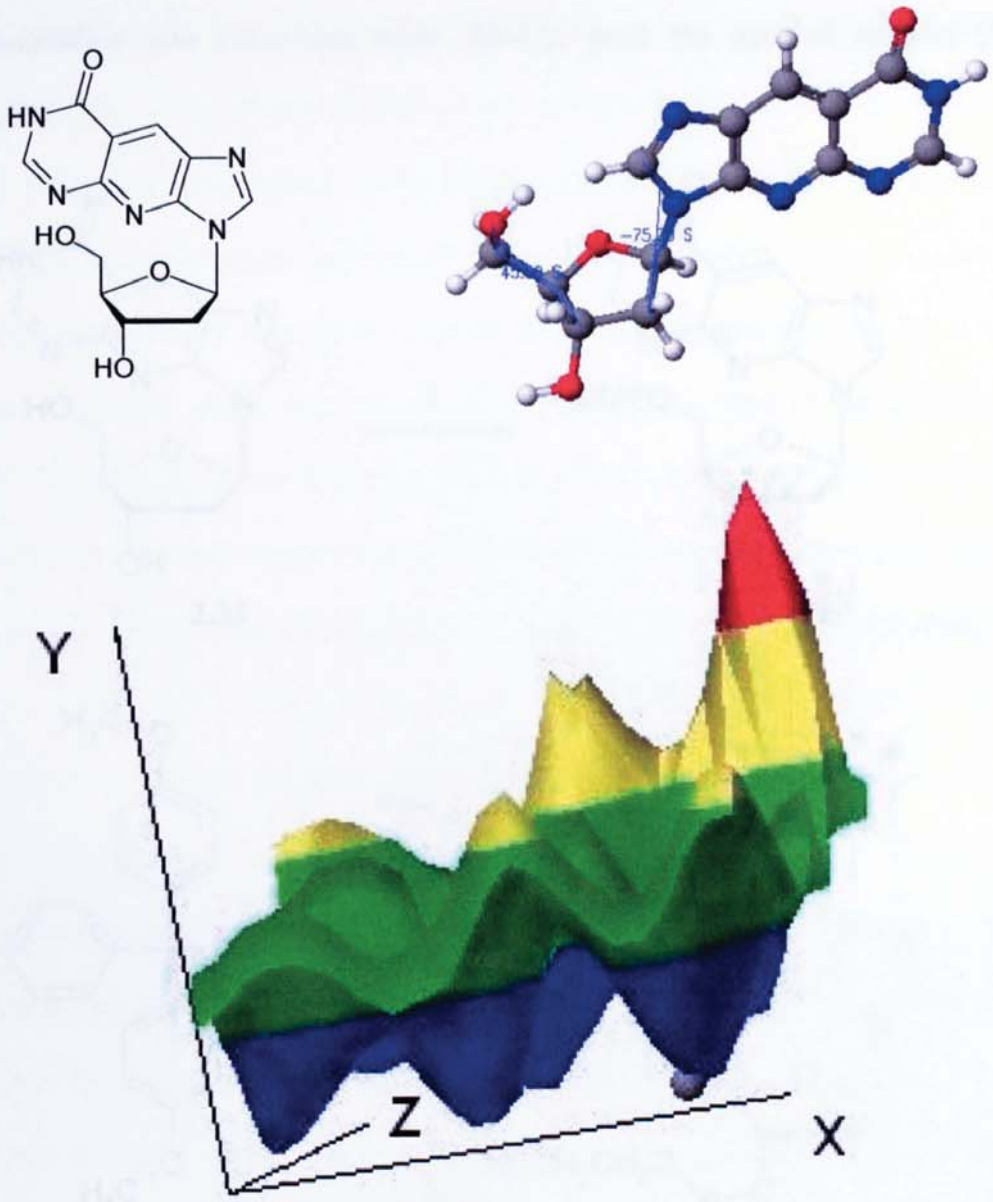

Figure 2.8 Three dimensional contour plot and lowest energy conformation from conformational analysis of strI. The X-axis represents rotation (-180 to 120°) about the C1'-N bond and the Z-axis represents rotation (-180 to 120°) about the glycosidic C5'-C4' bond. The calculated energy (-95.64 to -85.88 kcal mol^{-1}) for all conformations is given on the Y-axis axis. Blue, yellow and red represent conformations that are lowest, intermediate and highest in energy, respectively. The ball and stick structure represents the conformation at the point indicated by the grey sphere on the contour plot.

times) precipitation into petroleum ether (60-80), gave the purified product (50%) (**Scheme 2.12**).

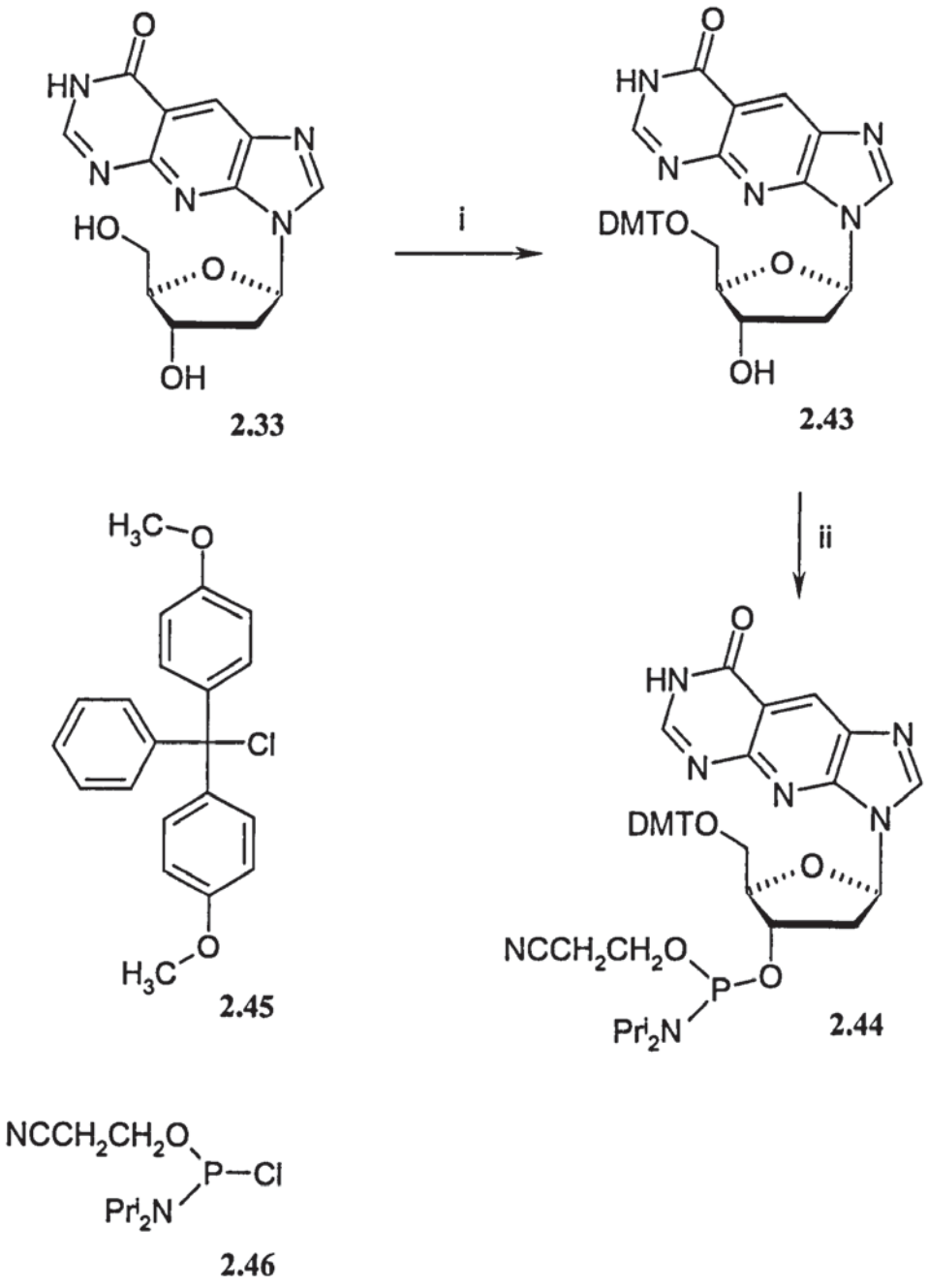

Scheme 2.12 Preparation of strI phosphoramidite. Reaction conditions, i; **2.45** (DMTCl), pyridine, DIPEA, rt; ii, **2.46**, DIPEA, rt.

2.9 Preparation of 5'-*O*-(4,4'-dimethoxytrityl)-3-(2-deoxy-β-D-ribofuranosyl)-8*H*-imidazo[4',5':5,6]pyrido[2,3-*d*]pyrimidin-8-one 2.43

The DMT group was the chosen as the protecting group for the primary alcohol of a nucleoside prior to solid phase synthesis because of its selectivity, ease of preparation, stability and compatibility to reagents used in solid phase synthesis (SPS). It is readily cleaved following SPS under mild conditions. In many cases DMTCl reacts readily and efficiently with the primary alcohol in dry pyridine. The addition of DIPEA or DMAP is generally effective for less reactive primary alcohols. Ammonium perchlorate has been demonstrated to be effective for relatively unreactive primary alcohols (Groebke et al. 1998).

With a limited amount of strI **2.33** available the initial attempts to prepare the DMT derivative of strI was carried out on a small scale and monitored by TLC. No significant reaction was detected in pyridine even following the addition of an excess of DMTCl. The reaction was repeated with the addition of DIPEA, but again no reaction was indicated by TLC analysis. The reaction mixture was stirred overnight following the addition of DMAP. TLC analysis indicated only starting materials. Ammonium perchlorate was then added with continued stirring. Again analysis indicated no significant reaction and only starting materials was recovered. It was thought that the failure of strI to react with DMTCl might be due to its insolubility in pyridine. Imidazolium mesylate and DIPEA in DMF has been reported to be an efficient reagent for the preparation of the DMT derivatives of nucleosides. This procedure was attempted but gave no significant reaction.

The possibility that strI might adopt a conformation that would sterically hinder the reaction with DMTCl was discounted following conformational analyses (**Section 2.8**).

The possible contamination of the strI with metal ions which could inhibit the reaction, was considered. A scaled up synthesis of strI was followed through and efforts were made to ensure that there was no metal ion contamination. All filter aid (celite) and sand used in chromatography columns was acid washed prior to use. For the preparation of the DMT derivatives of benzene expanded DNA analogues Liu et al. (2005a) used a large excess of DMTCl and DIPEA in pyridine. These conditions were followed using the new batch of metal ion free strI . Unlike previously the strI **2.33** dissolved after stirring for 1 h to give a clear solution. TLC analysis indicated negligible strI with three fluorescent spots of higher R_f. The compound with the lowest R_f being the most intense. It was noted that on initial treatment of the TLC plate with vanillin reagent, the fluorescent spots and excess DMTCl all stained orange. However, following heating the plate, the DMTCl remained orange and the fluorescent compound turned brown. This was taken as an indication that all the fluorescent spots contained the DMT group since strI its self only stains brown on heating with the reagent. Following quenching the reaction solution with methanol and evaporation under vacuum, TLC analysis only showed the two lower fluorescent spots, the compound of highest R_f having disappeared.

Separation and purification of the reaction product by dry column vacuum chromatography gave the desired DMT derivative of strI **2.43** in over 60% yield, a very minor fraction of strI **2.33** and a further fraction, which was characterised as the di-DMT derivative from ^{1}H NMR and accurate mass determination. The fluorescent compound of high R_f that was detected initially and decomposed during workup was thought to be a tri-DMT derivative; the N8 to DMT bond being cleaved following treatment with methanol to give di-DMT-

strI. NMR and MS analysis was consistent with DMT-strI **2.43** and indicated high purity **(Scheme 2.12)**.

2.10 Preparation of 5'-*O*-(4.4'-Dimethoxytrityl)-3-(2-deoxy-β-D-ribofuranosyl)-8*H*-imidazo[4',5':5,6]pyrido[2,3-*d*]pyrimidin-8-one 3'-*O*-(2-cyanoethyl)-*N,N*-diisopropyl)-phosphoramidite 2.44.

With the successful preparation of DMT-strI **2.43** the synthesis of the target phosphoramidite **2.44** required for the solid phase synthesis of the planned oligonucleotides was achieved by reaction with 2-cyanoethyl-*N,N*-diisopropylchlorophosphoramidite **2.46** under standard conditions i.e. dry THF in the presence of DIPEA at rt, TLC analysis indicated the reaction was complete after 3 h and only one product was detected. Workup and purification by dry column vacuum chromatography gave the target DMT-strI phosphoramidite **2.44**. Phosphorus NMR gave the expected downfield doublet for the phosphoramidite diasteroisomers and a doublet due to H-phosphonate contamination. The H-phosphonate was removed by repeated precipitation from DCM by the addition to petroleum ether. The purified phosphoramidite **2.44** was isolated as a white powder in 50% yield. NMR and MS analysis confirmed the structural assignment and purity **(Scheme 2.12)**.

The phosphoramidite was subsequently used to prepare the selected oligonucleotides via solid phase synthesis **(Chapter 4)**.

2.11 Possible alternative synthetic routes to key intermediates equivalent to 5-Amino-4-(2,2-dicyanovinyl)-1-(2'-deoxy-3',5'-di-*O*-*p*-toluoyl-β-D-ribofuranosyl)-imidazole 2.28 and 5-Amino-6-cyano-3-(2'-deoxy-β-D-ribofuranosyl)-imidazo[4,5-*b*]pyridine 2.29.

The previous work has demonstrated the potential of developing a relatively high yielding multi-stage synthesis from readily available starting materials to give the target family of PSNs (Clayton et al. 2002). The synthesis of the chlorosugar **2.16** from 2-deoxy-D-ribose is efficient and capable of yielding a high quality product provided the reaction and storage conditions are strictly adhered to (**Scheme 2.3**). While the outcome of the glycosylation reaction shown in **Scheme 2.7** is heavily dependent upon reaction conditions and the quality of reagents, the work to date has shown that the required 5 β-nitroimidazole isomer **2.22** can be prepared in acceptable yields and in gram quantities. Although 4-unsubstituted-5-aminoimidazoles are unstable on storage and rapidly degrade on exposure to air, NMR analysis has demonstrated that the initial catalytic hydrogenation of the 5-nitroimidazole **2.22** is highly selective and gives the 5-aminoimidazole **2.40** in high yields with no significant by-products. However, the reaction with EMMN **2.41** to produce the key intermediate **2.28** has proved to be problematic giving consistently low yields of around 30%, at best 37%. The subsequent reactions involving cyclisation, deprotection and ring formation to yield the target PSBs have been shown to be high, to near quantitative in yield. A yield of 30% for an individual step is acceptable initially in a multi-stage synthesis to produce a limited quantity of a specific compound for evaluation purposes. However, with the aim of developing an efficient, practical and versatile multi-stage synthesis to key intermediates capable of making a variety of PSNs readily accessible, possible alternative

routes compatible with the current work to **2.28** or an equivalent are necessary and they have been investigated (**Scheme 2.13**).

The presence of a nitro group activates aromatic ring systems to nucleophilic attack and in the case of 4(5)-nitroimidazoles, the carbon β to the nitro group is susceptible (**Scheme 2.14**). The hydride ion itself is a poor leaving group in aromatic nucleophilic substitution and is not directly displaced. However, if a suitable leaving group is incorporated in the attacking nucleophile the effective displacement of hydrogen from an aromatic ring can be realised and this is termed Vicarious Nucleophilic Substitution (VNS) according to Makosza (Makosza 1997; Makosza & Owczarczyk 1989). Through this mechanism it has been shown that the unsubstituted β carbon of 4(5)-nitroimidazoles can be efficiently functionalised with a dichloromethyl group using the trichloromethyl cation generated *in situ* from chloroform and strong base at low temperature. The reaction of the trichloromethyl cation with aromatic nitro compounds was originally proposed to proceed through a carbene intermediate but has since been demonstrated to proceed through the classic VNS mechanism (Crozet et al. 2002; Makosza & Owczarczyk 1989; M^{c}Bee et al. 1971) (**Scheme 2.15**).

With substitution at the carbon β to the nitro group, the aminoimidazole product from the subsequent reduction of the nitro group would be expected to be stable, as is **2.28**, and other 5(4)-C-substituted 4(5)-aminoimidazoles.

The VNS reaction requires the initial blocking of the acidic imidazole nitrogen. For the preliminary investigations the 1-benzyl derivative was chosen as it is known to be relatively stable under the various reaction conditions but labile under hydrogenolysis, the

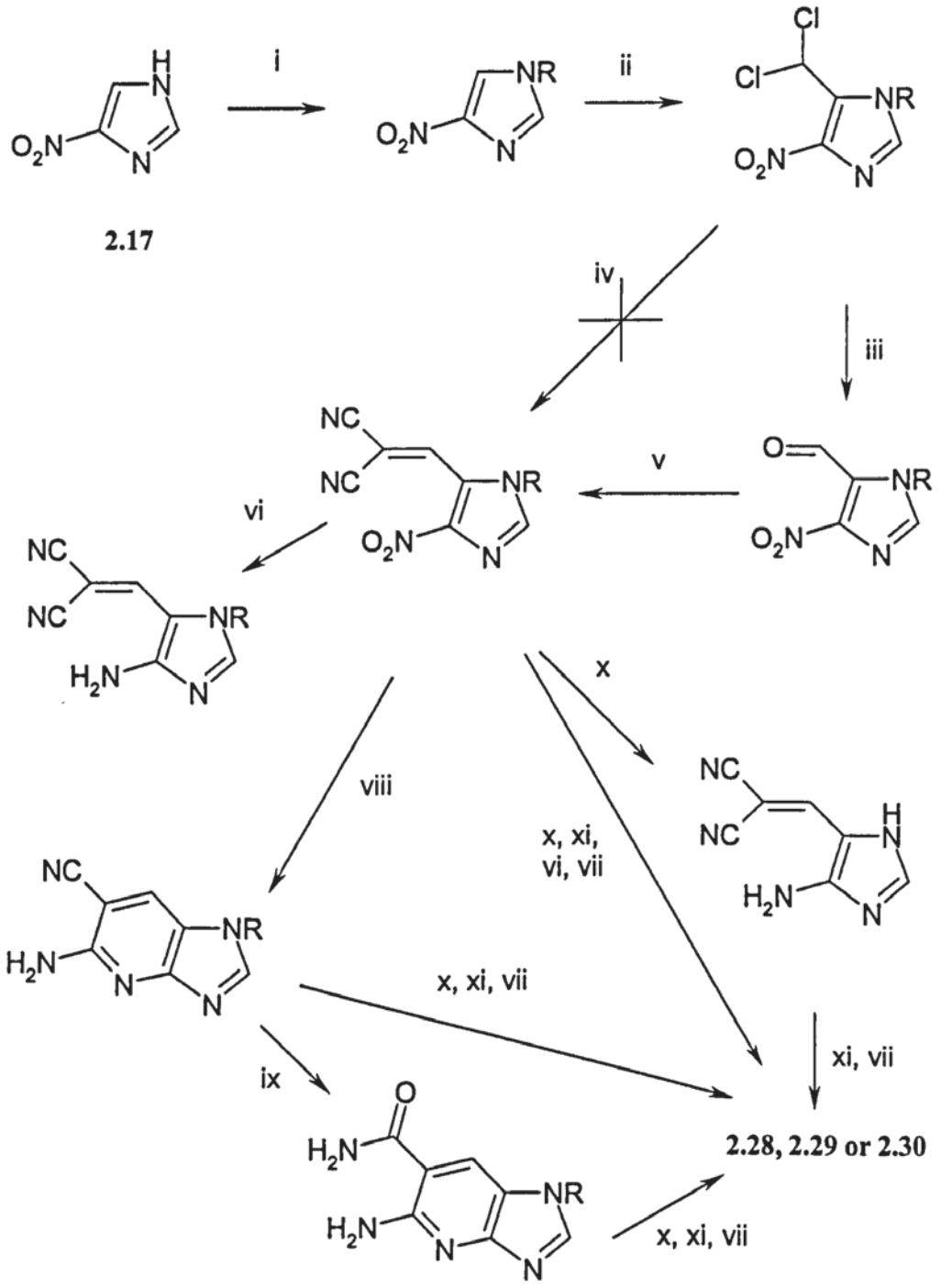

Scheme 2.13 Potential alternative routes to targeted key intermediates, i, alkyl halide/base, R= e.g. $PhCH_2$; ii, VNS, CCl_3^- ; iii, formic acid, heat; iv, malononitrile, heat; v, Knoevenagel reaction, malononitrile; vi, reduction; vii, base; viii, reduction under basic conditions; ix, H_2O_2, conc. NH_3 (aq); x, deprotection; xi, glycosylation with **2.16**.

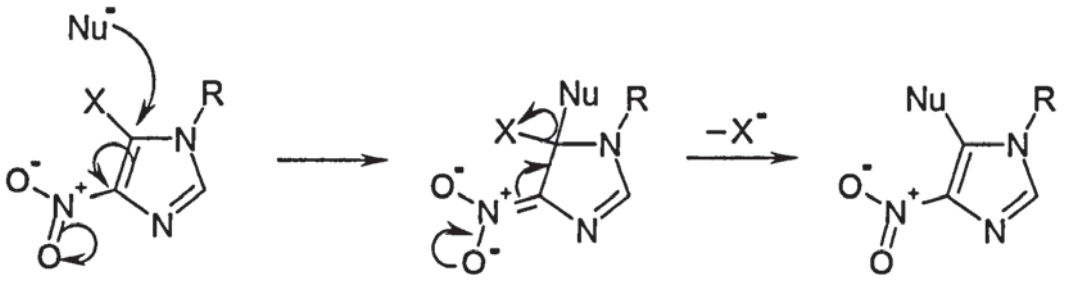

Scheme 2.14 Nucleophilic substitution of 4-nitroimidazoles.

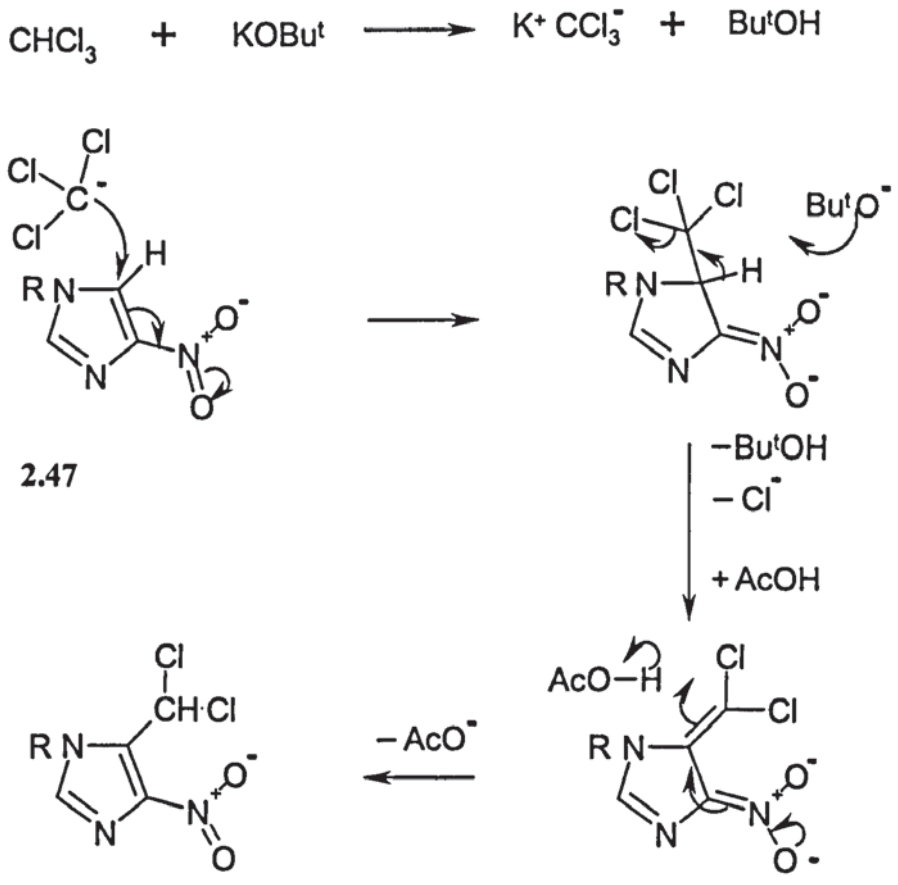

Scheme 2.15 Mechanism for the dichloromethylation of **2.47.**

deprotection conditions. The *p*-methoxybenzyl derivative has been also been reported in the literature (Siddiqui et al. 1999). One report in particular (Chen et al. 2002) suggested that the 1-protected-5-nitroimidazole is the major product when nitroimidazole **2.17** is reacted with benzyl chloride and K_2CO_3 in DMF. The report was compared to a second article where benzyl bromide and $KOBu^t$ in DMSO were used as the alternative conditions but which suggested that the 1-protected-4-nitroimidazole were the products formed in high yields (Ostrowski 1999). From the previous work it was decided to employ the pre-formed 4(5)-nitroimidazole potassium salt **2.51** and benzyl bromide in THF, DMF and DMSO (**Scheme 2.16**). With the exception of using THF as a solvent, where no significant reaction was detected; TLC analysis of all the other reactions indicated the same major product and one minor component. Following a standard work up procedure i.e. adding water,

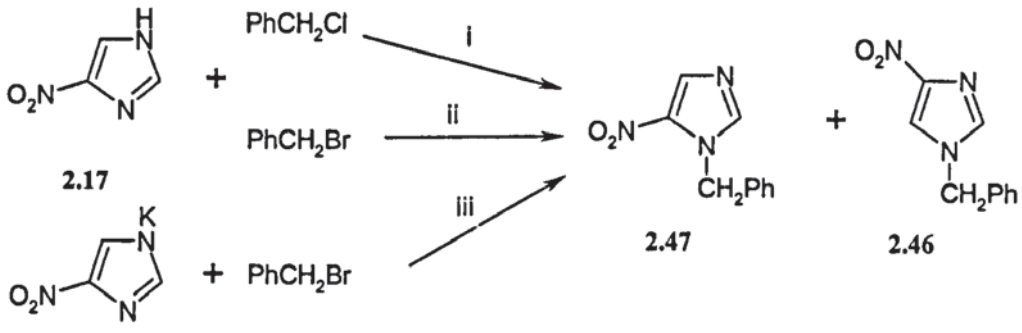

Scheme 2.16 Preparation of 1 N benzyl protected nitroimidazole. Reagents and conditions, i, K_2CO_3, DMF, 4 h, 70 °C; ii, $KOBu^t$, DMSO, 12h, rt; iii, 4(5)-nitroimidazole potassium salt, DMF or DMSO, rt, 1 h.

extracting with $CHCl_3$ followed by aqueous washing, then drying with anhydrous $MgSO_4$ and evaporation under vacuum, ^1H NMR analysis indicated one major product with 5-10% of an isomeric minor compound. Separation was readily achieved by the addition of ether and cooling to -20 °C to give the main product as a crystalline solid. Evaporation of the ether filtrate gave a yellow residue which slowly solidified under vacuum. ^1H NMR analysis indicated that this residue consisted of up to 57% of the minor isomeric product. While the yield in using a simple ether tituration for purification was 73%, a further crop could be readily obtained by flash chromatography of the ether residues. ^{13}C NMR of the major purified product confirmed that it was the 1-benzyl-4-nitroimidazole **2.46** product and not the 5 isomer **2.47.** Use of the 1-benzyl-4-nitroimidazole **2.46** derivative could be beneficial as 4-aminoimidazoles have been demonstrated to be inherently more stable than their 5-amino isomers.

Subsequent, effective nucleophilic substitution of hydrogen, due to the activating effect of the nitro group, efficiently functionalised the position beta to the nitro group with a dichloromethyl group (**Scheme 2.15**).

Conversion of the dichloromethyl group produced the corresponding aldehyde intermediate capable of undergoing a wide range of transformations. Direct reaction of the dichloromethyl derivative with malononitrile failed to give the desired 5-dicyanomethylene-4-nitroimidazole intermediate. However, the aldehyde readily reacted with malononitrile, via a Knoevenagel condensation, to give the desired 5-dicyanomethylene-4-nitroimidazole intermediate in 55% yield (**Scheme 2.13**). Suggested

conditions for completion of the planned pathway to the target compounds **2.28**, **2.29** and **2.30** *via* this 5-dicyanomethylene-4-nitroimidazole intermediate, are given in **Scheme 2.13**.

Chapter 3

Solid Phase Synthesis (SPS) of Pyridine-Stretched Oligonucleosides (PSOs)

3.1 Background to solid phase synthesis (SPS)

The first published account of the synthesis of a dinucleotide was of a thymidine dimer by Michelson and Todd (1955) using solution chemistry. In the late 1950s, Khorana developed the phosphodiester method, which became the template for subsequent synthetic procedures (**Scheme 3.1**) (Khorana 1968). The phosphodiester method proved to be compatible with solid support chemistry developed by Merrifield (1963) for the synthesis of proteins. In 1975, Letsinger was able to construct simple di- and trinucleotides using solid support chemistry (Lestinger et al. 1975). Letsinger had modified the procedure to utilise a phosphitetriester (phosphotriester) intermediate which improved selectivity and versatility as well as being significantly faster than the phosphodiester method (**Scheme 3.1**). This scheme formed the basis of operation of the first automated DNA synthesizers, which were introduced by Vega Biotechnologies and Biosearch in the 1970s (Willis 2004). Due to the inherent drawbacks of small scale solution chemistry that include the need for regular separation, isolation, extraction, and purification procedures, loss on transfer, continuous analysis, accumulation of residues from reagents, and the difficulty of ensuring standard and reproducible conditions over variable-scale reactions, these multi-stage

Scheme 3.1 The early phosphodiester (DCC dicyclohexylcarbodiimide) and phosphite-triester methods of dinucleotide synthesis (Simmonds 1992).

reactions would be impracticable without the development of automated solid phase synthesis. Even with manual solid support chemistry, the synthesis of short oligonucleotides is tedious, problematic and severely limited due to air and water sensitivity of the reagents and the need for strictly controlled, standardized reaction conditions to ensure maximum yield at every stage.

With so many reaction cycles required to construct an oligonucleotide sequence of even

Table 3.1 Correlation between coupling efficiency per cycle, length of oligonucleotide synthesized, and overall yield (Brown & Brown 1991).

Oligonucleotide length	Coupling efficiency				
	90%	95%	97%	98.5%	99.5%
10mer	*38.7*	*63.0*	*76.0*	*87.3*	*95.6*
20mer	*13.5*	*37.7*	*56.1*	*75.0*	*90.9*
50mer	–	*8.10*	*22.5*	*47.7*	*78.2*
100mer	–	–	*4.90*	*22.4*	*60.88*
150mer	–	–	*1.07*	*10.52*	*47.38*
200mer	–	–	–	*4.94*	*36.9*

moderate length, maximising the yield per cycle is essential. Any reduction in cycle efficiency results in a near exponential reduction in overall yield in relation to the length of the target oligonucleoside. With this comes the problem of subsequent purification as any residual contamination from n-1 sequences, for example, would yield a difficult-to-separate-combination of many, very similar analogues. One can only wonder at the overall efficiency of the natural enzymatic replication of DNA. This is best demonstrated by the correlation of coupling efficiency and actual overall yield to the length of the oligonucleotide (**Table 3.1**).

The final refinements to the general automated synthesis procedure that is used today for oligodeoxyribonucleotides, and more recently oligoribonucleotides (Gait et al. 1991), were introduced by Caruthers, a former student of Letsinger. Caruthers's modifications included replacing the chloride leaving group in the phosphite-triester by an amine to give a phosphoramidite (Beaucage & Caruthers 1981; Matteuci & Caruthers 1981). This modification dramatically increases shelf-life, allowing researchers to prepare these

materials well in advance or for them to be supplied commercially as solids or as ready-to-use stock solutions (Glen Research 2006; Link Technologies 2005).

Caruthers collaborated with Hood to develop the first automated DNA synthesizer using this new technology, which was introduced in 1983 (Atkinson & Smith 1984). Currently, there are several companies specializing in the automated synthesizer market, and there is a constant effort to find ways to increase reaction yields and introduce new chemical modifications (Beaucage & Iyer 1992; 1993a-c) with potential applications for use not only as therapeutics, diagnostics, and high-throughput screening, but also within the field of nanotechnology and molecular computers. A combination of advances in material, valve and computer technology, and further refining of the necessary chemistry, has enabled these instruments to become a not uncommon piece of laboratory equipment.

Several companies now supply custom made oligonucleotides to order (Glen Research 2006). With these developments in automated solid phase synthesis of oligonucleotides, and the commercial availability of reagents of consistent/guaranteed quality, the incorporation of synthetic nucleoside analogues into designed oligonucleotide sequences is entirely feasible and practical. If a targeted and suitably protected nucleoside phosphoramidite derivative can be prepared, it should be possible to incorporate it into an oligonucleotide with known and specified sequence.

3.2 Automated solid phase oligonucleotide synthesis using phosphoramidites

Many solid support materials have been used for DNA synthesis over the years including; Sephadex, silica gel, polydimethylacylamide, polyacrylmorpholide, Kieselguhr-polydimethylacrylamide composites, cellulose, borosilicate glass beads of controlled pore

size (CPG), a Teflon© laminated membrane system (MemSyn™), various polystyrene resins, and also gels based on derivatised Porex® X-4920 (Devivar et al. 1999). The generally preferred solid support for synthesis of small batches of oligonucleotide products is borosilicate glass in the form of controlled pore glass beads (CPG). CPG has the benefits of high mechanical strength, insolubility and chemical inertness, and is available commercially with certificates of analysis covering the actual loading and performance under standard conditions. CPG can be purchased ready functionalized with terminal aminopropyl groups.

Reaction of CPG with a suitable deoxyribonucleoside-3'-succinate ester, such as the 4-nitro-phenyl, gives succinyl amide linkages. The use of such spacer groups is required to ensure efficient access by the various reagents and washes used. Removal, following synthesis of the target oligonucleotide, is readily achieved by hydrolysis. This procedure requires the preparation of the succinyl or similar derivative of the required 3' terminal nucleotide of the target oligonuclotide and attachment of this to the solid support (Pon & Yu 1997; Pon et al. 1988; Walsh et al. 1997). More recently solid supports with universal linkers have been developed and are commercially available (Glen Research 2006; Link Technologies 2005). These traceless universal supports are functionalized so that the intended terminal 3' oligonucleotide, as the relevant phosphoramidite, can be directly and efficiently attached to the solid support using standard synthesizer protocols (Azhayev & Antopolsky 2001).

Prior to the coupling of the nucleoside or analogue with the solid support, the 5' hydroxyl group requires suitable protection, with the dimethoxyltrityl group (DMT) being the one of choice due to its general ease of preparation, selectivity for the primary hydroxyl group,

stability under the reaction conditions and its ease of removal (Atkinson & Smith 1984). The secondary 3' hydroxyl group is then converted to the 2-cyanoethyl-*N,N*-diisopropyl)-phosphoramidite (Brown & Brown 1991). If there are any primary amino groups in the base of the nucleoside or synthetic analogue, then these also require protection. In the case of the natural DNA, RNA and a growing number of base- and sugar-modified nucleoside analogues, the required phosphoramidites are commercially available in suitably protected form (Glen Research 2006).

Traditionally, the protecting groups of choice, because of their proven compatibility with the reaction sequences and their ease of removal, are benzoyl in both deoxyadenosine (benzoyl dA) and deoxycytosine (benzoyl dC), and isobutyryl for deoxyguanosine

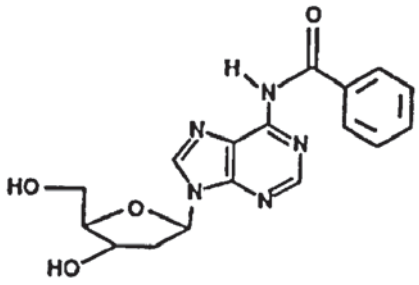

benzoyl dA

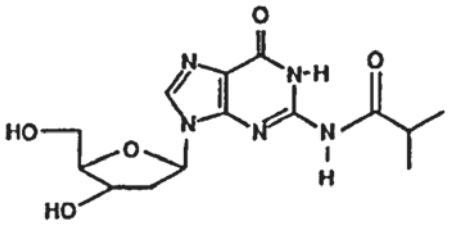

Isobutyryl dG

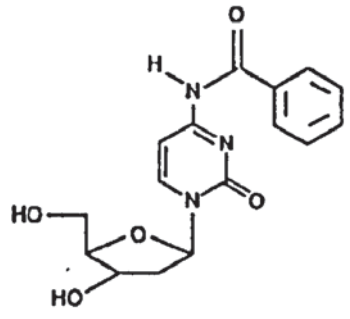

benzoyl dC

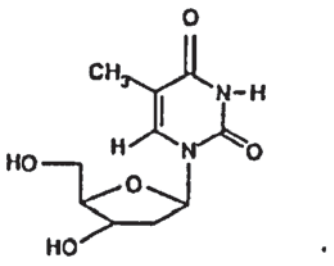

Unprotected T

(isobutyryl dG). Deoxythymidine is sufficiently unreactive and therefore does not need protecting. Although these protecting groups are still used, there have been many developments in the use of alternatives to improve cleavage and deprotection under milder conditions, compatible with oligonucleotide conjugates of other compounds (Devivar et al. 1999). Automated solid phase synthesis using phosphoramidites is shown in **Scheme 3.2.** Detritylation of the 5' OH group of the nucleoside attached to the solid support is followed by tetrazole-catalysed coupling to the desired phosphoramidite to form an internucleotide phosphitetriester bond.

Tetrazole acts as a weak acid and nucleophile to form a reactive tetrazolide intermediate of the nucleoside phosphoramidite. Tetrazole may be replaced by derivatives such as 5-ethylthio-1*H*-tetrazole (ETT). It is important that this step and all of the others are as high yielding as possible. Yields should be 99% or higher although slightly lower yields may be acceptable for short oligonucleotides (**Table 3.1**). Any 5' OH groups that fail to couple with the phosphoramidite are capped by acylation using acetic anhydride, to prevent build up of shorter, n-1 sequences (Fearon et al. 1997). The phosphitetriester group is then oxidized under mild conditions to phosphotriester. The cycle is repeated until the required length of oligonucleotide sequence has been synthesized. The oligonucleotide product is then cleaved from the solid support and the base-labile protecting groups are then removed by treatment with aqueous ammonia at elevated temperature, usually overnight. The oligonucleotide product is then analysed, purified, quantified and de-salted if necessary, ready for subsequent studies.

Scheme 3.2 Automated solid phase synthesis (SPS) using phosphoramidites. Reagents, detritylate (3% CCl_3CO_2H, CH_2Cl_2; couple (0.25 M 5-ethylthio-1*H*-tetrazole, CH_3CN); cap (acetic anhydride, 10% methylimidazole, 2,6-lutidine, THF); oxidize (0.02 M iodine, pyridine, THF, H_2O); deprotect/cleave (conc. NH_3 (aq), 55 °C, 16 h) (Walsh 1999).

3.3 Oligonucleotide purification and analysis

There is a variety of methods for the purification of oligonucleotides from automated synthesis of which reversed phase (RP) or anion exchange high pressure liquid chromatographic (HPLC) methods provide useful amounts of material of very high purity (Brotschi et al. 2005). RP-HPLC was the method of choice in this project work as the equipment was readily available and standard protocols had been established for this type of analysis (Herold & Hummel 1991).

3.4 Solid phase synthesis of inosine and pyridine-stretched inosine oligonucleotides

The target sequences identified for the thesis work are listed in **Table 3.2.** Sequences **S1** to **S16** were prepared (1 μM scale) by automated solid phase synthesis following the standard procedure (Beckmann 1994). The dA, dC, dG, dT and dI phosphoramidites were commercially available (Link Technologies 2005) and the strI phosphoramidite was obtained by chemical synthesis as described in the preceding chapter. Acceptable coupling efficiencies were achieved by observing the orange colour of the dimethoxytrityl cation produced during each detritylation step. Synthesis was performed in the "trityl-off" mode. Synthesised sequences were cleaved and deprotected using concentrated aqueous ammonia giving the products for purification by semi-preparative RP-HPLC (Pingoud et al. 1989).

3.5 Reversed phase HPLC analysis of oligonucleotide products

G-rich oligonucleotides in particular are known to form a series of hairpin and partially paired hyperstructures with differing partitioning properties, and therefore varying retention times (Brotschi et al. 2005). In order to eliminate or reduce hyperstructure formation as far as possible, all analyses and semi-preparative purification runs were performed at 80 °C (Herold & Hummel 1994). Oligonucleotide sequences were analysed using UV detection at 260 nm and purified at 285 nm using solvent system A with 0-25% solvent system B during 20 min. Solvent system A was composed of 0.1 M aqueous triethylammonium acetate (TEAA, 10%) and CH_3CN (2%) at pH 7.0, and solvent system B was composed of 0.1 M aqueous TEAA (10%) and CH_3CN (80%) at pH 7.0. A mobile phase flow rate = 1 ml min^{-1} was used throughout.

Table 3.2 Oligonucleotide sequences **S1** to **S16** prepared by the phosphoramidite method and purified by RP-HPLC.

Sequence		t_R (min)	ε at $A_{260\,nm}$	Mass
5'-ATAATATTAT	**S1**	12.60	108,900	3023.5597
5'-GCGGCGCCGC	**S2**	10.63	85,500	3028.5362
5'-AIAAIAIIAI	**S3**	12.23	121,950	3328.5927
5'-ICIICICCIC	**S4**	12.02	85,500	3208.5362
5'-AIAAIAIIAI	**S5**	11.26	104,130	3193.5382
5'-ICIICICCIC	**S6**	9.72	67,680	3073.4817
5'-AAAAGAAAAGGGGGGA	**S7**	12.12	198,450	5058.9269
5'-AAAAGAACAGGGGGGA	**S8**	12.64	191,160	5034.9156
5'-TCCCCCCTTTTCTTTT	**S9**	11.75	115,920	4682.7786
5'-TCCCCCCTITTCTTTT	**S10**	12.23	147,600	5038.8282
5'-TCCCCCCTITTCTTTT	**S11**	11.85	116,361	4716.7739
5'-AGGGGGGAAAAGAAAA	**S12**	12.12	198,450	5058.9269
5'-AGGGGGGAIAAGAAAA	**S13**	12.06	195,120	5110.9218
5'-AGGGGGGAIAAGAAAA	**S14**	12.05	119,556	5086.9109
5'-AGGGGGGAAIAGAAAA	**S15**	12.04	195,120	5110.9218
5'-AGGGGGGAAIAGAAAA	**S16**	12.06	119,556	5086.9109

3.6 HPLC chromatographs

The HPLC profiles of three representative oligonucleotide sequences are shown in **Figures 3.2, 3.3** and **3.4.** The first sequence contains just the DNA bases A and G, the second contains a single strI substitution, and the third a single I substitution. The analytical run of each crude oligonucleotide sequence shows that, typically, more than one product is present; the major product being the desired target sequence together with minor impurities (upper traces). During the semi-preparative purification runs, the chromatography column is deliberately overloaded and the major fraction collected, which contains the target sequence (middle traces). The purity of the target sequence is then confirmed by a final analytical run (lower traces).

3.7 Desalting and quantification of oligonucleotide products

The purified oligonucleotide sequences were desalted (to remove the mobile phase TEAA buffer salts) by short column reversed phase chromatography, then stock solutions of purified, desalted oligonucleotides were quantified for UV thermal melting studies (Greig et al. 1996). To calculate the oligonucleotide concentrations used in the UV studies, the extinction coefficients for I (7,740) and strI (11,600) at 260 nm were measured accurately. The extinction coefficients of the DNA bases A (15,400), C (7,300), G (11,700) and T (8,800) are given in the literature (Barawakar et al. 1996).

With the necessary oligonucleotide products in hand, evaluation of their duplex and triplex forming properties was undertaken. The results of these studies are detailed in the following chapter.

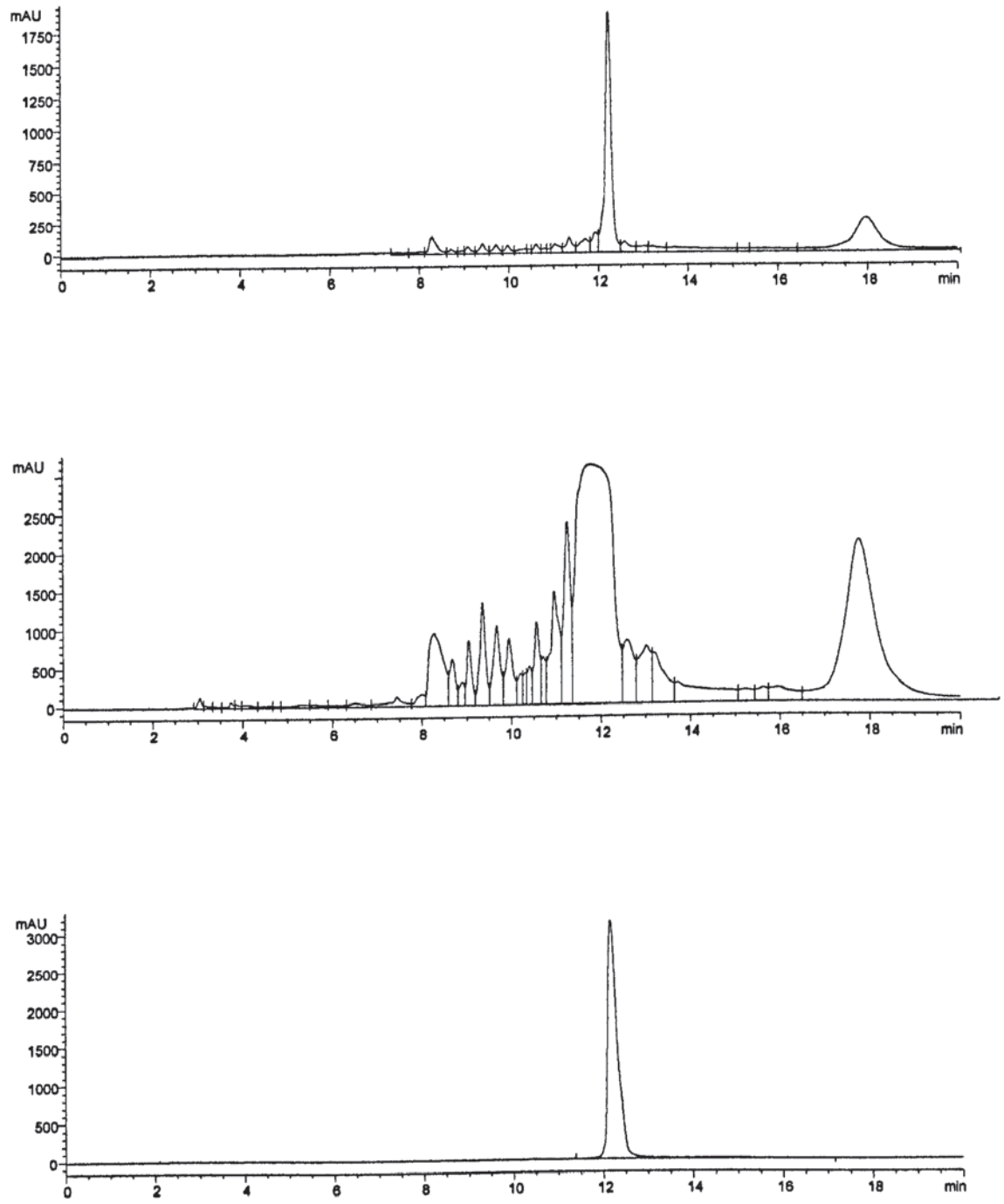

Figure 3.2 HPLC profiles of oligonucleotide 5'-AAAAGAAAAGGGGGGA (**S7**), analytical run of the crude sequence (upper trace), semi-preparative purification run (middle trace) and analytical run of the purified sequence (lower trace).

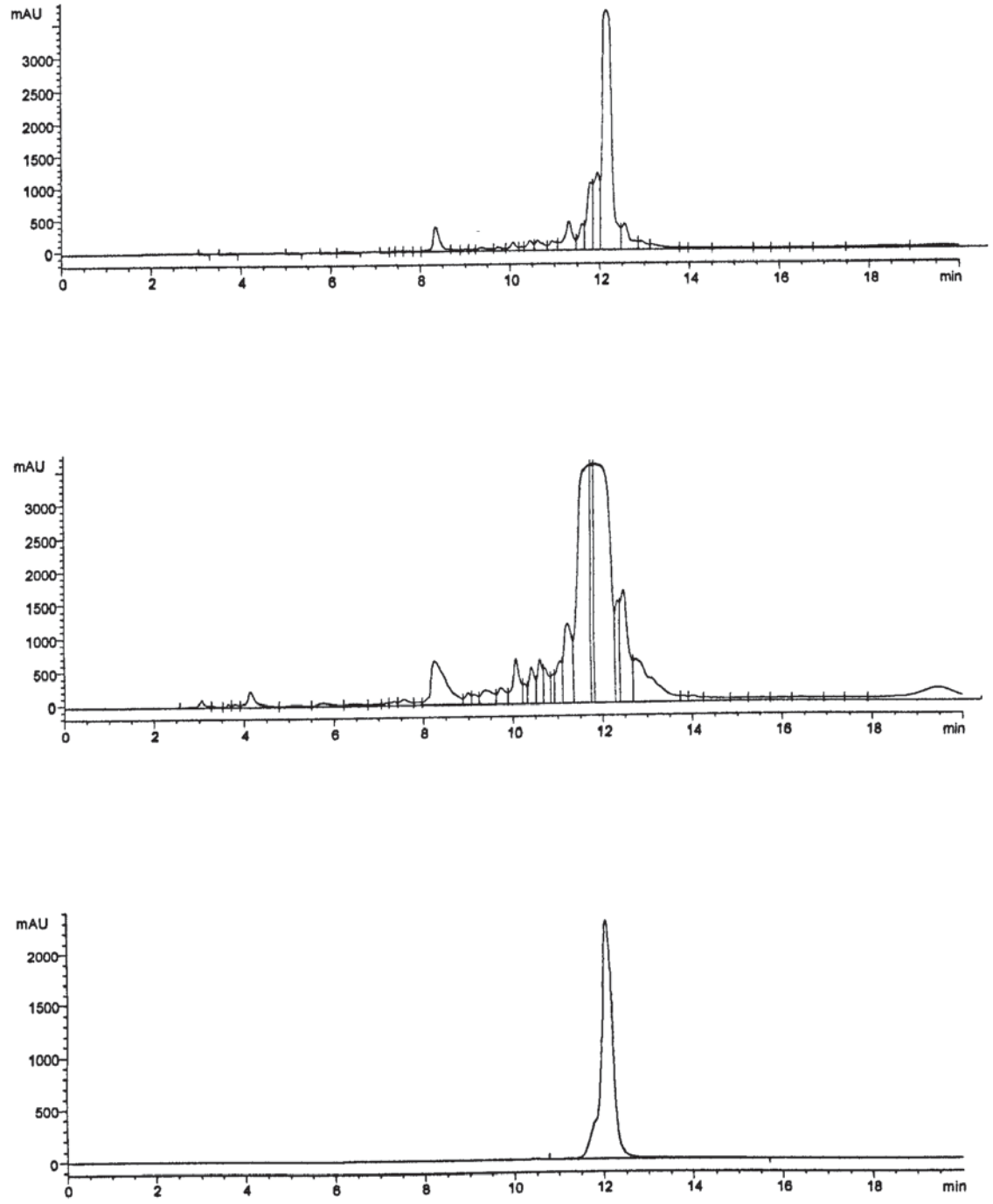

Figure 3.3 HPLC profiles of oligonucleotide 5'-AAAAGAAIAGGGGGGA (**S15**), analytical run of the crude sequence (upper trace), semi-preparative purification run (middle trace) and analytical run of the purified sequence (lower trace).

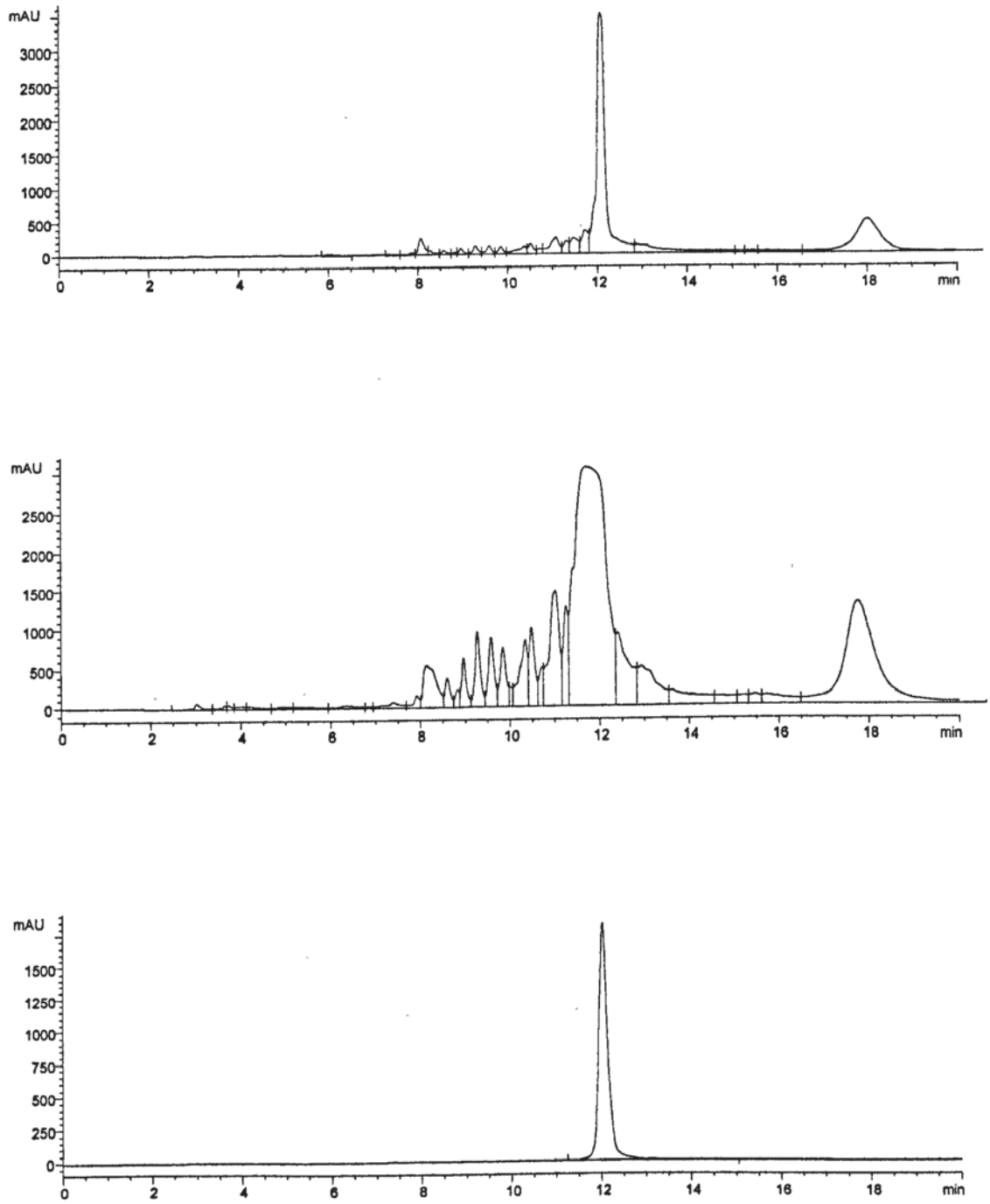

Figure 3.4 HPLC profiles of oligonucleotide 5'-AAAAGAAIAGGGGGGA (**S16**), analytical run of the crude sequence (upper trace), semi-preparative purification run (middle trace) and analytical run of the purified sequence (lower trace).

Chapter 4

DNA Molecular Recognition Properties of Pyridine-Stretched Oligonucleotides (PSOs)

4.1 Selection of strI for evaluation in PSOs

The aim of the thesis work was to synthesize and evaluate the molecular recognition properties of pyridine-stretched oligonucleotides (PSOs) containing the pyridine-stretched analogue of inosine (strI). The synthetic route developed described in **Chapter 2** for the preparation of strI is versatile allowing access to other members of this new series of pyridine-stretched base (PSB) analogues of adenine (strA) and diaminopurine (strD) (Calyton et al. 2002). There is the possibility to access further PSB analogues of guanine (strG), isoguanine (str-*iso*-G) and xanthine (strX). Attention was focused on the incorporation of strI into the first PSO sequences as no additional protection was required for the base, unlike strA, strD and the others (**Chapter 2**). This more direct route to the strI phosphoramidite for automated synthethesis of PSOs was the key factor in selecting this as the model PSB for evaluating the new PSOs.

4.2 Stacking capabilities of benzene-stretched and pyridine-stretched bases

Part of the rationale for incorporating PSBs into oligonucleotides was to determine whether the extended base ring system could be accommodated and whether it could increase or alter the stability of duplex and triplex structures compared with the natural DNA purine

and pyrimidine bases. Use of PSOs promises increased binding to single stranded and double stranded nucleic acid targets by enhancing base stacking, contributing favourably to the entropy of hybridization but not necessarily reducing electrostatic repulsion between charged backbones. Recent studies on oligonucleotides containing the benzene-stretched analogues **xA** and **xT** indicate that their duplex stabilizing properties are attributed to increased base stacking rather than a reduction in the electrostatic repulsion between the negatively charged phosphodiester backbones of paired strands (Liu et al. 2003). If this trend is mirrored in the PSO series then base stacking should be a dominant factor in duplex and triplex formation. Base stacking is known to significantly stabilise single stranded nucleic acids and their double and triple stranded hybrids (Brotschi et al. 2005; Lin et al. 1995; Saenger 1984) where the extended base systems benefit from favourable σ-π interactions, which outweigh destabilizing π-π interactions between adjacent bases (Hunter & Saunders 1990). It can be seen that overlap is potentially greater in PSBs compared with purine and pyrimidine bases (**Figure 4.1**).

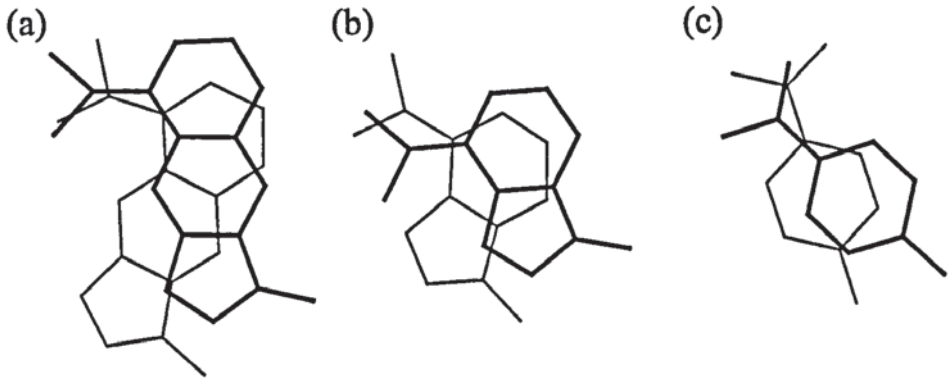

Figure 4.1 Illustration of the potential stacking possibilities between adjacent bases, (a) PSBs (b) purines and (c) pyrimdines in canconical A-form DNA structures.

4.3 Tautomerisation and electrostatic potential of strI

Pyridine-stretched inosine, strI, can adopt a number of possible tautomers, as can inosine (I) and its benzene-stretched analogue, bstrI (**Figure 4.2**). Semi-empirical calculations on the various possible base tautomers were performed using AM1 parameters to provide the heats of formation. Although the heats of formation are calculated in the gas phase, they indicate that strI, like inosine and benzene-stretched analogue, adopts the preferred t1 tautomer (**Figure 4.2**). It is this t1 tautomer that should allow Watson-Crick pairing with A and C by two hydrogen bonds in duplexes. This t1 tautomer should also allow Hoogsteen bonding in triplexes by two hydrogen bonds and also reversed Hoogsteen bonding, albeit by one hydrogen bond. The inosine t2 tautomer is marginally higher in heat of formation (+3.8 kcal mol^{-1}) compared with its most stable tautomer, suggesting that either could make contributions to base pairing and triplex formation. However, the analogous strI t2 tautomer is unlikely to contribute as it shows a significant increase in heat of formation (+8.1 kcal mol^{-1}). Of the other two alternative tauomers, strI t4 is least likely to contribute as evidenced by its substantially higher calculated heat of formation (+19.4 kcal mol^{-1}), which may be attributable to the loss of aromatic stabilization in the pyridine ring.

Space-filling models of the most stable tautomers I t1, bstrI t1, and strI t1 with electrostatic potentials, were generated and these are shown in **Figure 4.3**. Similar electrostatic charges at their Watson-Crick hydrogen bonding edges (left hand side as shown) suggest equal capabilities of forming hydrogen bonds with A and C, for example. The main difference in electrostatic potential between strI and the other two structures can be seen at the pyridine nitrogen.

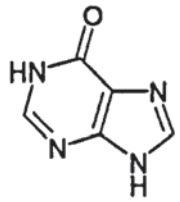

I t1: most stable

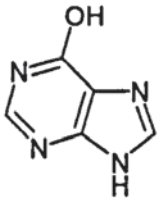

I t2: +3.8 kcal mol^{-1}

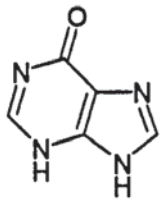

I t3: +14.0 kcal mol^{-1}

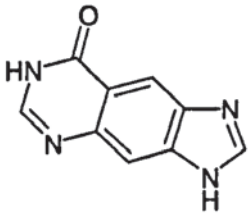

bstrI t1: most stable

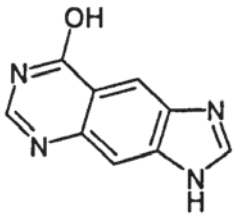

bstrI t2: +8.0 kcal mol^{-1}

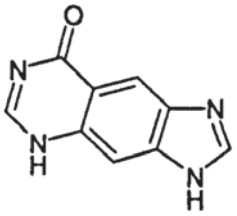

bstrI t3: +9.7 kcal mol^{-1}

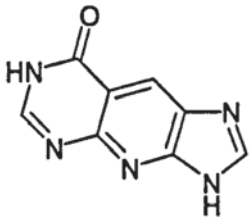

strI t1: most stable

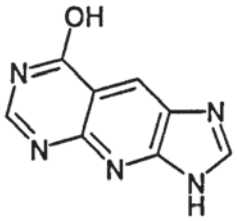

strI t2: +8.1 kcal mol^{-1}

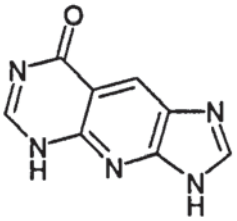

stI t3: +6.0 kcal mol^{-1}

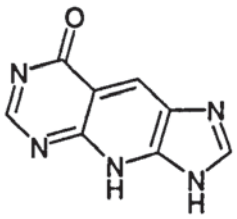

strI t4: +19.4 kcal mol^{-1}

Figure 4.2 Stabilities of tautomers of inosine (I), benzene-stretched inosine (bstrI) and pyridine-stretched inosine (strI) free bases calculated from relative heats of formation using AM1 parameters (Fujitsu Corporation 2005). Numbers are normalized to the most stable tautomer.

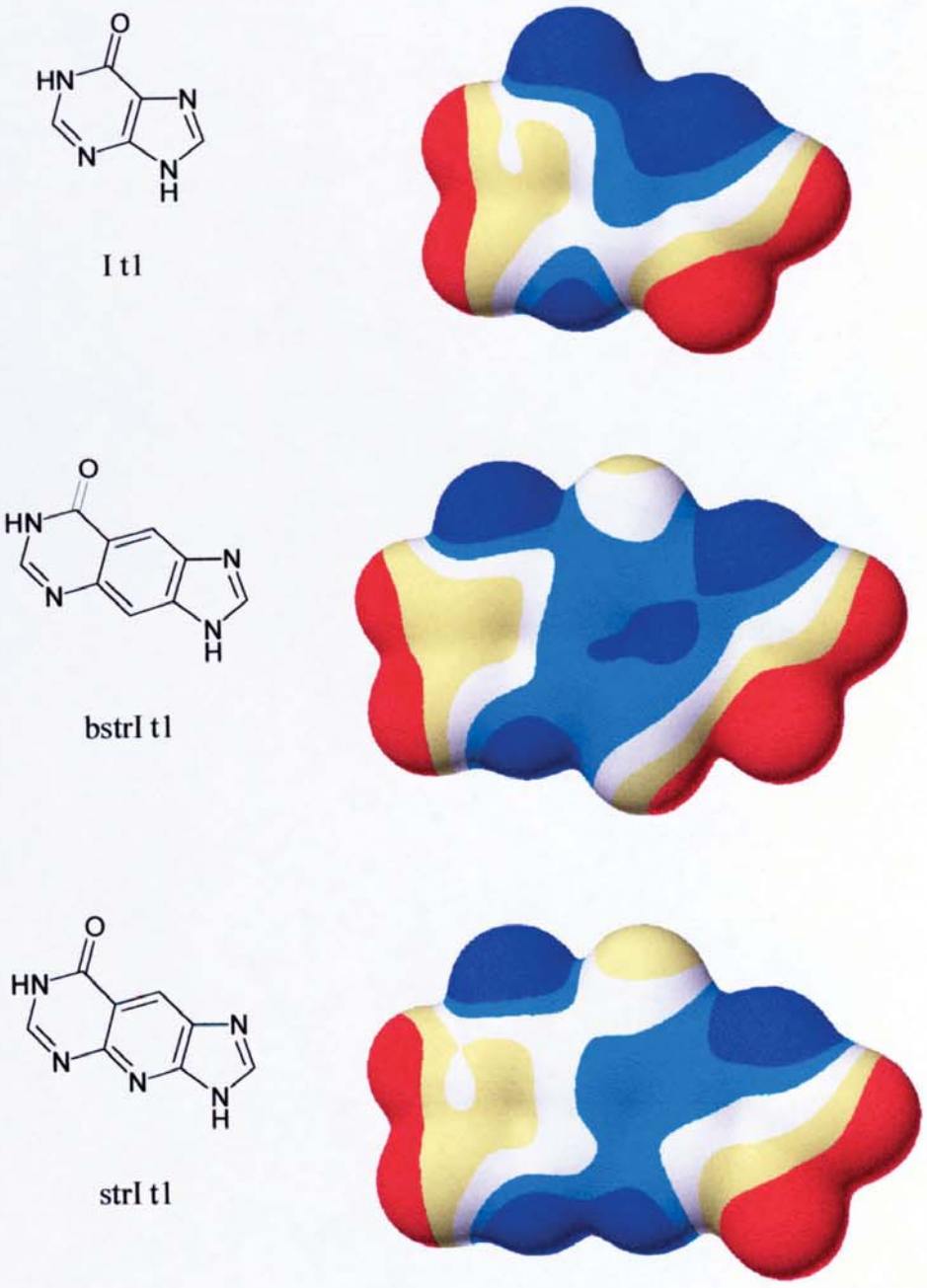

Figure 4.3 Space-filling models of the free bases inosine (I), benzene-stretched inosine (bstrI) and pyridine-stretched inosine (strI) with electrostatic potentials mapped on the surfaces. Geometry optimization and electrostatics were calculated using AM1 parameters (Fujitsu Corporation 2005). The electrostatic scale of -50 to +50 is depicted by red = positive potential, and blue = negative potential.

4.4 Calculated log P values

Ultimately, if PSO are to find applications in biological systems, aqueous solubility and partitioning between hydrophilic and hydrophobic environments within cells will be an important factor, especially to the biodistribution of these structures (Agrawal & Temsamani 1996). Theoretical calculations of log P values for model PSBs, where methyl replaces the sugar, gives values of log P = -0.51 for 9-methyladenine and log P = -0.37 for its pyridine-stretched analogue (Fujitsu Corporation 2005). This indicates similar partitioning of the pyridine-stretched base to that of the natural DNA base. The dramatically increased hydrophobicity of the benzene-stretched analogue (calculated log P = +0.56) may pose solubility problems in aqueous media, which in turn would impede its partitioning and DNA molecular recognition properties. The presence of the pyridine ring nitrogen appears to be significant in terms of partitioning and the potential biological applicatons of planned PSOs.

4.5 Methods for measuring duplex and triplex stabilities

There is a wide variety of spectroscopic, immunological, chemical and enzymatic methods available for the study of duplex and triplex structures (Soyer & Potaman 1995). Physicochemical methods of analysis include X-ray crystallography, electron microscopy, variable temperature ultraviolet (UV) spectrophotometry, nuclear magnetic resonance (NMR), electron spin resonance (ESR), infrared (IR) and Raman spectroscopy, optical rotatory dispersion (ORD), circular dichroism (CD), differential scanning calorimetry (DSC) and spectrofluorimetry (Liu et al. 2005c; Reither & Jeltsch 2002). In addition to a number of chemical methods, DNAse footprinting, gel co-migration using ^{32}P-radiolabelled

material, and two-dimensional agarose electrophoresis provide separation techniques for quantifying formation of duplex, triplex and other nucleic acid structures (Soyer & Potaman 1995).

4.5.1 Melting temperature (Tm) determination by variable temperature UV spectrophotometry (VT-UV)

Variable temperature UV spectrophotometry provides a direct, simple but effective method for the analysis of DNA duplex and triplex structures. The technique requires only small amounts (micromoles) of purified oligonucleotides and avoids the need for the radioactive ^{32}P-labelling for detection in gel electrophoresis. Measurement of the change in hyperchromicity of a duplex structure at a fixed wavelength allows the melting temperature (Tm) of the duplex to be determined directly (Huang & Miller 1993; Huang et al. 1996). The Tm value represents the helix-to-coil transition where half of the duplex structure remains intact but half has dissociated to give single strands. If melting curves are measured at varying oligonucleotide concentrations, then the thermodynamic parameters such as Gibbs free energy, enthalpy and entropy associated with duplex formation, may be calculated (Breslauer 1986; Liu et al. 2005b).

The thermal melting behaviour of the self-complementary oligonucleotide 5'-dATAATATTAT **S1** is shown in **Figure 4.4**. The percentage change in hyperchromicity measured at absorbance wavelength A = 260 nm is plotted against temperature (°C). The curve shows a clear inflection. The mid-point of the inflection is measured as the maximum point on the first derivative plot (not shown) and is taken as the Tm value. Thus, a Tm = 28.4 ± 0.5 °C was determined for **S1** according to **Figure 4.4**.

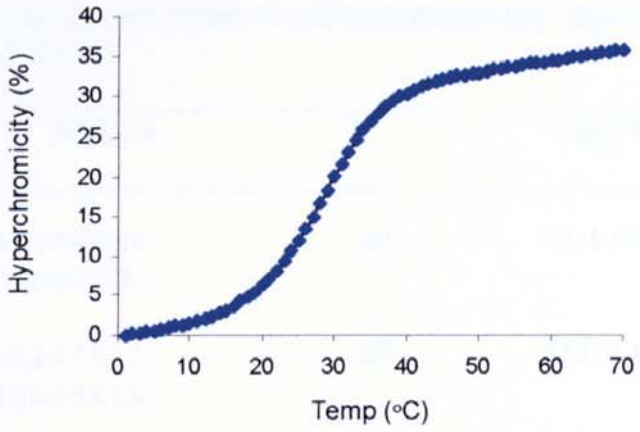

Figure 4.4 UV thermal melting curve of self-complementary duplex 5'-ATAATATTAT (**S1**) recorded at A = 260 nm and strand concentration 5 μM with Tm = 28.4 ± 0.5 °C determined from the first derivative plot (not shown).

4.6 Stability of self-complementary duplexes containing strI.A and strI.C base pairs

Self-complementary oligonucleotide sequences **S1** to **S6** where T and G residues are replaced, in turn, by inosine (I) and pyridine-stretched inosine (strI), were studied by VT-UV. The Tm values listed in **Table 4.1** give a direct measure of the duplex structures formed from the self-complementary strands. The measurements were carried out at pH 7.0 to mimic physiological conditions. Use of Tris.HCl buffer and monovalent (Na^+), divalent (Mg^{2+}) and polycation (spermine) are standard conditions for duplex and triplex formation (Singleton & Dervan 1994; Soyfer & Potaman 1996).

Table 4.1 indicates that replacement of pyrimidine base T by purine base I in **S2** increases duplex stability by 4.6 °C. Replacement of T by the pyridine-stretched tricylcic base strI in **S3** substantially increases duplex stability by 14.3 °C. The increase in Tm values are consistent with the two hydrogen bond Watson-Crick base pairing as shown in **Figure 4.5**.

Table 4.1 Thermal melting properties of self-complementary duplex sequences containing I and strI in place of T and G.

Duplex		Tm (°C)
5'-ATAATATTAT 3'-TATTATAATA	**S1**	28.4 ± 0.5
5'-AIAAIAIIAI 3'-IAIIAIAAIA	**S2**	33.0 ± 0.5
5'-A<u>I</u>AA<u>I</u>A<u>II</u>A<u>I</u> 3'-<u>I</u>A<u>II</u>A<u>I</u>AA<u>I</u>A	**S3**	42.7 ± 0.5
5'-GCGGCGCCGC 3'-CGCCGCGGCG	**S4**	46.0 ± 0.5
5'-ICIICICCIC 3'-CICCICIICI	**S5**	15.3 ± 0.5
5'-<u>I</u>C<u>II</u>C<u>I</u>CC<u>I</u>C 3'-C<u>I</u>CC<u>I</u>C<u>II</u>C<u>I</u>	**S6**	44.4 ± 0.5

Conditions, 5.0 μM DNA strand concentration in a 25 mM Tris.HCl buffer at pH 7.0 containing 100 mM NaCl, 10 mM $MgCl_2$ and 0.5 mM spermine. Strand concentration for sequence **S4** was 2.3 μM. I represents inosine and <u>I</u> represents strI.

It seems likely that the increased duplex stability is due to the increased base overlap and improved base stacking when pyrimidine base T is replaced by purine I and further by tricyclic strI. The relative distances between the phsophodiester backbones along the length of each duplex is preserved in **S2** and **S3** avoiding any need for distortion of the helical structure to accommodate the wider base pairs. This is the first example of a DNA duplex containing a hydrogen-bonded base pair involving a purine and tricylic pyridine-stretched, purine analogue.

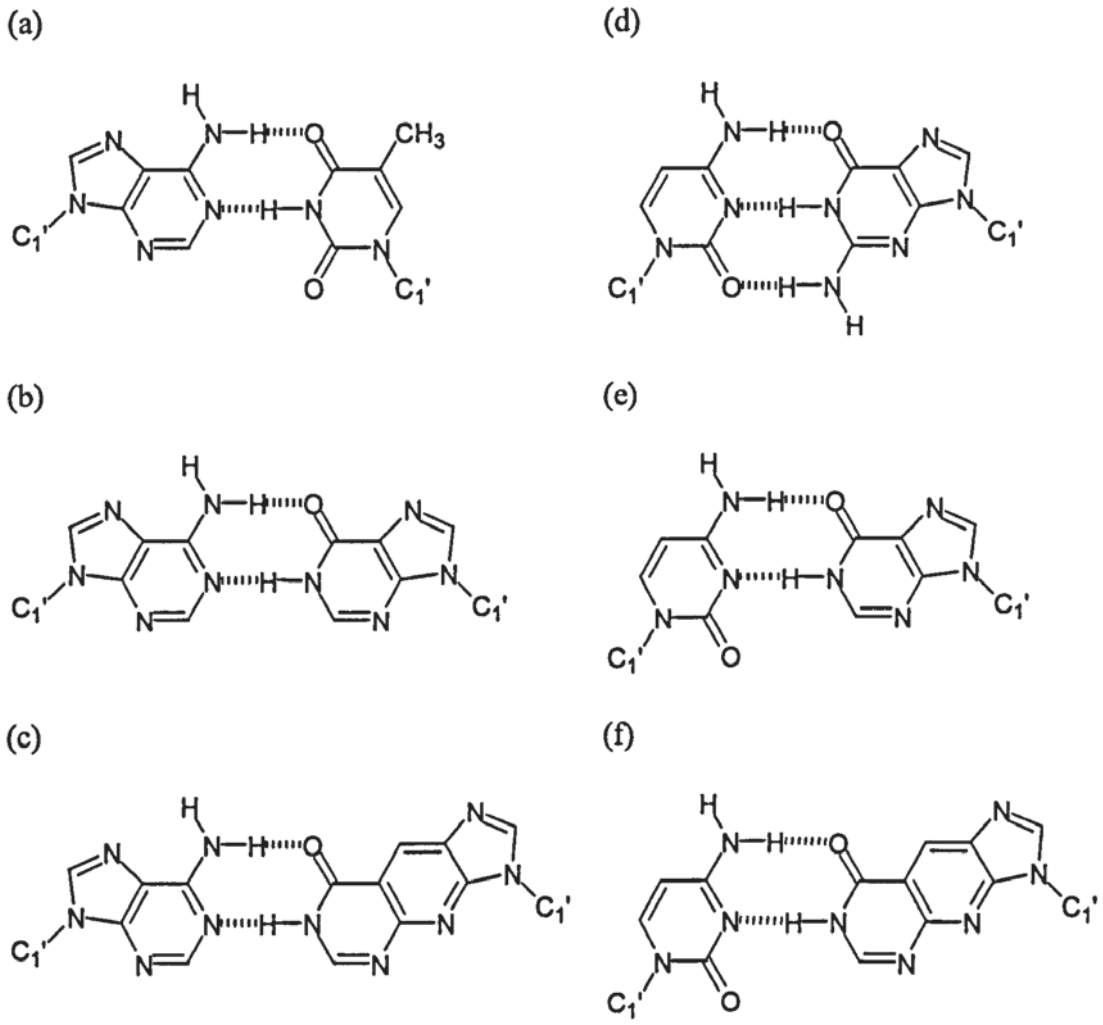

Figure 4.5 Two hydrogen bond Watson-Crick purine.pyrimidine base pair (a) A.T compared with proposed canonical purine.purine base pair (b) A.I and purine.pyrimidine-stretched purine pair (c) A.I. Two hydrogen bond Watson-Crick purine.pyrimidine base pair (d) C.G compared with proposed canonical purine.purine base pair (e) C.I and purine.pyrimidine-stretched purine pair (f) C.I.

Watson-Crick hydrogen bonding between pyrimidine.purine base pair C.G involves three hydrogen bonds. This is illustrated in **Figure 4.5**(d). The stability provided by this extra hydrogen bond is reflected in the increased stability of the self-complementary duplex

formed from **S4** compared with the duplex formed from **S1**. The increase is nearly 2 °C per C.G pair. This value would no doubt increase if **S4** were to be measured at a comparable total strand concentration of 5 μM. Hyperstructure formation during HPLC purification of **S4** gave a low yield of oligonucleotide product, therefore the strand concentration of 2.3 μM of **S4** was the highest achievable with the purified material available. Replacement of G by I is significantly destabilizing to duplex **S5**. This is most likely attributable to the loss of one of the three O...H-N hydrogen bonds per C.I base pair (**Figure 4.2**). Duplex stability substantially improves when I is replaced by strI in **S6** (**Table 4.1**). Indeed, the stability of duplex **S6** is only 1.6 °C lower than **S5** suggesting that the enthalpic loss associated with the reduced hydrogen bonding capability is compensated for, and nearly fully restored by the improved stacking between the strI residues in **S6**. Again, a regular backbone distance in **S4**, **S5** and **S6** avoids distortion of the helical structure.

4.7 Stability of non-self-complementary duplexes containing strI.A and strI.C base pairs

Having considered self-complementary duplexes, it was of interest to investigate the stability of strI in a different sequence context by incorporating the base into olgonculeotides that are not self-complementary. Sequences **S9**, **S10** and **S11** were separately targeted to **S7** and **S8** and their duplex stabilites determined by VT-UV (**Figure 4.6**). The Tm values are given in **Table 4.2.** Replacement of the A.T pair in **S7.S9** by an A.I pair in **S7.S11** or an A.I in **S7.S10** was destabilizing (**Figure 4.5**(a-c)). In this context, to maintain the hydrogen bonding pattern, the duplexes **S7.S11** and **S7.S10** must undergo

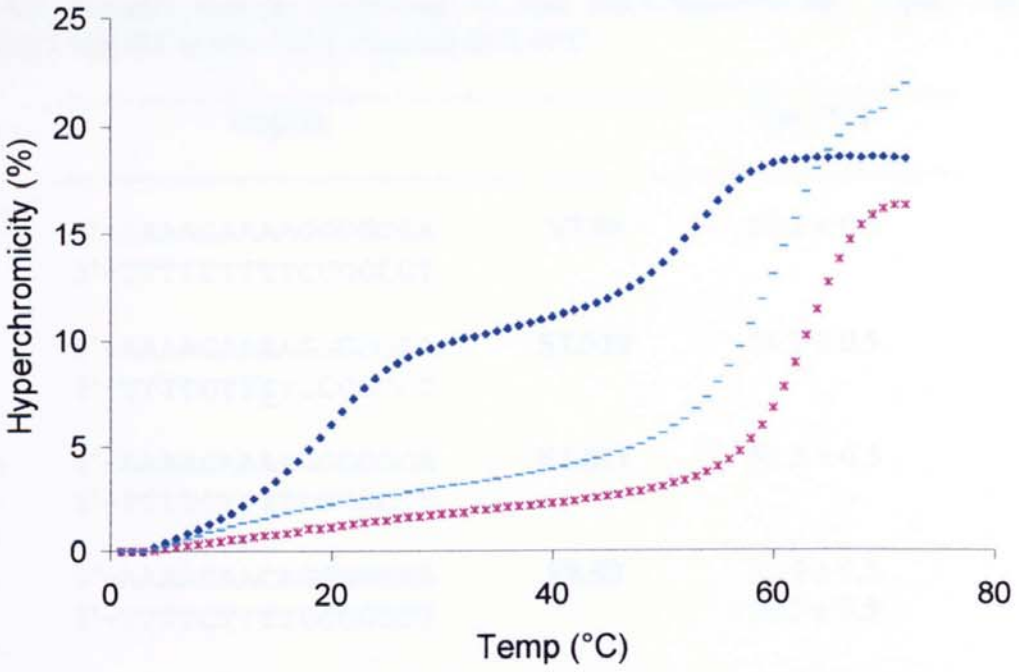

Figure 4.6 UV thermal melting curve of duplex structures **S8.S9** (dark blue diamonds), **S8.S10** (light blue dashes), **S8.S11** (purple crosses) recorded at A = 260 nm and total strand concentration 5 μM.

some backbone distortion to accommodate these "bulged" base pairs, and may account for the decrease in stability; -4.7 and -6.5 °C respectively, compared with the undistorted **S7**.**S9** duplex (**Figure 4.5**(a-c)). The duplex structure **S8**.**S9**, with its deliberate C.T mismatch (**Figure 4.7**(a)) was prepared and its stability compared with duplexes **S8.S10** and **S8**.**S11** (**Table 4.2**). The values listed in **Table 4.2** were determined from first derivative plots of the melting curves given in **Figure 4.6**. Duplex **S8.S11** was more stable than duplex **S8.S10** and **S8.S9** by +2.7 and +10.4 °C respectively. This is again consistent with Watson-Crick base pairing across the series where accommodation of the C.I pair would involve "bulging" and backbone distortion of the duplex (**Figure 4.7**(a-c)).

Table 4.2 Thermal melting properties of non self-complementary duplex sequences containing I and strI in place of T targeted to A or C.

Duplex		Tm (°C)
5'-AAAAGAAA**A**AGGGGGGA 3'-TTTTCTTT**T**TCCCCCCT	**S7.S9**	63.2 ± 0.5
5'-AAAAGAAA**A**AGGGGGGA 3'-TTTTCTT**I**TCCCCCCT	**S7.S10**	56.7 ± 0.5
5'-AAAAGAAA**A**AGGGGGGA 3'-TTTTCTT**I**TCCCCCCT	**S7.S11**	58.5 ± 0.5
5'-AAAAGAA**C**AGGGGGGA 3'-TTTTCTTT**T**TCCCCCCT	**S8.S9**	52.5 ± 0.5 19.5 ± 0.5
5'-AAAAGAA**C**AGGGGGGA 3'-TTTTCTT**I**TCCCCCCT	**S8.S10**	60.2 ± 0.5
5'-AAAAGAA**C**AGGGGGGA 3'-TTTTCTT**I**TCCCCCCT	**S8.S11**	62.9 ± 0.5

Conditions, 2.5 μM individual DNA strand concentration giving 5 μM total concentration in a 0.5 mM Tris.HCl buffer at pH 7.0 containing 100 mM NaCl, 10 mM $MgCl_2$ and 0.5 mM spermine. I represents inosine and I represents strI.

In the C.T motif the bases are further apart therefore hydrogen bonding would be lost or substantially hampered by the electrostatic repulsion between the lone pairs of electrons of the O2 atoms of C and T (**Figure 4.7**(a)). A very intriguing feature apparent in the **S8.S9** is the transition at 19.5 ± 0.5 °C that occurs before the double helix melts (**Figure 4.6**). This transition was present in both the melting and cooling curves, which were essentially superimposable. This type of profile is very characteristic of triplex formation yet it is

(a)

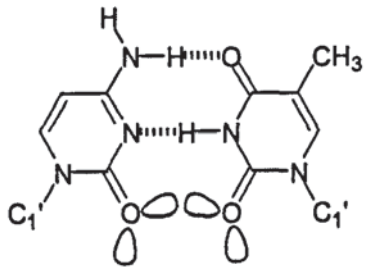

(b)

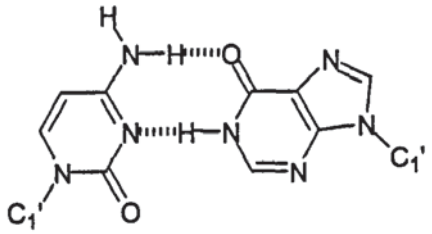

(c)

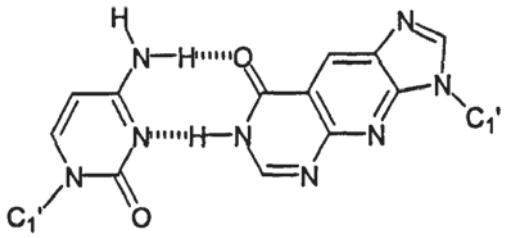

Figure 4.7 Two hydrogen bond Watson-Crick pyrimidine.pyrimidine base pair (a) C.T where (b) I replaces T and (c) I replaces I.

difficult to see how this might arise. One possibility is that a second strand of **S8** could align parallel with the purine strand of the **S8.S9** duplex to form a triple helical structure **S8*S8.S7.** This is unlikely for two reasons; firstly, homopurine TFOs form antiparallel triplexes when targeted to the purine strand of purine.pyrimidine duplexes (Buchini &

Leumann 2003). Here, in **S8**, the base sequence 5' to 3' is the exact reverse of that required for stable triplex formation. Secondly, the duplex structures **S8.S10** and **S8.S11** contain the exact same purine and pyrimidine sequences, except for the single base pair replacements, yet no transition is observed other than the clear duplex melting transition. The melting and cooling curves were repeatedly measured with exactly the same outcome each time. Although the analyses were reproducible, no satisfactory explanation for the "extra" transition could be determined. The C.T mismatch in duplex **S8.S9** could have promoted formation of partial duplex structures to try to avoid the energetic penalty imposed by the mismatch. However, this would have required formation of duplex structures oriented parallel, which is unlikely.

4.8 Triple helix formation involving possible reversed Hoogteen pairing

Targeting of polypurine.polypyrimidine DNA duplexes at neutral pH is possible using polypurine TFOs comprising A and G residues. The TFO aligns antiparallel to the A.T and G.C paired purine target sequence by reversed Hoogsteen hydrogen bonding to form triplex structures A*A.T and G*G.C (**Figure 4.8**).

To test whether incorporation of I and strI would have an influence on triplex stability, the target duplex structure **S9.S7** was prepared by mixing equimolar amounts of **S9** and **S7**. Triplexes were formed by adding separately an equimolar amount of third strand **S12, S13** or **S14**. The stabilities of the triplex structures were assessed by VT-UV. The melting profiles for the three triplex structures are shown in **Figure 4.9** and the results given in **Table 4.3.**

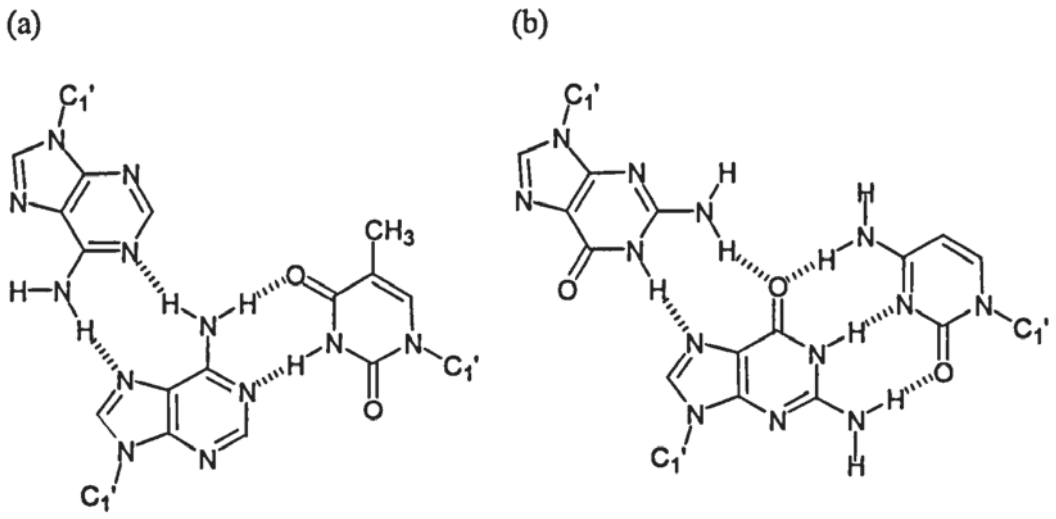

Figure 4.8 Reversed Hoogsteen paired triplexes with A and G targeted to A.T and G.C base paired duplexes (a) A*A.T, (b) G*G.C.

Replacement of A by I or strI allows formation of similar structures albeit with one hydrogen bond connecting the third stand base to the Watson-Crick paired A.T target (**Figure 4.10**). The melting profile of the fully paired triplex **S12*S9.S7** gave a biphasic curve characteristic of a DNA triplex. The first transition at lower temperature represents the melting temperature of the third (TFO) strand as it dissociates from the duplex. The second transition occurs at a higher temperature and corresponds to dissociation of the two strands of the target duplex, Tm = 28.0 ± 1 and 63.8 ± 0.5 °C respectively (**Table 4.3**). Close inspection of the two profiles for **S13*S9.S7** and **S14*S9.S7** reveals no clear triplex melting transition. However, in both cases there are significant increases in hyperchromicity over a broad temperature range before melting of the duplex. This is very characteristic of viable triplex structures.

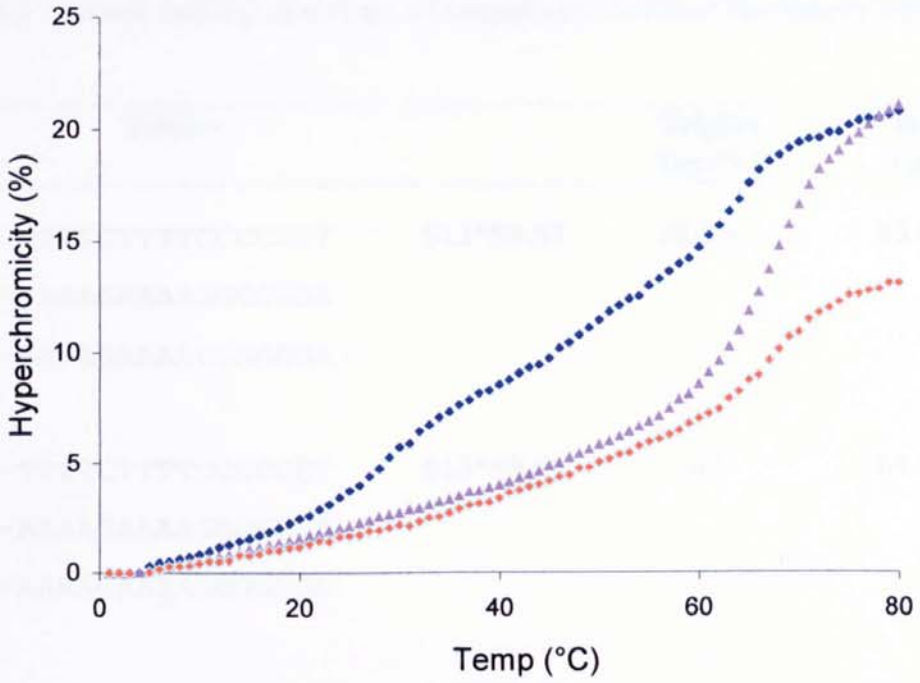

Figure 4.9 UV thermal melting curve of triplex structures **S12*S9.S7** (dark blue diamonds), **S13*S9.S7** (purple triangles), **S14*S9.S7** (red diamonds) recorded at absorbance = 260 nm and total strand concentrations of 5.4 μM.

It is well documented that triplex structures can and do form with sufficient stability yet give no distinct, well defined melting temperature transition in the UV (Parel & Leumann 2001). This circumstantial evidence supports formation of viable triplex structures but without the precise Tm values it is not possible to determine exactly whether I or strI provide better, equal or poorer stability compared with A when each is separately targeted to an A.T pair.

Mixing studies by the Job method (Liu et al. 2005b) is a straight forward procedure to determine the 2:1, or other, stoichiometry of the proposed triplex structures, and gel shift assays (Simon et al. 1999) or DNAse footprinting can provide a quantitative measure of

Table 4.3 Thermal melting properties of antiparallel, reversed Hoogsteen triplexes.

Triplex		Triplex Tm (°C)	Duplex Tm (°C)
3'-TTTTCTTTTCCCCCCT	**S12*S9.S7**	28.0 ± 1	63.8 ± 0.5
5'-AAAAGAAAAGGGGGGA			
3'-AAAAGAAAAGGGGGGA			
3'-TTTTCTTTTCCCCCCT	**S13*S9.S7**	n.t.	64.4 ± 0.5
5'-AAAAGAAAAGGGGGGA			
3'-AAAAGAAIAGGGGGGA			
3'-TTTTCTTTTCCCCCCT	**S14*S9.S7**	n.t.	64.5 ± 0.5
5'-AAAAGAAAAGGGGGGA			
3'-AAAAGAAIAGGGGGGA			

Conditions, 1.8 μM individual DNA strand concentration giving 5.4 μM total conentration in a 0.5 mM Tris.HCl buffer at pH 7.0 containing 100 mM NaCl, 10 mM $MgCl_2$ and 0.5 mM spermine. I represents inosine and I represents strI. n.t. represents no defined triplex transition but in these two cases significant increases in hyperchromicity were observed.

triplex stability (Ranasinghe et al. 2005). However, with no quantity of strI oligonucleotide or phosphoramidite remaining, use of these methods would have required complete resynthesis.

With the preliminary evaluation of strI revealing some interesting DNA molecular recognition properties, the thesis research project was concluded at this stage. The success of the chemical synthesis work and the promising DNA molecular recognition properties of

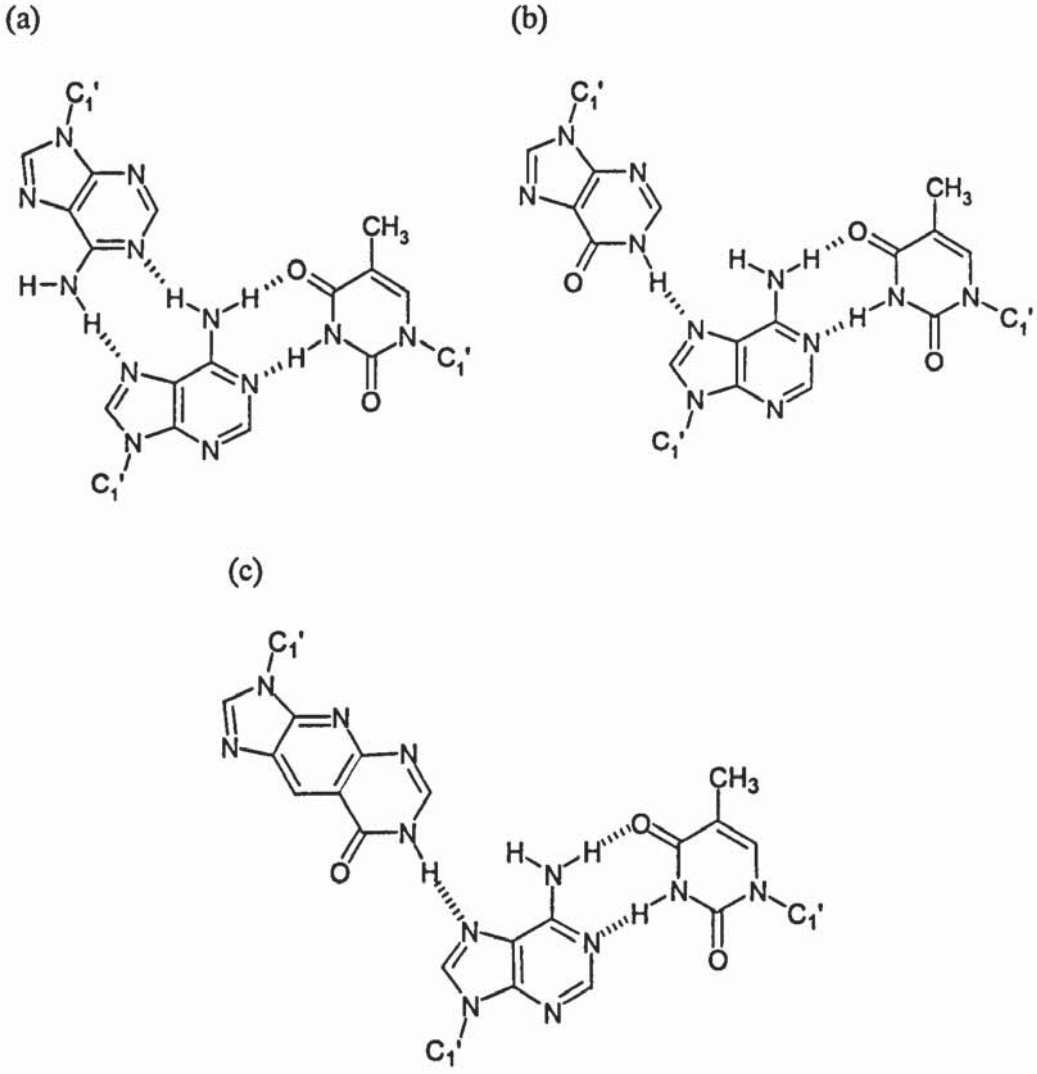

Figure 4.10 Comparison of the hydrogen bonding pattern of triplex structures (a) A*A.T, (b) I*A.T and (c) strI*A.T formed by A, I or strI targeted to an A.T base pair.

PSOs containing strI as a model, pave the way for the future synthesis of the complete series of pyridine-stretched bases in PSOs and full evaluation of their duplex and triplex forming properties. With the complete series eventually in hand, there is the possibility to extend the genetic alphabet beyond the DNA bases and their recently reported benzene-stretched homologues (Gao et al. 2005).

Chapter 5

Metronidazole Oligonucleotide Conjugate Formation

5.1 Nitroimidazoles as drugs

Metronidazole **5.1**, Tinidazole **5.2** and benznidazole **5.3** belong to a class of nitroimidazolyl containing drugs that have been used for more than 40 years. Such compounds have been used for the effective treatment of a wide range of anaerobic bacterial and protozoan infections due their selective ability to damage and cleave microbial DNA under oxygen deficient conditions (Edwards 1993; Oliveira 2003; Tocher 1997). While the incidence of drug resistance is still low it is reported to be on the increase thus, any developments that improve drug delivery, increase localized concentration or modify the mode of action of such nitroimidazole compounds would be of benefit (Dachs et al. 1995; Reysset 1996; Townson et al. 1994).

More recently, with their ability to localize within oxygen-deficient tissue, nitroimidazole derivatives such as etanidazole **5.4** have been used as radiotherapy sensitizers in the treatment of hypoxic tumours. Their use as agents in chemotherapy have also been investigated (Ali et al. 1993; Parrick & Porssa 1995; Tocher 1997). Hypoxic regions develop when the rate of tumor growth exceeds the normal required blood supply and results in solid tumors with a relatively strong, chemically reducing environment. Such hypoxia severely limits the efficacy of current radiotherapeutic and chemotheraputic

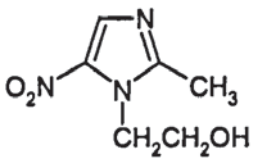

5.1

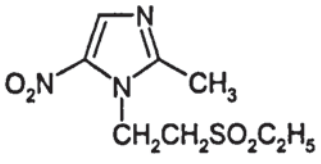

5.2

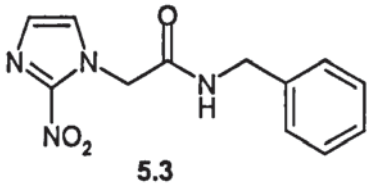

5.3

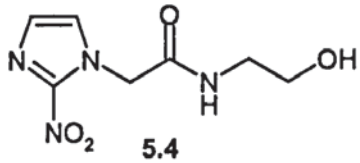

5.4

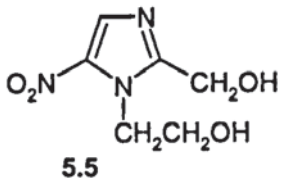

5.5

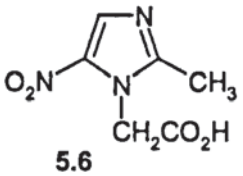

5.6

treatments. Nitroimidazoles have been shown to cause greatest DNA damage at A.T regions. Thus site-specific delivery of nitroimidazoles by linkage to triplex-forming oligonucleotides (TFOs) could possibly cause catastrophic but controlled damage resulting in hypoxic cell death (Edwards 1993; Parrick et al. 1993).

The nitroimidazoles are effective under anaerobic reducing conditions where they act as prodrugs, activated within a cell by reduction. They show limited toxicity to healthy aerobic cells and thus exhibit relatively few side effects. Side effects that can occur are, at worse, short term with cessation of treatment. There is concern that many nitroimidazole based drugs, including metronidazole, give a positive Ames test. However, indications are that mutagenesis by nitroimidazoles occurs only under anaerobic conditions and that they have little or no effect on mammalian cells (Hartmann 2002; Menendez 2001). The aerobic metabolites of metronidazole include metronidazole itself as a consequence of a "futile cycle" (**Figure 5.1**), 1-(2-hydroxyethyl)-2-hydroxymethyl-5-nitroimidazole **5.5** and 1-acetic acid-2-methyl-5-nitroimidazole **5.6**. Most concern about potential long-term toxicity has focused on the 2-hydroxyethyl metabolite **5.5**. Better targeting and delivery of

metronidazole to the anaerobic sites could significantly reduce the levels of this metabolite in aerobic tissue (Connor 1977; Pendland 1994). A significant amount of work has been devoted to understanding the mode and mechanism of action of nitroimidazoles. The effectiveness of this class of biologically active compounds is due to their ability to undergo a variety of metabolic pathways, depending on the local cellular environment. They have the capacity to undergo up to a six electron transfer but the initial activity is due to a reversible one electron transfer within a cell, which results in diffusion through the cellular membrane of the nitroimidazole derivative due to a concentration gradient. In the case of anaerobic bacteria, the reductive process appears to follow, at maximum, a two electron transfer to the corresponding nitroso derivative with the possibility of a reversible two electron reduction to the hydroxylamine derivative and ultimate conversion to the

Figure 5.1. Reductive activation of nitro-aromatic compounds. Feasible reduction steps are dependant on the electron affinity of the intermediates (Tocher 1997).

amine depending on local intracellular conditions.

The mechanism of DNA cleavage and the identity of the cleaved primary DNA reduction product are not certain. Indications are that it is a radical mechanism involving the protonated nitro radical anion ($ArNO_2^{\cdot}H$) (**Figure 5.1**).

Work on radiosensitization of hypoxic tumours has demonstrated that a 2-nitroimidazole derivative of netropsin, a DNA minor grove targeting oligopyrrole antibiotic **5.7**, is capable of entering a cell and binding to DNA. The radiosensitization efficacy was found to be poor, possibly due to a quenching effect of the netropsin residue. However aerobic cytotoxicity was high with significant cellular uptake. Although strong binding to DNA was demonstrated, anaerobic cytotoxicity was not determined. Using a 5-nitroimidazole residue attached to a sequence-specific TFO could be a potential selective anaerobic cytotoxin that might overcome the undesirable aerobic activity associated with the oligopyrrole conjugate (Parrick & Porssa 1993; Parrick et al. 1993).

The recent development of DNA modified glass electrodes could prove to be very useful for studying the potential cytotoxic effects due to DNA damage of the reactive reduction

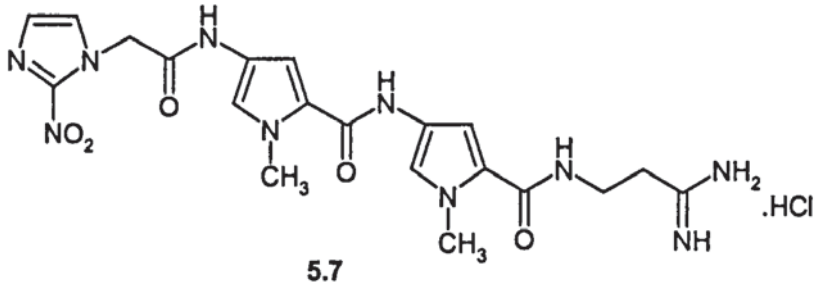

5.7

products from 4-unsubstituted-5-nitroimidazole derivatives such as metronidazole on selected DNA sequences via reduction *in situ*, especially when linked to a site-specific TFO (de Abreu 2002; La-Scalea 2002).

5.2 Synthesis of metronidazole oligonucleotide 5.11

The 2-cyanoethyl-*N,N*-diisopropylphosphoramidite derivative **5.8** of metronidazole was prepared by reaction of **5.1** with 2-cyanoethyl-*N,N*-diisopropylchlorophosphoramidite **2.46** in the presence of diisopropylamine, under anhydrous conditions (**Scheme 5.1**). Although the literature indicates a longer reaction time for the phosphitylation of 3′-hydroxyl groups of nucleosides, analysis (TLC) showed that the reaction was complete after 20 min, indicating the increased reactivity of the primary hydroxyl group of metronidazole over the secondary 3′-hydroxyl group of nucleosides (Sinha 1984). Purification of the phosphitylated product **5.8** was achieved by flash column chromatography to give a high yield of 89%. Analysis of **5.8** by proton NMR, a single aromatic proton peak at 8.0 ppm, no H-phosphonate peaks and in the ^{31}P NMR spectra a single peak at 51.4 ppm confirmed its

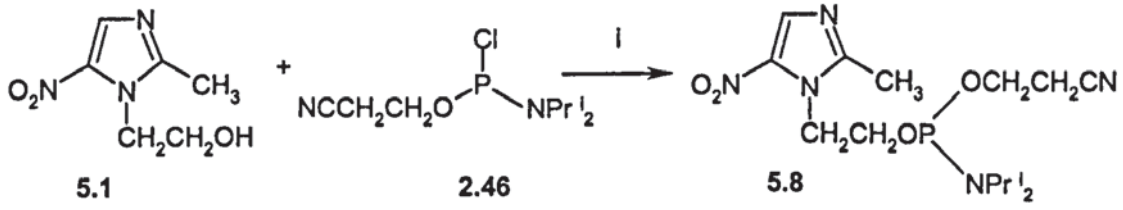

Scheme 5.1 Preparation of the metronidazole phosphoramidite. Reagents and conditions, i. Pr^i_2NH, THF, Argon, rt

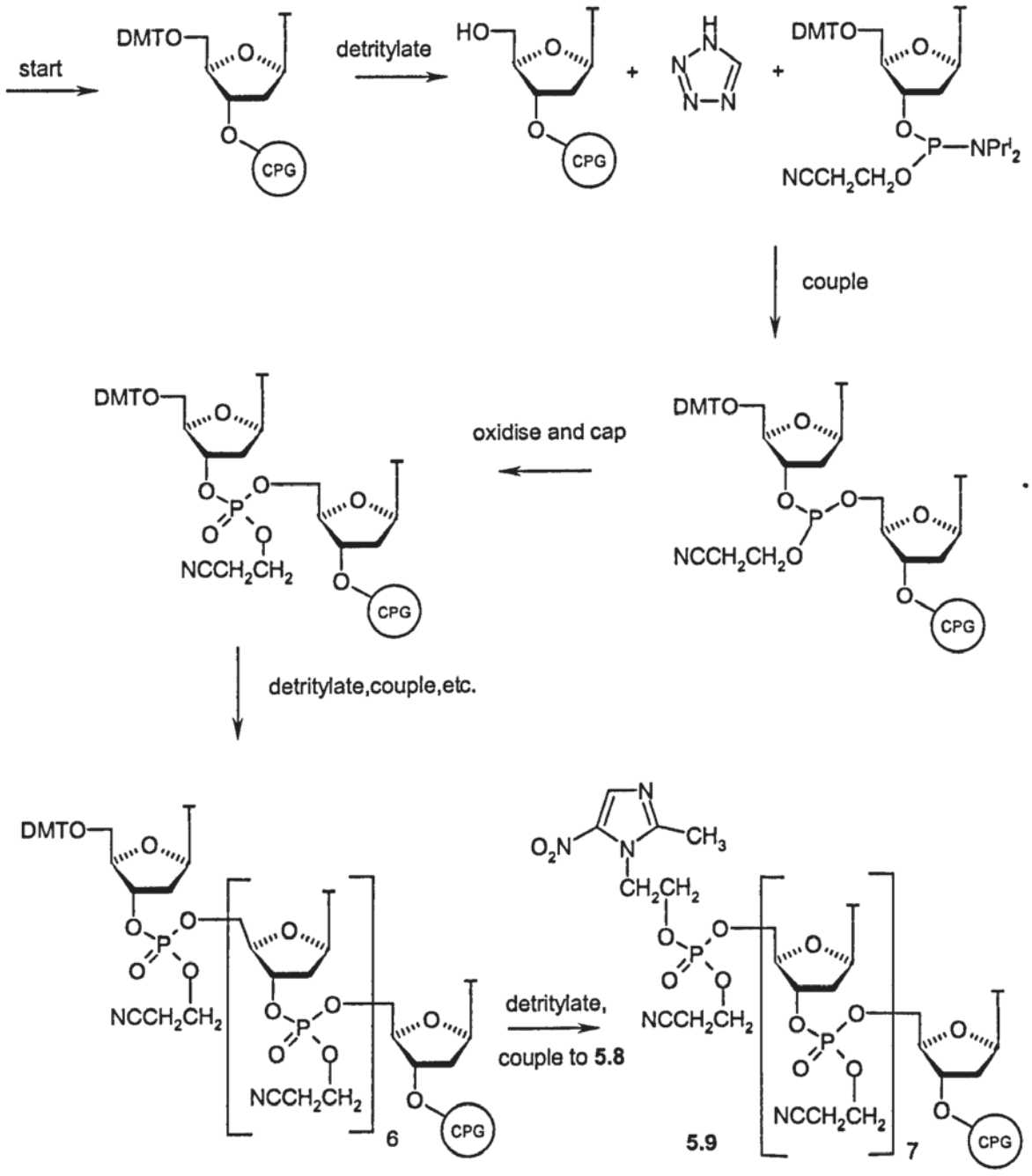

Scheme 5.2 Reaction cycle for the solid phase synthesis of dT_8 metronidazole conjugate, where T represents the base thymine, DMT, the dimethoxytrityl protecting group and CPG, the derivatized solid support.

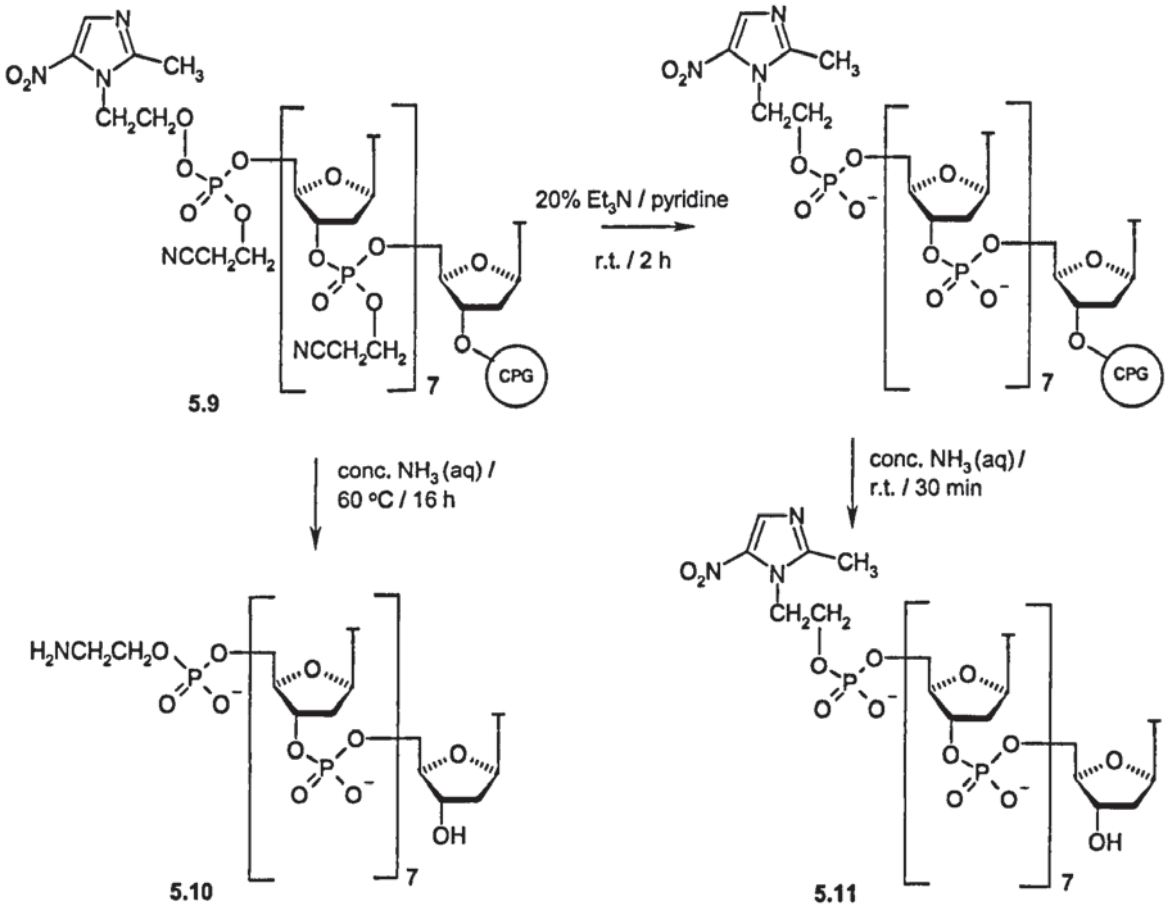

Scheme 5.3 Cleavage and deprotection to generate the dT_8 metronidazole conjugate.

identity and indicated that the product was of high purity. The stability of the product was confirmed after prolonged storage at ca. 4 °C and subsequent re-analysis by proton NMR. In order to demonstrate that the metronidazole phosphoramidite derivative could be covalently linked to a potential TFO, a sample was used in a solid phase DNA synthesis to give a protected, succinyl-CPG-supported dT_8 conjugated to metronidazole at the 5'-end **5.9** using standard reaction cycles and coupling times (**Scheme 5.2**) (Sinha 1984).

The dT_8 sequence was selected because the unconjugated dT_8 sequence has been characterized along with its mitozolomide and temozolomide conjugates by HPLC and electrospray mass spectroscopy (ESMS), thus the analogous dT_8 metronidazole conjugate could be compared directly (Walsh 1999). Analysis by HPLC and ESMS of the product from the initial attempt to remove the dT_8 metronidazole conjugate from the solid support and, deprotect the phosphate linker groups using standard conditions of conc. NH_3 (aq) at 60 °C for 16 h indicated that degradation of the metronidazole moiety had occurred. RP-HPLC purification and MS analysis showed that a dT_8 ethylamine conjugate **5.10** (MW

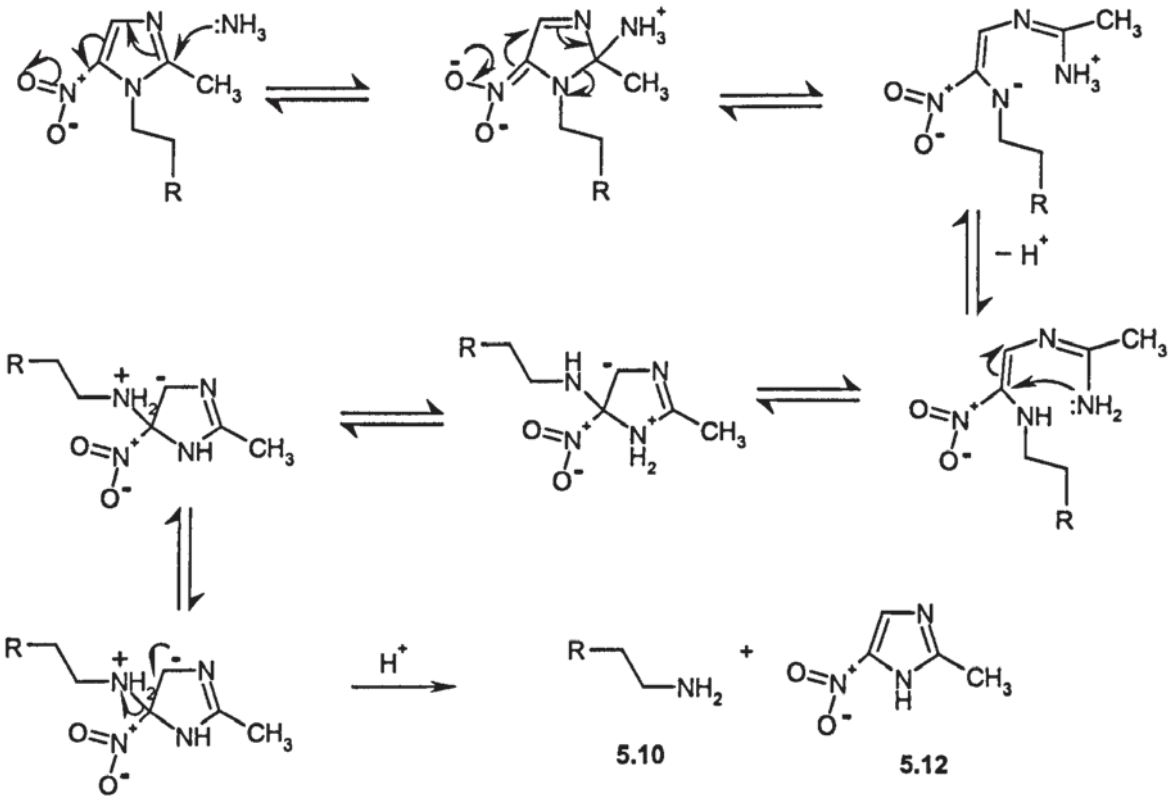

Scheme 5.4 Possible mechanism for the formation of dT_8 ethylamine conjugate.

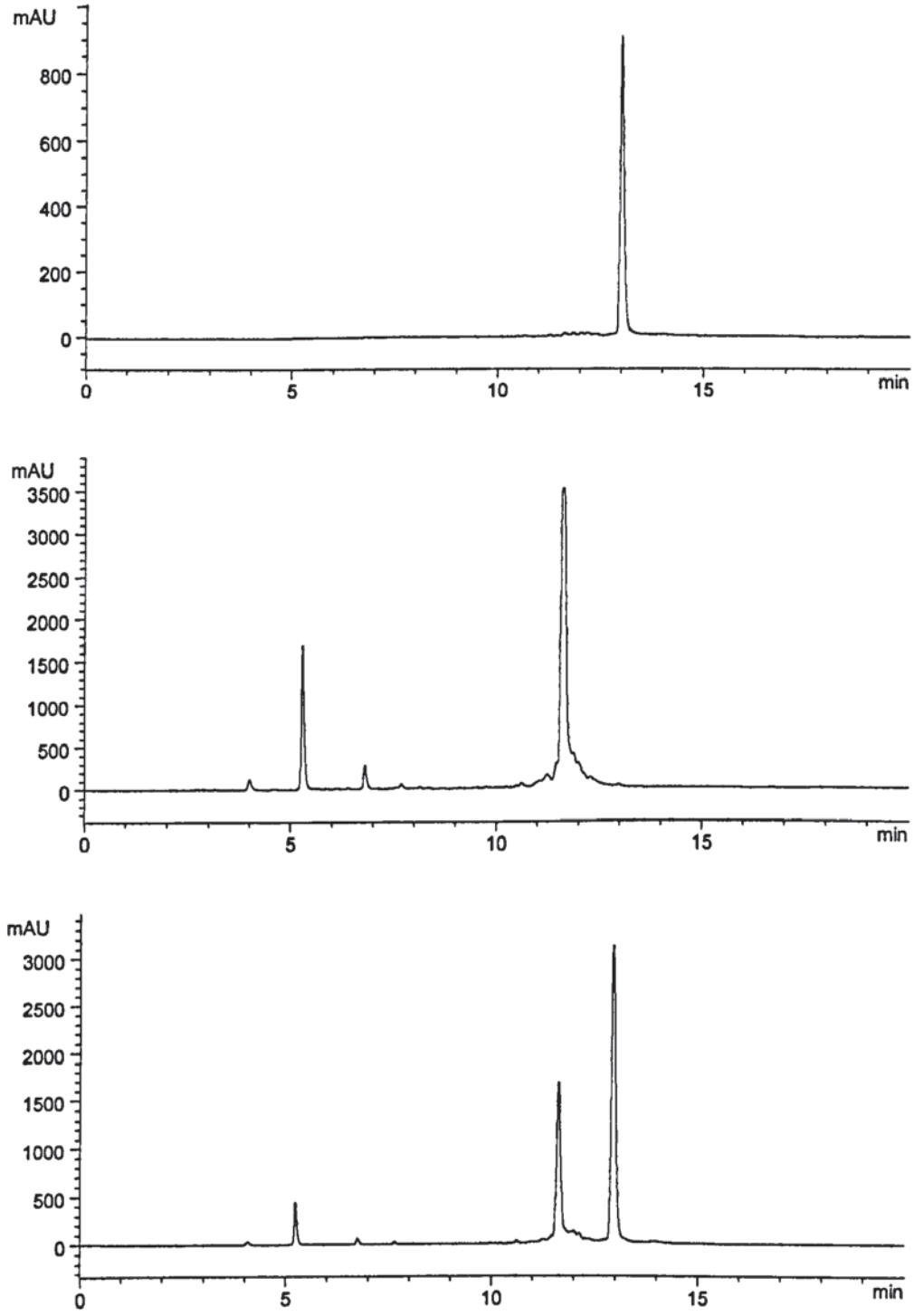

Figure 5.2 HPLC profiles of, the target dT_8 metronidazole conjugate with retention time 13.3 min (upper trace), dT_8 aminoethyl conjugate with retention time 11.6 min (middle trace) and a mixture of both conjugates (lower trace).

found 2494.1; calculated 2492.4) had been produced (**Scheme 5.3**). Formation of **5.10** could have been possible through a ring-opening, ring-closing mechanism resulting in the elimination of 1-methyl-5-nitroimidazole **5.12** (**Scheme 5.4**). Clearly the standard deprotection conditions were incompatible with the metronidazole group. However, a sequential procedure using milder conditions involving deprotection with 20% triethylamine-pyridine at rt for 2 h and cleavage from the solid support with conc. NH_3 (aq) at rt for 30 min was successful (**Scheme 5.3**). ESMS analysis following semi-preparative HPLC showed that the target conjugate **5.11** (MW found 2604.2; calculated 2603.4) had been successfully prepared (**Figure 5.2**).

5.3 Attempts to reduce metronidazole

With the ultimate reduction product of the metronidazole residue being an aromatic amine, it was attempted to synthesize and isolate the reduction products of metronidazole for evaluation of potential aerobic toxicity. Catalytic hydrogenations over palladium on carbon and Raney nickel and reduction using nickel boride/HCl were tried (Seltzman 1993; Sullivan 1982). When initial TLC analysis indicated significant product spots separation using flash chromatography was attempted, however in all cases decomposition occurred during workup yielding intractable mixtures and no identifiable products.

Primary 5-aminoimidazole derivatives, unsubstituted at the 4-position, have been shown to be very unstable and only recently shown to have any potential synthetic utility requiring rapid reduction and, either reaction *in situ*, possibly as a readily hydrolysable amidine derivative, or further reaction with minimal workup under an inert atmosphere (Al-Shaar 1992). Storage even under inert atmosphere has proved to be impractical due to rapid

deterioration, with possibly catalysis by trace amounts of oxygen and/or degradation products.

Having demonstrated that an oligonucleotide-metronidazole conjugate can be successfully synthesized by solid phase chemistry further work to link metronidazole to a selected sequence for testing to assess possible antiviral activity, cellular uptake and biostability has not been undertaken due to time constraints as studies on the pyridine-stretched work was the main focus of this thesis (**Chapters 2, 3, 4**).

Chapter 6

Prelimary Studies on Pyridine PNAs: Design and Synthesis of Potential Intermediates

Peptidic nucleic acids (PNAs) are synthetic molecules, designed and synthesized in the early 1990's by Buchardt and Nielsen with the aid of computer-assisted model building. The rationale was to produce a DNA mimic capable of binding with high sequence-specificity to a chosen target whlist being resistant to enzymic degradation *in vivo* (Hyrup & Nielsen 1996; Ray & Noerden 2000). They are DNA analogues with a pseudopeptide backbone consisting of *N*-(2-aminoethyl)glycine units with the bases attached to the glycine nitrogen via carbonyl methylene linkers (**Figure 6.1**). Because of their strong binding affinity for DNA and their biological stability they have been the focus of extensive investigation as potential antigene and antisense therapeutic agents (**Section 1.3**). They have been shown to be capable of high sequence specificity and can form highly stable triplexes with DNA and thus have the potential to selectively suppress gene expression. A wide range of backbone and base modifications have been studied and work has been directed to overcome their potential limitations due to low aqueous solubility and poor cellular uptake (Iwase & Murakami 2002; Koppelhus & Nielsen 2003).

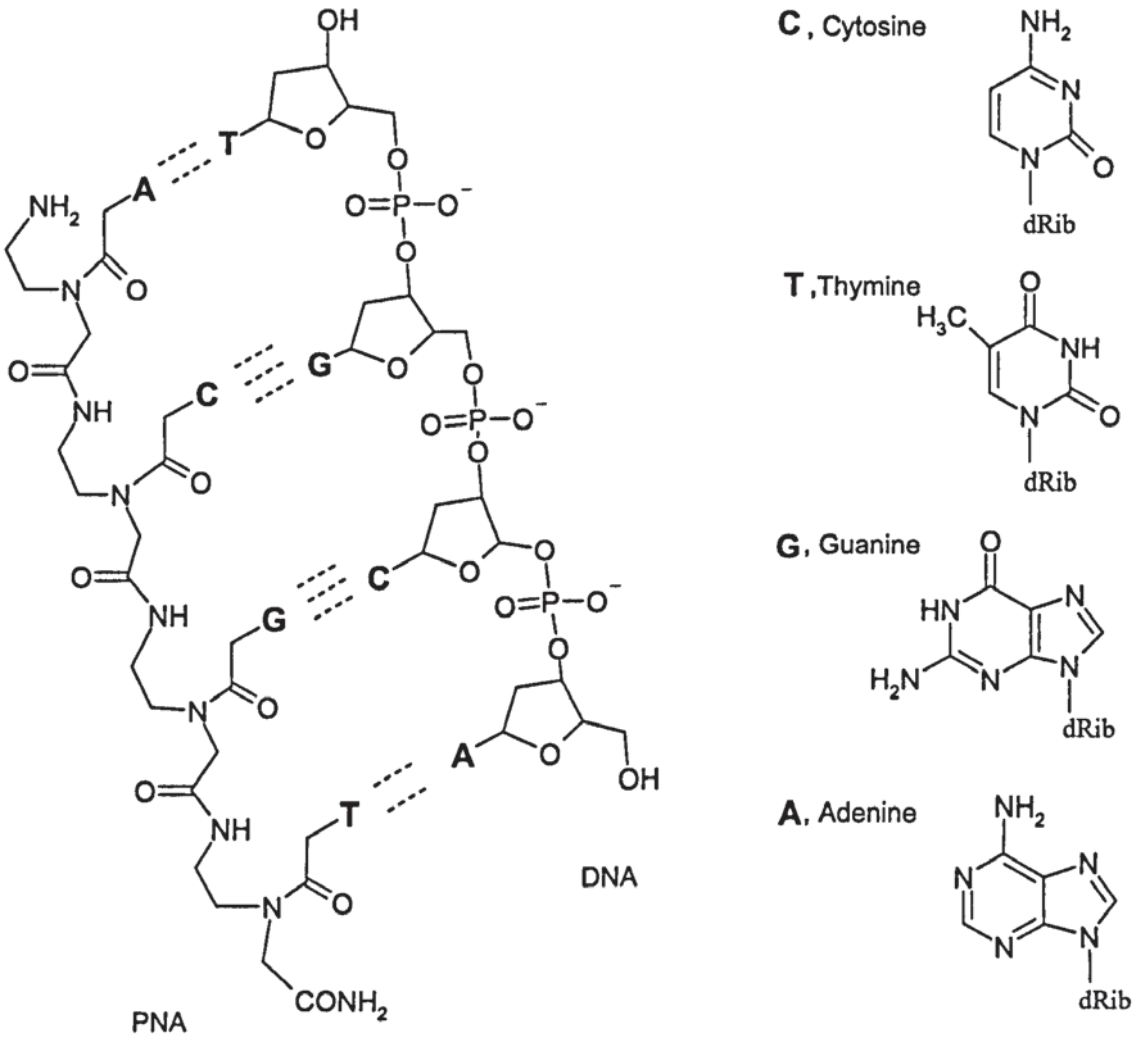

Figure 6.1 Chemical structures of DNA and PNA, where A, C, G and T designate the naturally occurring bases in DNA and dRib represents 2'-deoxyribose.

A PNA_2-DNA triplex is observed from the interaction between a C-rich PNA sequence and a GC-rich DNA duplex. Formation of the required Hoogsteen hydrogen bonds in the triplex needs the cytosine **6.1** to form N3 protonated cytosine (C^+) **6.2**, thus the stability of structures involving C^+*G.C triplets is pH dependent being most stable in the pH range of 5.0-5.5 (**Figure 6.2**).

The synthesis and incorporation into a TFO or a triplex-forming PNA of a neutral analogue of cytosine, able to form the required hydrogen bonding independent of pH, would improve

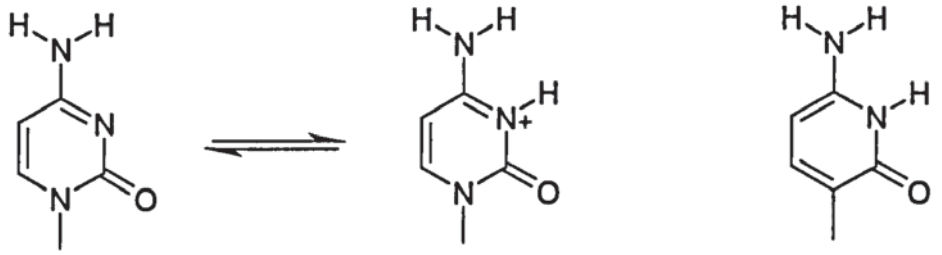

Cytosine **6.1** Cytosine$^+$ **6.2** Pyridine analogue **6.3**

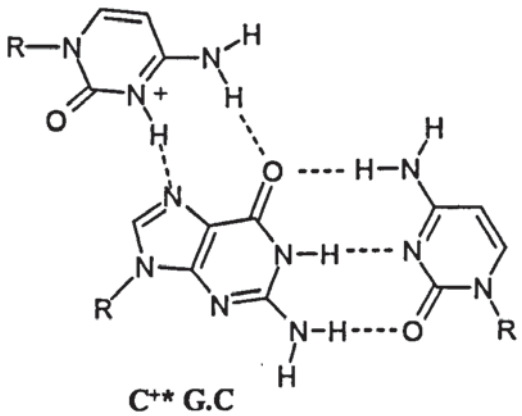

C$^+$* G.C

Figure 6.2 Protonated cytosine triplex with G.C. R is the point of attachment to the relevant sequence of the cytosine analogues.

stability and binding under physiological conditions. Neutral C^+ analogues based on the pyrimidine nucleus such as pseudo-isocytosine **6.9** and 6-oxocytosine **6.10** do produce pH-independent triplex stability, however **6.9** is susceptible to tautomerisation and hence triplex formation can be compromised (Egholm et al. 1995; Hyrup & Nielsen 1996). Recently it has been shown that 1,8-naphthyridine-2,7(*1,8H*)-dione **6.11**, a cytosine analogue which does not need protonation to form Hoogsteen-type triplets, increases triplex stability at pH 7 compared to cytosine and pseudocytosine. Replacement of the pyrimidine nucleus with that of a pyridine **6.3** suggests that tautomerization and pH dependency can be overcome (**Figure 6.3**) (Christensen et al. 2002).

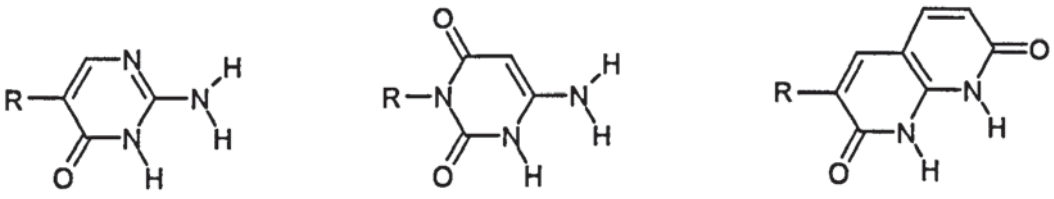

6.9 **6.10** **6.11**

Figure 6.3 Possible pyridine analogues for Cytosine$^+$ which do not require protonation.

A possible route to the proposed C^+ analogue-containing PNA starting from 2,6-difluoropyridine **6.4** is outlined in **Figure 6.4**. With the potential of *ortho* directed lithiation and nucleophilic substitution of fluorine, **6.4**, being commercially available, was considered as a versatile synthon (Queguiner 1994). The conversion of **6.4** to 2-methoxy-6-aminopyridine-3-carboxylic acid has been reported, however the yields were low due to the formation of regioisomers. The reported procedure was followed with the intention of introducing the required side chain at position-3 using ethyl bromoacetate and sequential displacement of the fluoro groups to give the required substituents (Coldwell et al. 1995; Hirokawa 2000; Hirokawa 2003). The synthetic route is outlined in **Scheme 6.1.**

Initially the amination reaction of 2,6-difluropyridine **6.4** gave low yields although no by-products were detected. GLC analysis showed only starting material and product. However, as the reaction scale was increased, a maximum of 50% yield of the 2-amino-5-fluoropyridine **6.5** was obtained. Protection of the amino group as the t-butyl amide **6.6** was near quantitative. The literature states that lithiating **6.6** with n-butyllithium followed by quenching gives an approx. 1:1 mixture of 3- and 5-substituted pyridines (Coldwell 1995). However, following this procedure and quenching with ethyl bromoacetate gave only a complex mixture of products which could not be effectively separated. This was concluded to be due to the susceptibility of the bromo ester to α-lithiation. Using t-butyllithium, lithiation proceeds exclusively *ortho* to the amide group (Queguiner 1994). In order to block this site, the reaction mixture was quenched with trimethylsilyl chloride to give a mixture of the starting amide **6.6** and the required product **6.7** that were separated by

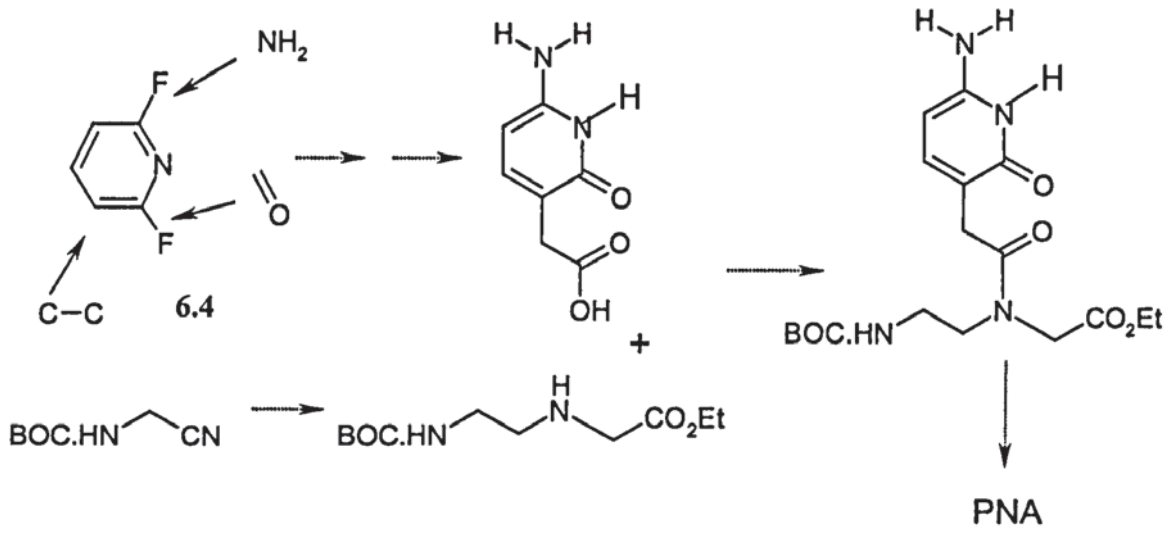

Figure 6.4 Proposed route to pyridine PNA from difluoropyridine.

flash column chromatography. Numerous attempts to lithiate **6.7** *ortho* to the fluoro group, using upto 6 equivalents of t-butyllithium and quenching with methyl iodide failed and, surprisingly, only unreacted starting material could be recovered in any significant quantity from the reaction mixtures (Hirokawa 2000; Hirokawa 2003). Lithiation of 2,6-difluoropyridine **6.4** with LDA and quenching with the bromo ester again gave only inseparable mixtures. In order to determine the efficiency of the lithiation of the pyridine nucleus, the reaction was repeated except methyl iodide was used to quench the reaction mixture to eliminate possible side reactions. Analysis by ^{1}H NMR and ^{19}F NMR of the crude reaction products showed a mixture of starting material, mono- and di-methylpyridines **6.4**, **6.9** and **6.10**, their ratio was readily determined by integration. Rationalization of the results obtained, assuming only mono lithiated species are present, requires LDA to react with methyl iodide slower than the sequential lithiation and quenching of 2,6-difluoropyridine (**Figure 6.5**). Work in this field has been limited due to

the work directed towards the synthesis of pyridine stretched bases (PSBs). However, the work has demonstrated the potential usefulness of difluoropyridine for the synthesis of 2,3,6- and 2,3,4,6-substituted pyridines.

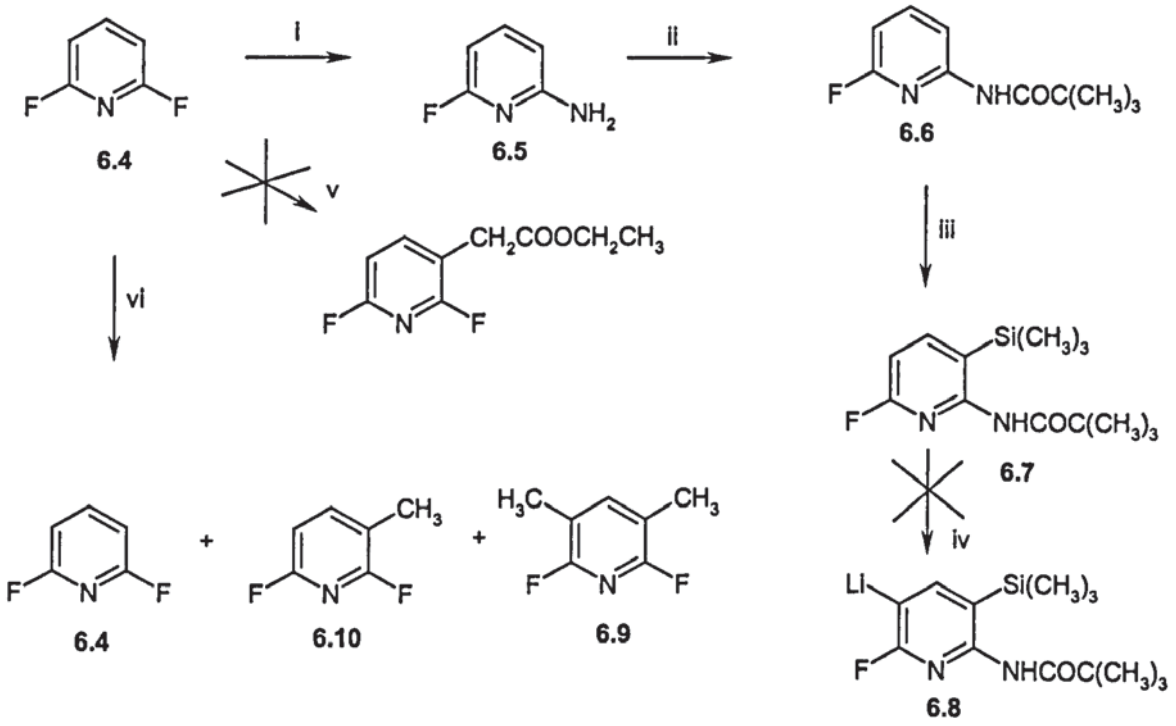

Scheme 6.1 Reactions of 2,6-difluoropyridine. Reagents and conditions, i, conc. NH_3 (aq), Pr^iOH, 120 °C, sealed bomb; ii, $(CH_3)_3CCOCl$, CH_2Cl_2, rt; iii, Bu^nLi, THF, $(CH_3)SiCl$, -78 °C; iv, Bu^tLi, Et_2O, -78 °C, MeI; v, LDA, $BrCH_2COOC_2H_5$, -78 °C; vi, LDA, THF, MeI, -78 °C.

Chapter 7

Experimental

7.1 Materials and methods

NMR spectra were recorded on a Bruker AC-250 spectrometer at ^{1}H (250.1 MHz) referenced to tetramethylsilane (TMS), ^{13}C (62.9 MHz) referenced to dimethylsulphoxide [$(CD_3)_2SO$], ^{31}P (101.3 MHz) referenced to 85% H_3PO_4 (aq) and ^{19}F (235.3 MHz) referenced to CF_3CCl_3. NMR COSY and NOESY experiments were performed on a Jeol 400 instrument. Mass spectra were recorded in atmospheric pressure chemical ionisation ($APCI^{+/-}$) or elecrospray ionisation (ES^{-}) mode with a Hewlett-Packard HP 5989B MS Engine apparatus using a HP 59987A API-electrospray LC/MS interface. Accurate mass measurements were recorded using a LCT Premier MS System. Oligonucleotides were prepared on a Beckman Oligo 1000 DNA Synthesiser following the manufacturer's protocol (Beckmann Instruments Incorporated 1994). HPLC analyses and purifications were carried out on a Hewlett-Packard 1100 instrument using a HPLC Technology C18 Reversed Phase Column. Infrared spectra were recorded using a Mattson Galaxy 2020 FT-IR Spectrophotometer. Ultraviolet spectra were recorded using a Unicam PU8730 Spectrophotometer. Melting points were measured on a Gallenkamp Electrothermal Digital apparatus and are uncorrected. Flash column chromatography was performed using Sorbsil C60 silica using the method described by Still, Kahn and Mitra (1978). Dry column vacuum chromatography was performed with Merck Silica gel 60 (15-40 μm) using the method described by Pedersen and Rosenbohm (2001) (Harwood 1985). TLC was carried

out on pre-coated Merck 60 F254 aluminium-backed plates and visualized using UV (254 and 360 nm) and vanillin reagent: vanillin (6 g), ethanol (250 mL) and conc. sulphuric acid (2mL). Anhydrous solvents were purchased from Aldrich, Fisher or were distilled from the appropriate drying agent. Off-the-shelf reagents and purchased reagents of unspecified purity were checked by TLC and high concentration ^{1}H NMR. If considered suspect, purification by recrystallization, distillation, flash chromatography or by a standard published method was performed (Leonard et al. 1995; Perrin et al. 1980). Air- and water-sensitive reactions were carried out using glassware pre-dried at 250 °C for 2 h, cooled in a dessicator over NaOH with silica gel as an indicator and then purged with argon. Alternatively the glassware was flame dried under an argon purge. For the handling and transferring of air- and/or water-sensitive reagents standard protocols were followed using canullar, syringe and septum techniques with pre-dried equipment (Anon 1994; Leonard et al. 1995).

7.2 Chemical Synthesis

2-Deoxy-1-*O*-methyl-α/β-D-ribofuranose 2.14

To a stirred solution of 2-D-deoxyribose **2.13** (40.0 g, 0.3 mol) in MeOH (600 ml) a solution of acetyl chloride (1.35 ml, 0.02 mol) in MeOH (70 ml) was added dropwise over 20 min at rt. After a further 15 min stirring, Ag_2CO_3 (13.1 g, 0.047 mol) was added and stirring continued for a further 20 min. The resultant mixture was filtered through celite (acid washed) and the filter cake washed with MeOH (3 x 30 ml). The filtrate plus washings were concentrated under reduced pressure and dried under high vacuum to yield

the title compound **2.14** (44.1 g, >99%) as a very light brown oil. TLC analysis (EtOAc-MeOH 4:1) R_f 0.40; ^{1}H NMR [$(CD_3)_2SO$]: δ 1.63, 1.93, 2.23 (2H, 3 x m, 2-CH_2 α,β), 3.20 (1.5H, s, 1-ß-OCH_3), 3.22 (1.5H, s, 1-α-OCH_3), 3.39, 3.48, 3.65 (2H, 3 x m, 5-CH_2 α,β) 3.89, 4.08 (1H, 2 x m, 3-CH α,β), 4.63 (1H, m, 5-OH α,β, D_2O exchangeable), 4.88, 4.94 (1H, 2 x m, 1-CH α,β) 4.85, 4.98 ppm (1H, 2 x br, 3-OH α,β, D_2O exchangeable).

2-Deoxy-3,5-di-*O*-toluoyl-1-*O*-methyl-α/β-D-ribofuranose 2.15

The pentofuranose **2.14** (44 g, 0.3 mol) was co-evaporated twice with pyridine (2 x 140 ml) before being dissolved in dry pyridine (170 ml) and cooled to >0 °C with an ice/NaCl/water bath under argon. *p*-Toluoyl chloride (100 g, 0.65 mol) was added dropwise over 40 min and the resultant pinkish slurry allowed to warm to rt. After stirring for a further 24 h the reaction mixture was evaporated under reduced pressure and concentrated under high vacuum. The residue was partitioned between ether (400 ml) and water (400 ml). The organic layer was washed with 0.5 M HCl (aq) (3 x 200 ml), saturated $NaHCO_3$ (aq) (3 x 200 ml) and 5% NaCl (aq) (3 x 200 ml). The ether layer was dried over anhydrous $MgSO_4$, concentrated under reduced pressure and dried under high vacuum to yield the title compound **2.15** as a clear, light-orange coloured syrup. Further drying under high vacuum on a slowly rotating rotary evaporator caused crystals to slowly form. On further standing the product **2.15** slowly solidified to a pale buff mass (114.6 g, >99%). TLC analysis (EtOAc-Hexane 1:2) R_f 0.49; 0.52. ^{1}H NMR ($CDCl_3$): δ 2.40 (8H, m, 2'-CH_2, 2 x 4-tol-CH_3), 3.36 (1.5H, s, 1'-β-OCH_3), 3.43 (1.5H, s, 1'-α-OCH_3), 4.45 (2H, m, 5'-CH_2), 5.22

(1H, m, 4′-CH), 5.41 (1H, m, 1′-CH), 5.61 (1H, m, 3′-CH), 7.23 (4H, m, 3,5-tol-CH), 7.97 ppm (4H, m, 2,6-tol-CH).

1-Chloro-2-Deoxy-3,5-di-*O*-toluoyl-α-D-ribofuranose 2.16

Method A

Glacial acetic acid (70 ml) was saturated with HCl (g) and the solution cooled to 10-15 °C. The pentofuranose **2.15** (11.3 g, 30.0 mmol) was added as a solution in acetic acid (45 ml) with mechanical stirring. After stirring for a further 20 min the precipitate was filtered, washed with ether (2 x 20 ml) and dried under high vacuum to yield the title compound **2.16** (8.45 g, 73%) as a white powder. Analysis as for method B.

Method B

The pentofuranose **2.15** (50 g, 0.13 mol) was dissolved in glacial acetic acid (150 ml) by stirring at rt for 20 min under argon. The solution was cooled to 10-15 °C and 4 M HCl in dioxane (150 ml, 0.6 mol) was added dropwise over 5 min. The resultant pale, straw-coloured solution was seeded with a small amount of **2.16** and stirred briefly until a precipitate started to form. The stirring was stopped and the reaction mixture stood for 40 min with cooling (ice/water). The resultant white slurry was broken up by swirling the flask and filtered rapidly. The filter cake was packed down, washed with cold ether (3 x 30 ml) and dried under high vacuum to yield the title compound **2.16** (34.1 g, 67%) as a white solid. TLC analysis (EtOAc-Hexane 1:2) R_f 0.58; ^{1}H NMR ($CDCl_3$): δ 2.42 (6H, s, 2 x 4-

tol-CH_3), 2.78 (1H, m, 2′-CH), 2.85 (1H, m, 2′-CH), 4.62 (1H, m, 5′-CH_2), 4.67 (m, 1H, 5′-CH), 4.78 (1H, m, 4′-CH), 5.57 (1H, m, 3′-CH), 6.47 (1H, d, *J* 4.8 Hz, 1′-CH), 7.25 (4H, q, 3,5-tol-CH), 7.96 (4H, q, 2,6-tol-CH) ppm.

4(5)-Nitroimidazole silver salt 2.18

4-Nitroimidazole **2.17** (4.52 g, 40 mmol) was dissolved in conc. NH_3 (aq). (70 ml) to give a clear yellow solution. A solution of silver nitrate (6.8 g, 40 mmol) in water (40 ml) was added dropwise over 20 min with moderate stirring at rt. After stirring for a further 10 min the resultant pale yellow precipitate was filtered off, washed well with ethanol and dried under high vacuum to yield the title compound **2.18** (8.16 g, 93%) as a pale yellow/white chalky powder.

4(5)-Nitroimidazole lithium salt 2.19

A solution of $LiOH.H_2O$ (0.84 g, 20 mmol) in MeOH (10 ml) was added dropwise to a stirred mixture of 4-nitroimidazole **2.17** (2.26 g, 20 mmol) and MeOH (20 ml) at rt. After stirring for a further 30 min the clear dark orange solution was evaporated under reduced pressure and the resultant orange/brown solid was dried under high vacuum to give the title compound **2.19** (2.33 g, 98%). ^{1}H NMR [$(CD_3)_2SO$]: δ 7.34 (1H, s, CH), 7.89 ppm (1H, s, CH); ^{13}C NMR [$(CD_3)_2SO$]: δ 127.4 (CH), 142.7 ppm (CH), (CNO_2) not observed.

4(5)-Nitroimidazole sodium salt 2.20

A solution of NaOH (1.6 g, 40 mmol) in MeOH (10 ml) was added dropwise to a stirred mixture of 4-nitroimidazole **2.17** (4.5 g, 40 mmol) and MeOH (40 ml) at rt. After stirring for a further 10 min a trace of insolubles was filtered off, the clear yellow solution was evaporated under reduced pressure and the residue recrystallised from EtOH to give the title compound **2.20** (4.2 g, 79%) as yellow crystals. ^{1}H NMR [$(CD_3)_2SO$]: δ 7.14 (1H, s, CH), 7.75 ppm (1H, s, CH); ^{13}C NMR [$(CD_3)_2SO$]: δ 131.0 (CH), 145.6 ppm (CH), (CNO_2) not observed.

4(5)-Nitroimidazole cesium salt 2.21

Powdered 4-nitroimidazole **2.17** (15.0 g, 133 mmol) was added to MeOH (150 ml) and stirred at rt. An aqueous solution of CsOH (23.2 ml 50% w/w, 133 mmol) was added dropwise with stirring. After a further 30 min stirring the clear yellow solution was filtered from a trace of insolubles, evaporated under reduced pressure and dried under high vacuum to give the title compound **2.21** (37.7 g, 97%) as a yellow/orange solid. This product was used for the initial comparison experiments with the other nitroimidazole salts but for subsequent work the salt was recrystallised from Pr^{i}OH and dried under vacuum to give the title compound **2.21** as yellow/orange crystals (73% recovery). ^{1}H NMR [$(CD_3)_2SO$]: δ 7.09 (1H, s, CH), 7.71 ppm (1H, s, CH); ^{13}C NMR [$(CD_3)_2SO$]: δ 132.6 (CH), 146.8 ppm (CH), (CNO_2) not observed; ^{13}C NMR DEPT 135 [$(CD_3)_2SO$]: δ 132.6 (+, 2-CH), 146.8 ppm (+, 4(5)-CH); MS (APCI$^-$) *m/z* 112 (M^-).

1-(2'-Deoxy-3',5'-di-*O*-toluoyl-β-D-ribofuranosyl)-4-nitroimidazole 2.24 and 1-(2'-Deoxy-3',5'-di-*O*-toluoyl-α-D-ribofuranosyl)-4-nitroimidazole 2.25

Method A

Sodium hydride 60% in oil (0.61 g, 15.2 mmol) was added to a solution of 4-nitroimidazole **5** (2.0 g, 17.7 mmol) in dry MeCN (40 ml) under argon. After stirring the resultant mixture for 15 min. at rt the protected chlorosugar **4** (6.0 g, 15.4 mmol) was added and stirring continued for a further 1 h. The reaction mixture was then filtered and the insolubles washed with MeCN. The combined filtrate plus washing were evaporated under reduced pressure and dried under high vacuum to yield a crude product mixture (2.79 g). The insolubles were filtered from the reaction and the reaction mixture was stirred with dichloromethane (DCM) (30 ml), filtered and washed with DCM (2 x 20 ml). The filtrate plus washings were evaporated and dried under vacuum to give recovered unreacted, protected chlorosugar **2.16** (3.54 g, 59% recovery). Flash chromatography (EtOAc-Hexane 1:1) was used to separate the crude product mixture into the two isomeric title compounds **2.24** (0.82 g, 28%) and **2.25** (0.47 g, 17%).

Analysis as for method B.

Method B

The silver salt **2.18** (4.7 g, 21.2 mmol) and protected chlorosugar **2.16** (8.23 g, 21.2 mmol) were refluxed (140 °C) together in xylene (120 ml) for 6 h with stirring. After cooling and standing overnight, the reaction mixture was filtered under reduced pressure and the insolubles washed well with $CHCl_3$. The filtrate and washings were removed at up to 60 °C

under high vacuum to yield the crude reaction mixture. Flash column chromatography (EtOAc:Hex 1:1) was used to isolate, from this mixture, two isomeric products, compound **2.24** (3.01 g, 31%) as fine white crystals and compound **2.25** (1.34 g, 14%) as an off-white glassy solid.

Compound **2.24**, TLC analysis (EtOAc-Hexane 1:1) R_f 0.40; mp 116-117.5 °C; ^{1}H NMR [$(CD_3)_2SO$]: δ 2.40 (s, 6H, 4-tol-CH_3), 2.93 (m, 2H, 2′-CH_2), 4.63 (s, 3H, 4′-CH, 5′-CH_2), 5.73 (s, 1H, 3′-CH), 6.43 (t, 1H, *J* 6.6 Hz, 1′-CH), 7.35 (2 x d, 4H, 3,5-tol-CH), 7.92 (2 x d, 4H, 2,6-tol-CH), 8.18 (s, 1H, 5-CH), 8.68 ppm (s, 1H, 2-CH); ^{13}C NMR [$(CD_3)_2SO$]: δ 21.36 (s, 4-tol-CH_3), 37.72 (s, 2′-CH_2), 64.17 (s, 5′-CH), 74.92 (s, 3′-CH), 82.56 (s, 4′-CH), 86.96 (s, 1′-CH), 119.39 (s, 5-CH), 126.63 (s, 4-tol-C), 129.58 (d, tol-CH), 136.44 (s, 2-CH), 144.21 (d, 1-tol-C), 147.77 (s, 4-CNO_2), 165.50 ppm (d, tol-CO); ^{13}C NMR DEPT. [$(CD_3)_2SO$]: δ 21.36 (s, +, 4-tol-CH_3), 37.72 (s, -, 2′-CH_2), 64.17 (s, -, 5′-CH), 74.92 (s, +, 3′-CH), 82.56 (s, +, 4′-CH), 86.96 (s, +, 1′-CH), 119.39 (s, +, 5-CH), 129.58 (d, +, tol-CH), 136.44 ppm (s, +, 2CH).

Compound **2.25**, TLC analysis (EtOAc-Hexane 1:1) R_f 0.27; ^{1}H NMR (d_6-DMSO): δ 2.39 (d, 6H, *p*-tol-CH_3), 2.93 (m, 2H, 2′-CH_2), 4.53 (s, 2H, 5′-CH_2), 5.01 (t, 1H, 4′-CH), 5.64 (s, 1H, 3′-CH), 6.46 (d, 1H, *J* 5.3 Hz, 1′-CH), 7.32 (2 x d, 4H, 3,5-tol-CH), 7.80 (2 x d, 4H, 2,6-tol-CH), 8.13 (s, 1H, 5-CH), 8.62 ppm (s, 1H, 2-CH); ^{13}C NMR [$(CD_3)_2SO$]: δ 21.37 (s, 4-tol-CH_3), 38.85 (s, 2′-CH_2), 64.20 (s, 5′-CH), 74.99 (s, 3′-CH), 84.33 (s, 4′-CH), 88.34 (s, 1′-CH), 119.53 (s, 5-CH), 126.63 (s, 4-tol-C), 129.50 (d, tol-CH), 135.71 (s, 2-CH), 144.25 (d, 1-tol-C), 147.47 (s, 4-CNO_2), 165.44 ppm (d, tol-CO); ^{13}C NMR DEPT. [$(CD_3)_2SO$]: δ 21.35 (s, +, 4-tol-CH_3), 38.85 (s, -, 2′-CH_2), 64.18 (s, -, 5′-CH), 74.94 (s, +, 3′-CH), 84.31

(s, +, 4'-CH), 88.30 (s, +, 1'-CH), 119.50 (s, +, 5-CH), 129.39 (d, +, tol-CH), 135.57 ppm (s, +, 2-CH).

1-(2'-Deoxy-β-D-ribofuranosyl)-4-nitroimidazole 2.38

To a solution of compound **2.24** (0.78 g, 1.7 mmol) in MeOH (30 ml), 40% (aq) $MeNH_2$ (8 ml) was added. The resultant solution was left to stand at rt overnight. The reaction solution was evaporated under high vacuum and the residue purified by flash chromatography (EtOAc-MeOH 9:1) to yield the title compound **2.32** (0.34 g, 87%). A sample was further purified by recrystallisation (EtOAc-MeOH 4:1) for analysis by COSY and NOESY NMR experiments to confirm structure (**Appendix 1**). TLC analysis (EtOAc-MeOH 9:1) R_f 0.42; ^{1}H NMR [$(CD_3)_2SO$]: δ 2.41 (m, 2H, 2'-CH_2), 3.56 (m, 2H, 5'-CH_2), 3.88 (d, 1H, 4'-CH), 4.34 (s, 1H, 3'-CH), 5.08 (t, 1H, 5'-OH), 5.37 (d, 1H, 3'-OH), 6.14 (t, 1H, *J* 6.4 Hz, 1'-CH), 8.11 (s, 1H, 5-CH), 8.59 ppm (s, 1H, 2-CH); ^{13}C NMR [$(CD_3)_2SO$]: δ 41.45 (s, 2'-CH_2), 61.49 (s, 5'-CH_2), 70.61 (s, 3'-CH), 87.17 (s, 4'-CH), 88.56 (s, 1'-CH), 119.58 (s, 5-CH), 136.26 (s, 2-CH), 147.40 ppm (s, 4-CNO_2); ^{13}C NMR DEPT. [$(CD_3)_2SO$]: δ 41.40 (s, -, 2'-CH_2), 61.43 (s, -, 5'-CH_2), 70.56 (s, +, 3'-CH), 87.10 (s, +, 4'-CH), 88.51 (s, +, 1'-CH), 119.55 (s, +, 5-CH), 136.22 ppm (s, 2CH).

1-(2'-Deoxy-α-D-ribofuranosyl)-4-nitroimidazole 2.37

To a solution of compound **2.25** (2.5 g, 5.4 mmol) in MeOH (100 ml), 40% (aq) $MeNH_2$ (25 ml) was added. The resultant solution was left to stand at rt overnight. The reaction solution was evaporated under high vacuum and the residue purified by flash

chromatoghraphy (EtOAc-MeOH 9:1) to yield the deprotected product **2.31** (1.03 g, 84%). A sample was re-purified by flash column chromatography using re-distilled solvents for analysis by COSY and NOESY NMR experiments to confirm the structure (**Appendix 1**). TLC analysis (EtOAc-MeOH 9:1) R_f 0.27; mp 118.5-119.5 °C; ^{1}H NMR [$(CD_3)_2SO$]: δ 1.94 (d, 1H, 2′-CH), 2.69 (q, 1H, 2′-CH), 3.43 (m, 2H, 5′-CH_2) 4.16 (s, 1H, 4′-CH), 4.31 (s, 1H, 3′-CH), 4.91 (t, 1H, 5′-OH), 5.52 (s, 1H, 3′-OH), 6.15 (d, 1H, *J* 7.1 Hz, 1′-CH), 8.06 (s, 1H, 5-CH), 8.56 ppm (s, 1H, 2-CH); ^{13}C NMR [$(CD_3)_2SO$]: δ 41.08 (s, 2′-CH_2), 61.76 (s, 5′-CH_2), 70.83 (s, 3′-CH), 87.95 (s, 4′-CH), 89.83 (s, 1′-CH), 120.01 (s, 5-CH), 136.48 (s, 2CH), 147.36 ppm (s, 4-C); ^{13}C NMR DEPT. [$(CD_3)_2SO$]: δ 41.07 (s, -, 2′-CH_2), 61.75 (s, -, 5′-CH_2), 70.82 (s, +, 3′-CH), 87.95 (s, +, 4′-CH), 89.83 (s, +, 1′-CH), 120.02 (s, +, 5-CH), 136.49 ppm (s, 2CH).

Ratio of product isomers from the glycosylation of chlorosugar 2.16 using metal salts 2.18, 2.19, 2.20 and 2.21 under varying conditions

The chlorosugar **2.16** (0.5 g, 1.3 mmol), 4/5 nitroimidazole salt **2.18, 2.19, 2.20** and **2.21** (2.6 mmol, 2 eq), 4Å molecular sieve (2 g) and dry acetonitrile (20 ml) were charged into an argon-purged dry flask and stirred at rt under argon. Samples were taken periodically and analysed by TLC (Et_2O). When no starting material **2.16** was detected the reaction mixture was filtered through celite. The filtrate and washings were evaporated under reduced pressure and the crude reaction product analysed by ^{1}H NMR. The ratio of the four

possible isomers was estimated from the integration of the anomeric proton signals (**Table 2.1**).

Stability of chlorosugar 2.16 in solution

Solutions of the chlorosugar **2.16** were prepared with the respective deuterated solvents in pre-dried, argon-purged NMR tubes and the tops were sealed with PTFE tape with an overlay of parafilm. The ^{1}H NMR spectra were recorded at intervals over a 24 h period.

1-(2'-Deoxy-3',5'-di-*O*-toluoyl-β-D-ribofuranosyl)-5-nitroimidazole 2.22

A solution of chlorosugar **2.16** (5.0 g, 12.9 mmol) in dry THF (500 ml) was added dropwise to a stirred mixture of 4(5)-nitroimidazole cesium salt **2.21** (3.8 g, 15.5 mmol) and dry THF (500 ml) at 60 °C over 30 min. After stirring at this temperature for a further 2 h the reaction mixture was allowed to cool to rt and filtered through a bed of filter aid. The filtrate and washings were evaporated under reduced pressure. The resultant crude mixture of isomers was dissolved in $CHCl_3$ (50 ml) and loaded onto a flash chromatography column (70 mm ID column, 150 mm silica, packed dry and degassed with a 1:1 mixture of Et_2O and $CHCl_3$) and eluted with a 1:1 mixture of Et_2O and $CHCl_3$. Evaporation of the collected fractions and drying under high vacuum gave the title compound **2.22** (4.1 g, 68%) as a white solid. Evaporation of subsequent fractions gave compound **2.24** (1.2 g, 20%) as a white solid. The structure assignments were comfirmed by NOESY experiments (**Appendix 1**).

Compound **2.22**, TLC analysis (Et_2O-$CHCl_3$ 1:1) R_f 0.49; mp 159-160 °C; υ_{max} (KBr)/cm^{-1} 752, 1092, 1111, 1280, 1374, 1466, 1528, 1723, 2938; ^1H NMR ($CDCl_3$): δ 2.42 (3H, s, 4-tol-CH_3), 2.46 (3H, s, 4-tol-CH_3), 2.52 (1H, m, 2'-CH), 3.12 (1H, m, 2'-CH), 4.74 (3H, m, 5'-CH_2 and 4'-CH), 5.64 (1H, m, 3'-CH), 6.74 (1H, t, *J* 6.3 Hz, 1'-CH), 7.24 (2H, d, 2,5-tol-CH), 7.30 (2H, d, 3,5-tol-CH), 7.84 (2H, d, 2,6-tol-CH), 7.97 (2H, d, 2,6-tol-CH), 8.05 (1H, s, 4-H), 8.11 ppm (1H, s, 2-H); ^{13}C NMR ($CDCl_3$): δ 21.70 (s, 4-tol-CH_3), 21.77 (s, 4-tol-CH_3), 40.86 (2, 2'-CH_2), 63.60 (s, 5'-CH_2), 74.14 (s, 4'-CH), 83.94 (s, 3'-CH), 88.99 (s, 1'-CH), 126.04 (s, 4-tol-C), 126.18 (s, 4-tol-C), 129.56 (d, tol-CH), 134.33 (s, 4-CH), 138.13 (s, 2-CH), 144.60 (s, 1-tol-C), 166.01 ppm (s, C=O); *m/z* (EI) 465 (M^+); Anal. Calcd. for $C_{24}H_{23}N_3O_7$: C, 61.9%; H, 5.0%; N, 9.0%. Found C, 61.7%; H, 4.9%; N, 8.8%.

5-Amino-1-(2'-deoxy-3', 5'-di-*O*-*p*-toluoyl-β-D-ribofuranosyl)-imidazole 2.40

Compound **2.22** (50 mg, 0.11 mmol), 5.0% Pd on C (50 mg) and d_8-THF (1 ml) were vigorously shaken with H_2 at atmospheric pressure and rt. After 2.5 h TLC analysis indicated no starting material remained. The reaction mixture was filtered through a d_8-THF wetted bed of pre-dried sand and filter aid, in a Pasteur pipette, using a slight argon pressure into a dry argon-purged NMR tube. The filter bed was washed with d_8-THF (2 x 0.25 ml). The resultant clear pale yellow solution was analyzed immediately by ^1H NMR. TLC analysis (EtOAc-MeOH-conc. NH_3 (aq). 10:1:1) R_f 0.57; ^1H NMR (d_8-THF): δ 2.37 (3H, s, 4-tol-CH_3), 2.39 (3H, s, 4-tol-CH_3), 2.55 (1H, m, 2'-CH), 2.97 (1H, m, 2'-CH), 4.01 (2H, br s, NH_2), 4.52 (3H, m, 5'-CH_2 and 4'-CH), 5.63 (1H, m, 3'-CH), 6.07 (1H, q, *J* 8.9,

5.4 Hz, 1'-CH), 6.15 (1H, s, 4H), 7.26 (5H, m, 3,5-tol-CH and 2H), 7.92 ppm (4H, d, 2,6-tol-CH).

Purification of ethoxymethylene malononitrile (EMMN) 2.41

EMMN **2.41** (12.0 g) supplied by Aldrich as a soft yellow/orange solid, was dissolved in Et_2O (40 ml) and loaded onto a flash chromatography column (70 mm ID column, 150 mm silica, packed dry and degassed with Et_2O). Elution with Et_2O, evaporation under reduced pressure and drying under vacuum gave **2.41** (4.6 g, 92% recovery) as a light yellow crystalline solid. TLC analysis (EtOAc-MeOH-conc. NH_3 (aq). 10:1:1) R_f 0.52.

5-Amino-4-(2,2-dicyanovinyl)-1-(2'-deoxy-3',5'-di-*O*-*p*-toluoyl-β-D-ribofuranosyl)-imidazole 2.28

Nucleoside **2.22** (8.0 g, 17.2 mmol), 5.0 % Pd on C (6.0 g) and dry THF (100 ml) were vigorously shaken with H_2 at atmospheric pressure and rt. After 2.5 h a sample was removed and TLC analysis indicated a significant spot, due to **2.40** and no starting material. The reaction flask was evacuated and purged with argon. Solid EMMN **2.27** (2.1 g, 17.2 mmol) was added rapidly to the reaction flask. The reaction mixture was resealed and swirled to dissolve and mix. After standing over night under argon the Pd on C was filtered off through a bed of celite (acid washed) and the filter cake washed with hot THF until the washing were near colourless (6 x 40 ml). The yellow/brown filtrate and washings were concentrated under reduced pressure and a maximum liquid temperature of 30 °C. EtOAc (50 ml) was added to the residue and kept in the freezer overnight. The insolubles were filtered off and washed with EtOAc (3 x 20 ml) and Et_2O (1 x 15 ml) to yield the title

compound **2.28** (3.3 g, 37%) as a yellow solid. TLC analysis (EtOAc-MeOH-conc. NH_3 (aq) 10:1:1) R_f 0.73; mp 194-196 °C; υ_{max} (KBr)/cm^{-1} 752, 1112, 1266, 1283, 1354, 1540, 1586, 1715, 2218, 2924, 3348; ^1H NMR [$(CD_3)_2SO$]: δ 2.39 (3H, s, 4-tol-CH_3), 2.41 (3H, s, 4-tol-CH_3), 2.72 (1H, m, 2'-CH), 2.86 (1H, m, 2'-CH), 4.53 (3H, m, 5'-CH_2 and 4'-CH), 5.63 (1H, d, 3'-CH), 6.09 (1H, dd, 1'-CH), 7.34 (2H, d, 3,5-tol-CH_3), 7.38 (2H, d, 3,5-tol-CH_3), 7.72 (2H, br s, NH_2), 7.79 (1H, s, C=CH), 7.83 (1H, s, 2-H), 7.86 (2H, d, 2,6-tol-CH), 7.95 ppm (2H, d, 2,6-tol-CH); ^{13}C NMR [$(CD_3)_2SO$]: δ 21.14 (s, 4-tol-CH_3), 21.17 (s, 4-tol-CH_3), 35.88 (s, 2'-CH_2), 58.63 (s, $C(CN)_2$), 63.96 (s, 5'-CH_2), 74.72 (s, 4'-CH), 81.69 (s, 3'-CH), 82.81 (s,1'-CH), 116.20 (s, 4C), 117.99 (s, CN), 118.56 (s, CN), 126.43 (s, 2 x 4-tol-C), 129.29 (d, tol-CH), 129.47 (2, tol-CH), 134.13 (s, 2-CH), 143.53 (s, C=CH), 143.84 (s, 1-tol-C), 144.08 (s, 1-tol-C), 150.02 (s, 5-C), 165.12 (s, C=O), 165.40 ppm (s, C=O); m/z (ES) 511 (M^+).

5-Amino-6-cyano-3-(2'-deoxy-β-D-ribofuranosyl)-imidazo[4,5-*b*]pyridine 2.29

Method A

Sodium hydroxide (1.0 g, 25 mmol) was dissolved in water (5 ml) and added to a stirred mixture of **2.28** (0.4 g, 0.78 mmol) and MeOH (40 ml). The reaction mixture was warmed to reflux. After 10 min TLC analysis indicated no starting material but one main spot was observed that was strongly fluorescent. The reaction mixture was cooled and neutralised with citric acid (20% w/v aq) to pH 7. The resultant mixture was filtered through a bed of filter aid the filter cake washed well with MeOH. The filtrate and washings were evaporated under reduced pressure. The residue was redissolved in warm MeOH, pre-

adsorbed on silica and purified by flash chromatography (EtOAc-MeOH/conc. NH_3 (aq) 15:1:1) to yield the title compound **2.29** (1.9 g, 88%) as a light yellow green powder. Analysis as for Method B.

Method B

Dowex 1x2-200 ion exchange resin (5.2 g) was stirred with NaOH aq (2 M, 50 ml) for 30 min. The ion exchange resin was filtered off and washed with de-ionised water until the washings were neutral and then washed with MeOH (2 x 40 ml). Suction was applied for 30 min to dry the resin. The prepared resin was added to **2.28** (2.8 g, 5.5 mmol) and MeOH (50 ml) and the resultant mixture stirred at r.t for 3 h. TLC analysis indicated no starting material present but only one fluorescent product spot was observed. The reaction mixture was filtered and the resin washed with hot MeOH (5 x 50 ml, 50 °C). The filtrate and washings were evaporated under reduced pressure. Et_2O (50 ml) was added to the residues. The insolubles were filtered off, washed with Et_2O (2 x 50ml) and dried under high vacuum to yield the title compound **2.29** (1.33 g, 89%) as light fawn-coloured solid. TLC analysis (EtOAc-MeOH-conc. NH_3 (aq) 5:1:1) R_f 0.55; mp 162-163.5 °C; υ_{max} (KBr)/cm^{-1} 940, 1099, 1432, 1576, 1630, 2216, 2923, 3223, 3337; ^1H NMR [$(CD_3)_2SO$]: δ 2.23 (1H, m, 2′-CH), 2.56 (1H, m, 2′-CH), 3.52 (2H, m, 5′-CH_2), 3.82 (1H, d, 4′-CH), 4.36 (1H, s, 3′-CH), 4.95 (1H, t, *J* 5.4 Hz, 5′-OH, D_20 exchangeable), 5.31 (1H, d, *J* 3.5 Hz, 3′-OH, D_2O exchangeable), 6.28 (1H, t, *J* 6.9 Hz, 1′-CH), 6.80 (2H, br s, NH_2, D_2O exchangeable), 8.25 (1H, s, 7-CH), 8.42 ppm (1H, s, 2-CH); ^{13}C NMR [$(CD_3)_2SO$]: δ 39.51 (s, 2′-CH_2), 61.89 (s, 5′-CH_2), 70.99 (s, 4′-CH), 82.71 (s, 3′-CH), 86.26 (s, 5-C), 87.89 (s, 1′-CH), 118.02 (s,

CN), 127.11 (s, C), 134.37 (s, 2-CH), 142.29 (s, 4-CH), 148.96 (s, C), 157.84 ppm (s, C); *m/z* ($APCI^+$) 276 (M+H). Accurate mass: calculated for $C_{12}H_{13}N_5O_3Na$ 298.0916; found 298.0919.

5-Amino-3-(2'-deoxy-β-D-ribofuranosyl)-imidazo[4,5-*b*]pyridine-6-carboxamide 2.30

Method A

Sodium hydroxide (3.0 g, 75 mmol) dissolved in water (15 ml) was added to MeOH (80 ml) followed by **2.28** (1.2 g, 2.3 mmol) and warmed to reflux. After 3 h of refluxing TLC analysis (EtOAc-MeOH-conc. NH_3 (aq) 5:1:1) showed **2.29** as a minor component with **2.30** as the major component and two minor spots of lower R_f value. The reaction mixture was cooled, neutralized with citric acid (20% w/v aq) and filtered. The filtrate and MeOH washings were combined and evaporated under reduced pressure. The residue was pre-adsorbed on silica and separated by flash chromatography (EtOAc-MeOH-conc. NH_3 (aq) 15:1:1). Residual methyl toluate was removed by sublimation (80 °C, 3 h) under high vacuum. A initial fraction of **2.29** (0.20 g, 0.8 mmol) was recovered. The main fraction yielded the title compound **2.30** (0.32 g, 67% based on recovered **2.29**) as an off-white solid. Analysis as for Method B.

Method B

H_2O_2 (2.3 ml 35% w/w, 23 mmol) was added to a stirred mixture of **2.29** (0.63 g, 2.3 mmol) in conc.NH_3 (aq). (25 ml). After stirring at rt for 30 min the reaction became clear. TLC analysis after stirring for 2 h indicated no starting material and only one product spot. The reaction mixture was partially evaporated under reduced pressure, after removal of

excess NH_3 a precipitate formed. The volume was reduced to approx. 10 ml and cooled in the fridge for 2 h. The precipitate was filtered off, washed with MeOH (2 x 5 ml) and dried under high vacuum to yield the title compound (0.53 g, 79%) as a very light yellow solid. TLC and NMR analysis indicated that the product was of high purity and this was thus without further purification. TLC analysis (EtOAc-MeOH-conc. NH_3 (aq) 10:1:1) R_f 0.32; mp 222-223.5 °C; ^{1}H NMR [$(CD_3)_2SO$]: δ 2.24 (1H, m, 2'-CH), 2.65 (1H, m, 2'-CH), 3.55 (2H, m, 5'-CH_2), 3.84 (1H, m, 4'-CH), 4.39 (1H, m, 3'-CH), 5.00 (1H, br, 5'-OH, D_20 exchangeable), 5.27 (1H, br, 3'-OH, D_2O exchangeable), 6.31 (1H, t, *J* 7.0 Hz, 1'-CH), 7.35 (1H, br s, N-H, D_2O exchangeable), 7.99 (1H, br s, N-H, D_2O exchangeable), 8.32 (1H, s, 4-CH), 8.36 ppm (1H, s, 2-CH); ^{13}C NMR [$(CD_3)_2SO$]: δ 45.58 (2'-CH_2), 67.94 (5'-CH_2), 77.05 (4'-CH), 89.99 (3'-CH), 94.28 (1'-CH), 120.59 (s, C), 132.26 (d, CH), 140.99 (s, C), 153.83 (d, CH), 156.48 (s, C), 161.15 (s, C), 168.41 ppm (s, C=O); *m/z* ($APCI^+$) 294 (M+H). Accurate mass: calculated for $C_{12}H_{15}N_5O_4Na$ 316.1022; found 316.1017.

3-(2'-Deoxy-β-D-ribofuranosyl)-8*H*-imidazo[4',5':5,6]pyrido[2,3-*d*]pyrimidin-8-one strI 2.33

Sodium metal (0.35 g, 15.3 mmol) was dissolved in EtOH (pre-dried over 3Å molecular sieve, 15 ml) under argon. Compound **2.30** (0.45 g, 1.53 mmol) and ethyl formate (1.1 g, 15.3 mmol) were added and the reaction mixture was stirred at 65 °C for 1 h. TLC analysis indicated no starting material remained. The reaction mixture was cooled and water (20 ml) added to give a clear colourless solution. Following neutralization with 2M HCl (aq) to pH 7 and upon stirring, the reaction turned cloudy. Stirring was stopped and the reaction

mixture placed in the fridge overnight. The precipitate was filtered, washed with water (2 x 5 ml) and MeOH (2 x 5 ml) and then dried under high vacuum to yield the title compound **2.33** (0.40 g, 85%) as a white chalky solid. The filtrate plus washings were evaporated under reduced pressure. Water (10 ml) was added to the residues and heated to boiling to give a clear solution. On cooling overnight in the fridge a small amount of solid crystallized. Work up as before gave a second small crop of **2.33** (44 mg, total yield 94%) as light yellow fine crystals. TLC analysis (EtOAc-MeOH-conc. NH_3 (aq) 5:2:2) R_f 0.15, (MeOH) R_f 0.66; mp>280 °C; υ_{max} (KBr)/cm^{-1} 807, 1086, 1235, 1392, 1605, 1686, 2925, 3214, 3504; ^{1}H NMR [$(CD_3)_2SO$]: δ 2.38 (1H, m, 2′-CH), 2.79 (1H, m, 2′-CH), 3.63 (2H, m, 5′-CH_2), 3.93 (1H, m, 4′-CH), 4.47 (1H, br s, 3′-CH), 5.03 (1H, br s, 5′-OH), 5.35 (1H, br s, 3′-OH), 6.57 (1H, t, *J* 6.7 Hz, 1′-CH), 8.29 (1H, s, 2-H), 8.73 (1H, s, 6-H), 8.91, (1H, s, 9-H), 12.30 ppm (1H, v br, NH); ^{13}C NMR [$(CD_3)_2SO$]: δ 45.58 (s, 2′-CH_2), 67.94 (s, 5′-CH_2), 77.05 (s, 4′-CH), 89.99 (s, 3′-CH), 94.28 (s, 1′-CH), 120.59 (s, C), 132.26 (s, CH), 140.99 (s, C), 153.83 (s, CH), 156.48 (s, C), 161.15 (s, C), 168.41 ppm (s, C=O); *m/z* (APCI$^+$) 304 (M+H). Accurate mass: calculated for $C_{13}H_{13}N_5O_4Na$ 326.0865; found 326.0870.

Conformational analysis of strI and analogues

Structural formulae representing nucleosides inosine, its benzene-stretched analogue and strI were prepared and subjected to CONFLEX™ minimisation. Two torsion angles corresponding to rotation around the C5'-C4' and glycosidic C1'-N bonds were defined and labelled. Both rotatable bonds were stepped through –120 to +180 degrees in 20 steps of 15

degrees. Each defined structure was geometry optimised using MOPAC PM3. A contour map was constructed by plotting the two torsion angles against energy representing calculated heat of formation. Blue, yellow and red coloration was used to denote, lowest, intermediate and highest energy conformations. The parameters used and keywords specified for the MOPAC PM3 calculations were:

```
**********************************************************************
**                    MOPAC2002 (c) Fujitsu                         **
**********************************************************************
                    PM3 CALCULATION RESULTS
**********************************************************************
*          MOPAC2002 Version 2.20CACHe   CALC.'D. Mon Sep  5 16:45:35 2005
*                          Microsoft(R) Windows 95/98/NT/2000.
* PM3     - THE PM3 HAMILTONIAN TO BE USED
* NOMM    - DO NOT MAKE MM CORRECTION TO CONH BARRIER
* STEP1   - FIRST  STEP-SIZE IN GRID =  15.00
* STEP2   - SECOND STEP-SIZE IN GRID =  15.00
* POINT1  - NUMBER OF ROWS IN GRID = 21
* POINT2  - NUMBER OF COLUMNS IN GRID = 21
* NODIIS  - DO NOT USE GDIIS GEOMETRY OPTIMIZER
* T=      - A TIME OF   10.0 DAYS    REQUESTED
* DUMP=N  - RESTART FILE WRITTEN EVERY  7200.000 SECONDS
* GRAPH   - GENERATE FILE FOR GRAPHICS
**********************************************************************

PM3 NOMM NODIIS GRAPH STEP1=15.000000 POINT1=21 STEP2=15.000000
POINT2=21 + T=10D
```

5'-*O*-(4.4'-Dimethoxytrityl)-3-(2'-deoxy-β-D-ribofuranosyl)-8*H*-imidazo[4',5':5,6]-pyrido[2,3-*d*]pyrimidin-8-one 2.43

After co-evaporation with dry pyridine (2 x 15 ml), strI (0.36 g, 1.2 mmol) was mixed with dry pyridine (20 ml) and DIPEA (0.5 ml, 40 mmol) under argon. DMTCl (2.4 g, 7.1 mmol) was added and the reaction mixture stirred at rt. After 1 h all the strI had dissolved to give a

clear yellow solution and TLC analysis indicated negligible starting material and three significant fluorescent spots which stained brown with vanallin reagent. The reaction mixture was quenched with MeOH (5 ml) and evaporated under high vacuum using a water bath temperature of 40 °C to give viscous orange oil. TLC analysis indicated that the fluorescent spot of highest R_f observed prior to evaporation had degraded and two fluorescent spots were observed, the compound with lower R_f being the major product. Following storage overnight at -20 °C the reaction mixture was separated with dry column vacuum chromatography using gradient elution (5% 2M NH_3-MeOH in EtOAc to 15% 2M NH_3-MeOH in EtOAc) to yield the title compound **2.43** (0.44 g, 61%) as a white solid and a minor fraction which was subsequently identified as the ditritylated derivative. The column was further eluted with EtOAc-MeOH-conc. NH_3 (aq) (10:1:1) to give a second small fraction of **2.43** together with a small amount of recovered starting material strI. TLC analysis (EtOAc-MeOH-conc. NH_3 (aq) 10:1:1) R_f 0.28, (MeOH) R_f 0.66; mp decomp. over 150 °C; ^{1}H NMR [$(CD_3)_2SO$]: δ 2.35 (1H, m, 2′-CH), 2.92 (1H, m, 2′-CH), 3.25 (2H, dd, 5′-CH_2), 3.67 (6 H, d, OCH_3), 4.03 (1H, m, 4′-CH), 4.52 (1H, br s, 3′-CH), 5.39 (1H, d, 3′-OH), 6.57 (1H, t, 1′-CH), 6.63-7.27 (13 H, dd + s, Ar), 8.28 (1H, s, 2-H), 8.70 (1H, s, 6-H), 8.80, (1H, s, 9-H), 12.50 ppm (1H, br, NH); ^{13}C NMR [$(CD_3)_2SO$]: δ 38.50, 54.96, 64.5, 70.77, 83.50, 85.38, 86.50, 114.50, 126.30, 126.53, 127.64, 129.59, 129.80, 134.90, 135.52, 135.62, 144.97, 146.50, 147.50, 150.05, 149.95, 147.99, 162.50; *m/z* (APCI$^-$) 605 (M). Accurate mass: calculated for $C_{34}H_{31}N_5O_6Na$ 628.2172; found 628.2178.

Dityryl derivative, accurate mass: calculated for $C_{55}H_{49}N_5O_8Na$ 930.3479; found 930.3468.

Attempted preparation 5'-*O*-(4.4'-Dimethoxytrityl)-3-(2'-deoxy-β-D-ribofuranosyl)-8*H*-imidazo[4',5':5,6]pyrido[2,3-*d*]pyrimidin-8-one 2.43

Method A

StrI **2.33** (75 mg, 0.25 mmol) was co-evaporated with dry pyridine (2 x 5 ml). Following the addition of dry pyridine (10 ml), 4,4'-dimethoxytrityl chloride **2.45** (100 mg, 0.30 mmol) was then added to the mixture. After stirring under argon at rt for 5 h, TLC analysis indicated a possible minor product plus **2.33** and 4,4'-dimethoxytrityl chloride. Following a further addition of **2.45** (100 mg, 0.30 mmol) the reaction mixture was stirred at rt overnight. TLC analysis indicated unreacted **2.20** and a possible minor product spot comparable to the previous TLC analysis. Attempts to work up the reaction mixture resulted in the recovery of **2.20** but no product was isolated. The reaction was therefore abandonded.

Method B

StrI **2.33** (95 mg, 0.31 mmol) was co-evaporated with dry pyridine (2 x 5 ml). Following the addition of dry pyridine (5 ml), **2.45** (130 mg, 0.38 mmol) and dry N,N-diisopropylethylamine (DIPEA) (38 mg, 0.37 mmol) were added and the resultant mixture stirred under argon for 3 h at rt. TLC analysis indicated negligible reaction. Dry 4-dimethylaminopyridine (DMAP) (46 mg, 38 mmol) was added and the reaction mixture stirred overnight. TLC analysis again indicated negligible reaction. Ammonium perchlorate (130 mg, 38 mmol) was added and then the reaction mixture stirred for a further 4 h. TLC analysis indicated negligible reaction and the reaction was abandoned.

Method C

i) Imidazolium mesylate

A sample of imidazole was initially purified by sublimation under high vacuum. Imidazole (4.0 g, 58.8 mmol) was dissolved in dry DCM (50 ml) at rt. Methanesulphonic acid (5.6 g, 58.8 mmol) was added dropwise with cooling in an ice-water bath. The reaction mixture was then allowed to warm to rt and the precipitate was filtered off. The precipitate was washed with dry DCM (3 x 20 ml) and dried under high vacuum to yield the title compound (8.3 g, 86.1%) as a white powder. ^{1}H NMR [$(CD_3)_2SO$]: δ 2.49 (3H, s), 7.62 (2H, s), 9.03 ppm (1H, s).

ii) Attempted preparation 5'-*O*-(4.4'-dimethoxytrityl)-3-(2'-deoxy-β-D-ribofuranosyl)-8*H*-imidazo[4',5':5,6]pyrido[2,3-*d*]pyrimidin-8-one 2.43

Compound **2.45** (112 mg, 0.33 mmol) was added to a stirred mixture of StrI **2.33** (100 mg, 0.33 mmol), imidazoilium mesylate (108 mg, 0.66 mmol) and DIPEA (85 mg, 0.66 mmol) in dry DMF (2 ml) at r.t under argon. Samples were taken at intervals and analysed by TLC. After stirring for 48 h no significant reaction was detected and the reaction was therefore abandoned.

5'-*O*-(4.4'-Dimethoxytrityl)-3-(2'-deoxy-β-D-ribofuranosyl)-8*H*-imidazo[4',5':5,6] pyrido[2,3-*d*]pyrimidin-8-one 3'-*O*-(2-cyanoethyl)-*N,N*-diisopropyl)-phosphoramidite 2.44

DIPEA (0.18 g, 1.8 mmol) was added to a solution of **2.43** (0.34 g, 0.56 mmol) in dry THF under argon. 2-Cyanoethyl-*N,N*-diisopropylchlorophosphoramidite (0.18 g, 0.76 mmol) was added and the reaction mixture was stirred at rt for 3 h. During which time a precipitate

formed and TLC analysis indicated negligible starting material **2.43** and a new product spot. The reaction mixture was evaporated under reduced pressure and stored over the weekend at -20 °C. The reaction mixture was separated with dry column vacuum chromatography using gradient elution (5% 2 M NH_3-MeOH in EtOAc to 15% 2 M NH_3-MeOH in EtOAc) to yield the crude title compound **2.44** (0.34 g, 75%). Purification by repeated (seven times) precipitation of a DCM solution of **2.44** (3 ml) into petroleum ether (60-80, 300 ml) gave the pure title compound **2.44** (0.23 g, 51%) as a white powder. TLC analysis (EtOAc-2M NH_3 in MeOH 10:1) R_f 0.40; ^1H NMR [$(CD_3)_2SO$]: δ 1.00–1.19 (12 H, m, 4 x CH_3), 2.67 + 2.77 (2 H, d x t, *J* 26.5, 5.8 Hz, CH_2OP), 2.88 (2 H, t, *J* 5.9 Hz, CH_2CN), 3.11 (1 H, m, 2'-CH), 3.18-3.80 (2 H, m, 2 x NCH), 3.65 (6 H, 2s, 2 x CH_3O), 4.05 (2 H, m, 5'-CH_2), 4.18 (1 H, m, 4'-CH), 4.79 (1 H, m, 3'-CH), 6.57 (1H, t, 1'-CH), 6.75-6.61 (4 H, m, Ar), 7.10-7.35 (9 H, m, Ar), 8.30 (1H, s, 2-H), 8.71 (1H, s, 9-H), 8.84, 8.83 (1 H, d, *J* 3.4 Hz, 6-CH); 12.48 (1H, br, NH) ppm; ^{31}P NMR [$(CD_3)_2SO$]: δ 147.8, 148.6 ppm; *m/z* (APCI$^-$) 805 (M^+). Accurate mass: calculated for $C_{43}H_{48}N_7O_7Na$ 828.3251; found 828.3264.

1-Benzyl-4-nitroimidazole 2.46

Method A

Benzyl chloride (5.75 ml, 50 mmol) was added to a stirred mixture of **2.17** (5.6 g, 50 mmol), anhydrous K_2CO_3 (3.45 g, 25 mmol) and dry DMF at rt. The reaction mixture was heated and stirred for 4 h at 70 °C. TLC analysis indicated one main product and one minor component. The reaction mixture was cooled and, following the addition of water (200ml),

extracted with $CHCl_3$ (3 x 50 ml). The combined extracts were washed with water (3 x 50ml) dried over anhydrous $MgSO_4$ and evaporated under reduced pressure to give yellow crystals and a yellow oil. Et_2O (10 ml) was added and the mixture shaken. The insolubles were filtered off, washed with Et_2O (2 x 5 ml) and dried under vacuum to give a first crop of the title compound **2.45** (4.38 g) as an off-white crystalline solid. The Et_2O filtrate and washings were combined mixed and cooled to -20 °C over night to give a second crop of the title compound (1.45 g, total yield 5.83 g, 58%). The analysis is given in method C.

Method B

Benzyl bromide (11.9 ml, 100 mmol) was added dropwise to a stirred solution of **2.17** (5.6 g, 50 mmol), $KOBu^t$ (3.45 g, 25 mmol) and dry DMSO under argon at rt. The reaction mixture was stirred over night and then quenched by pouring onto 200 ml of iced water followed by extraction with $CHCl_3$ (3 x 50 ml). The combined extracts were washed with water (3 x 50 ml) dried over anhydrous $MgSO_4$ and evaporated under reduced pressure to give a yellow slurry which slowly solidified under high vacuum.

Method C

i) 4(5)-Nitroimidazole potassium salt 2.51

Following the procedure outlined for **2.20** above, KOH (1.96 g, 35 mmol) was reacted with **2.17** (3.96 g, 35 mmol). The crude product was recrystallized from a mixture of EtOH and Pr^iOH to yield the title compound as light yellow crystals (2.04 g, 38%). ^1H NMR [$(CD_3)_2SO$]: δ 7.08 (1H, s, CH), 7.70 ppm (1H, s, CH); ^{13}C NMR [$(CD_3)_2SO$]: δ 132.6

(CH), 146.8 (CH); ^{13}C NMR DEPT [$(CD_3)_2SO$]: δ 132.0 (+, CH), 146.3 ppm (+, CH), (CNO_2) not observed.

ii) **1-Benzyl-4-nitroimidazole 2.46**

Benzyl bromide (0.86 g, 5 mmol) was added to a stirred solution of **2.48** (0.76 g, 5 mmol) in dry DMF (10 ml) at rt. A precipitate rapidly formed and after stirring for 1 h TLC analysis indicated one major product and one minor component. The reaction mixture was extracted with $CHCl_3$ (3 x 15 ml) following the addition of water (50 ml). The combined extracts were washed with water (3 x 15 ml), dried over anhydrous $MgSO_4$ and evaporated under reduced pressure. The residue was stirred with Et_2O (5 ml) cooled to -20 °C overnight, filtered, washed with cold Et_2O (2 x 5ml) and dried under high vacuum to yield the title compound **2.46** (0.74 g, 74%) as a light-buff solid. mp 79-80 °C, TLC analysis (Et_2O-petroleum ether (40-60) 2:1) R_f 0.59; ^{1}H NMR ($CDCl_3$): δ 5.20 (2H, s, CH_2), 7.24-7.27 and 7.41-7.42 (5H, 2 x m, H-Ph), 7.54 (1H, s, 2-H), 7.77 ppm (1H, s, 5-H); ^{13}C NMR [$(CD_3)_2SO$]: δ 50.86 (s, CH_2), 121.72 (s, 5-C), 128.08, 128.47 and 129.09 (3 x s, 5 x C(Ph)), 136.44 (s, 1-C-Ph), 137.56 (s, 2-C); ^{13}C NMR DEPT 90 [$(CD_3)_2SO$]: δ 50.86 (s, -, CH_2), 121.72 (s, +, 5-C), 128.08, 128.47 and 129.09 (3 x s, +, 2,3,4,5,6-C-Ph), 136.44 (s, -, 1-C-Ph), 137.56 ppm (s, +, 2-C), 4-CNO_2 not observed; (APCI$^+$) *m/z* 203 (M).

1-Benzyl-5-dichloromethyl-4-nitroimidazole 2.48

A solution of KOBu^t in THF (34 ml 1M, 34 mmol) was added to dry DMF (9 ml) and cooled to –95 °C using a hexane and liquid N_2 slush bath. A solution of 1-benzyl-4-nitroimidazole **2.46** (1.73 g, 8.5 mmol) and $CHCl_3$ (1.1 g, 9.2 mmol) in DMF (5 ml) was

added dropwise. The reaction mixture was stirred at -78 °C for 10 min and quenched by the dropwise addition of AcOH (4.2 ml) in MeOH (9 ml). The resulting mixture was allowed to warm to rt poured into water (100 ml) and extracted with Et_2O (3 x 50 ml). The ether extract was washed with water (3 x 50 ml), dried over anhydrous $MgSO_4$ and evaporated under vacuum. The crude product was purified by flash chromatography (Et_2O-$CHCl_3$-petroleum Ether (40-60) 2:2:1) to give the title compound **2.48** (1.64 g, 67% yield) as light red/brown solid. TLC analysis (Et_2O-$CHCl_3$ 1:1) R_f 0.55; ^1H NMR ($CDCl_3$): δ 5.60 (2H, s, CH_2), 7.24 (1H, s, CCl_2H), 7.33 (2H, m, 2 x CH(Ph)), 7.45 (3H, m, 3 x CH(Ph)), 8.00 ppm (1H, s, 2-CH); ^{13}C NMR [$(CD_3)_2SO$]: δ 50.20 (s, CH_2), 59.19 (s, CCl_2H), 127.88, 128.74 and 129.32 (3 x s, 5 x C(Ph)), 134.24 (s, 1-C-ph), 139.44 ppm (s, 2-C); ^{13}C NMR DEPT 90 [$(CD_3)_2SO$]: δ 50.20 (s, -, CH_2), 59.19 (s, +, CCl_2H), 127.88, 128.74 and 129.32 (3 x s, +, 5 x C(Ph)), 136.24 (s, -, 1-C-ph), 139.44 ppm (s, +, 2-C), 4-CNO_2 and 5-C not observed; ($APCI^+$) *m/z* 284, 286, 288 (M-1).

1-Benzyl-5-formyl-4-nitroimidazole 2.49

1-Benzyl-5-dichloromethyl-4-nitroimidazole **2.48** (0.5 g, 1,75 mmol) was refluxed with formic acid (5 ml, 70% w/v) for 6 h. The reaction mixture was cooled and neutralized with saturated $NaHCO_3$ (70 ml) and extracted with EtOAc (3 x 20 ml). The EtOAc extract was washed with water (2 x 20 ml), dried over anhydrous $MgSO_4$ and evaporated under reduced pressure. The residue was redissolved in EtOAc (20 ml) and treated with activated carbon (0.13 g, 5% by weight) and then filtered through a bed of silica. Evaporation of the filtrate and washings gave 1-benzyl-5-formyl-4-nitroimidazole **2.49** (0.26 g, 66%) as a pale yellow crystalline solid. TLC analysis (Et_2O-$CHCl_3$ 1:1) R_f 0.36; ^1H NMR ($CDCl_3$): δ 5.56 (2H, s,

CH_2), 7.22 (2H, m, 2 x CH(Ph)), 7.39 (3H, m, 3 x CH(Ph)), 7.7.59 (1H, s, 2-CH), 10.49 ppm (1H, s, CHO); MS (APCI$^-$) *m/z* 229 (M-2).

Attempted preparation of 1-benzyl-5-(2,2-dicyanovinyl)-4-nitroimidazole 2.50

The dichloro compound **2.48** (55 mg, 0.19 mmol) was mixed with powdered malononitrile (19 mg, 0.28 mmol) and heated to 95 °C for 90 min at rt under argon. TLC analysis indicated only starting material. Toluene (0.5 ml) and piperidine (2.4 mg, 0.28 mmol) were added and the reaction mixture stirrered for a further 90 min at 95 °C under argon. The water insolubles were extracted with i, $CHCl_3$ ii, EtOAc and iii, MeOH. TLC analysis of these extracts indicated only starting material and base line intractables. The reaction was therefore abandonded.

1-Benzyl-5-(2,2-dicyanovinyl)-4-nitroimidazole 2.50

Malononitrile (0.07g, 1.04 mmol) was added to a solution of the aldehyde **2.49** (0.24 g, 1.04 mmol) in EtOH (5 ml) and CH_2Cl_2(5ml). A catalytic amount of piperidine (1 drop) was added to the stirred solution at rt. Prior to the addition of the piperidine a sample was taken and subsequent TLC analysis indicated that the reaction proceeded rapidly without the piperidine addition. The reaction mixture was evaporated under reduced pressure to give a deep red residue. The product was purified by eluting through a short silica column first with $CHCl_3$, then with Et_2O-$CHCl_3$ 1:1 and finally with EtOAc. The light yellow crystals that formed on standing in some of the fractions (0.09 g) were collected by filtration. A second crop was obtained from evaporation of the product fractions (0.07 g) to

give the title compound **2.50** (55%). TLC analysis (Et_2O-$CHCl_3$ 1:1) R_f 0.20; mp 79.5-81.5 °C ^{1}H NMR [$(CD_3)_2SO$]: δ 5.47 (2H, s, CH_2), 7.30 (2H, m, 2 x CH(Ph)), 7.41 (3H, m, 3 x CH(Ph)), 8.36 (1H, s, 2-CH), 8.78 ppm (1H, s, $CH=C(CN)_2$); ^{13}C NMR [$(CD_3)_2SO$]: δ 49.78 (s, CH_2), 90.41 (s, $C(CN)_2$), 111.30 (s, CN), 112.18 (s, CN), 127.65, 128.60 and 128.95 (3 x s, 5 x C(Ph)), 135.01 (s, 1-C-Ph), 139.69 (s, 2-C), 147.13 ppm (s, $CH=C(CN)_2$); ^{13}C NMR DEPT 135 [$(CD_3)_2SO$]: δ 49.78 (s, -, CH_2), 127.65, 128.60 and 128.95 (3 x s, +, 5 x C (Ph)), 139.69 (s, +, 2-C), 147.13 ppm (s, +, $CH=C(CN)_2$), 4-CNO_2 not observed; (APCI$^+$) *m/z* 280 (M+1) also 322 (M+1+32, MeOH adduct). Accurate mass: calculated for $C_{14}H_8N_5O_2$ 278.0678; found 278.0671.

7.3 Experimental for Chapter 5

2-(2-methyl-5-nitro-imidazoyl)-ethyl-(2-cyanoethyl)-*N,N*-diisopropyl)-phosphor-amidite 5.8

2-Cyanoethyl-*N,N*-diisopropylchlorophosphoramidite (0.37 g, 4.65 mmol) was added to a stirred solution of metronidazole (0.53 g, 3.1 mmol) and diisopropylamine (0.31 g, 9.1 mmol) in dry THF (15 ml) under argon. After stirring for 1 h at rt the reaction mixture was evaporated under reduced pressure and dried under high vacuum. The phosphoramidite **5.8** (1.02 g, 89%) was isolated by flash column chromatography (EtOAc) and dried under high vacuum. TLC analysis (EtOAc) R_f 0.38; ^{1}H NMR [$(CD_3)_2SO$]: δ 1.03 (12H, q, 4 x CH_3), 2.50 (3H, s, CH_3), 2.71 (2H, t, CH_2), 3.43 (2H, m, OCH_2), 3.62 (2H, m, $N(CH)_2$), 3.85 (2H, m, OCH_2), 4.51 (2H, t, CH_2), 8.04 ppm (1H, s, 4-H); ^{31}P NMR [$(CD_3)_2SO$]: δ 51.45 ppm (s).

Synthesis of CPG bound, protected dT_8 metronidazole conjugate 5.9

Synthesis of **5.9** was carried out on a 1 μmol scale using phosphoramidite **5.8** (0.10 M solution in acetonitrile), succinyl CPG solid support and Beckman reagents. The standard cycle and coupling times recommended by the manufacturer were used (Beckmann Instruments Incorporated 1994).

Attempted deprotection and cleavage from CPG of dT_8-metronidazole conjugate: synthesis of conjugate 5.10.

The solid supported conjugate (10 mg, 0.24 μmol of oligonucleotide) from the DNA synthesiser was gently agitated with conc. NH_3 (aq) (0.5 ml) for 16 h at 60 °C. After filtering off the solid support, the filtrate was evaporated and the product dried overnight on a vacuum concentrator to give **5.10.**

HPLC analysis was carried out using gradient elution, with a flow rate of 1 ml min^{-1}, using an HPLC Technology C18 Reversed Phase Column (250 x 4.6mm) with solvent system A mixed with solvent system B (0-40%) during 20 min. A was composed of 1 M aqueous TEAA (10%) and MeCN (2%) at pH 7.0 and B was composed of 1 M aqueous TEAA (10%) and MeCN (80%) at pH 7.0; R_t 11.6 min.

Mass spectroscopy was carried out using negative ion electrospray analysis with the oligonucleotide samples dissolved in weakly basic NH_3 (aq) solution; Calculated mass 2492.4, found 2494.1.

1 M triethylammonium acetate buffer for HPLC

To about 300 mL of water, triethylamine (69.7 mL) was added and the mixture stirred. Acetic acid (28.6 mL) was then added slowly. Water was added to increase to total volume of solution to about 490 mL. The pH of the buffer was monitored using a pH meter whilst acetic acid was added dropwise until pH 7.0 was achieved. To this water was then added and the solution was made upto 500 mL.

BUFFER A: 2% CH_3CN in 0.1 M triethylammonium acetate buffer

To about 200 mL of water, 1.0 M triethylammonium acetate buffer stock solution (50 mL) was added. To this CH_3CN (10 mL) was added and the solution was made up to a total volume of 500 mL with HPLC grade water.

BUFFER B: 80% CH_3CN in 0.1 M triethylammonium acetate buffer

To 100 mL of water, 1.0 M triethylammonium acetate buffer stock solution (50 mL) was added. The solution was made up to a total volume of 500 ml with CH_3CN.

Deprotection and cleavage of dT_8-metronidazole conjugate from solid support: synthesis of 5.11

Deprotection was carried out using 17 mg of the solid supported conjugate from the DNA synthesiser by gently agitating with pyridine (0.8 ml) containing 20% Et_3N for 2 h at rt and then evaporating to dryness under high vacuum.

To cleave from solid support the deprotected, solid supported conjugate was agitated with 0.5 ml conc. NH_3 (aq) for 30 min. After filtering off the solid support, the filtrate was evaporated and the product dried overnight on a vacuum concentrator to give **5.11.**

HPLC analysis; conditions as for **5.10**; R_t 13.3 min.

Mass spectroscopy; conditions as for **5.10**; calculated mass 2603.4, found 2604.2.

The HPLC profile of a mixture of oligonucleotides **5.10, 5.11** and dT_8 gave three distinct peaks (**Figure 5.2**).

Attempted synthesis and isolation of the reduction products of metronidazole by catalytic hydrogenation

Catalytic hydrogenation of metronidazole was attempted under the following conditions. The catalyst loading is given as % by weight based on the weight of metronidazole taken;

i) 10% Pd/C (10% loading), methanol solvent, 1atm hydrogen pressure.

ii) 10% Pd/C (10% loading), methanol solvent, 50 psi hydrogen pressure.

iii) 10% Pd/C (25% loading), ethanol solvent, 50 psi hydrogen pressure.

iv) Raney Ni (10% loading), methanol solvent, 1 atm hydrogen pressure.

In all cases, attempts to work-up the reaction mixture, separate and identify the reaction products gave low yields of complex mixtures and intractable solids.

Nickel boride

Nickel acetate tetrahydrate (5 g, 20 mmol) was dissolved in water (75 ml) and sodium borohydride (3.02 g, 80 mmol dissolved in 40 ml water) was added dropwise with stirring

over 30 min at 10-15 °C. The black precipitate was filtered, washed with water (3 x 25 ml), washed with ethanol (50 ml) and dried under vacuum to yield nickel boride (1.4 g). The exact structure is not known but ratio of nickel to boron gives an empirical formula of Ni_2B (yield 55%).

Note: prolonged drying over phosphorus pentoxide under high vacuum is reported to produce a pyrophoric material (Seltzman & Berrang 1993).

Attempted reduction of metronidazole using nickel boride

Metronidazole (27 mg, 1.6 mmol) was added to a stirred mixture of nickel boride (500 mg, 3.9 mmol) in methanol (28 ml) at rt. After addition of hydrochloric acid (1 M, 7 ml) the reaction mixture was heated and stirred for 30 min at 60 °C. Following neutralization with NH_3 (aq), the insolubles were filtered off and the filtrate extracted with ether. The extract was dried and concentrated under vacuum. As with previous reduction attempts, separation by flash chromatography yielded numerous fractions containing small quantities of complex mixtures and the reaction was therefore abandoned.

7.4 Experimental for Chapter 6

2-Amino-6-fluoropyridine 6.5

2,6-Difluoropyridine (15 g, 130 mmol), conc. NH_3 (aq) (30 ml), Pr^iOH (30 ml) and a magnetic follower were charged into a steel bomb. The reaction mixture was stirred and heated to 120 °C for 6 h. After cooling the reaction mixture was dissolved in water and extracted with ether. Evaporation under reduced pressure and drying under high vacuum

gave the crude product **6.5** (7.6 g, 52%) as light grey crystals which were used without further purification. TLC analysis (Et_2O-petroleum ether (40-60) 1:2) R_f 0.17; mp 62-64 °C; ^1H NNR ($CDCl_3$): δ 4.82 (2H, s, 1 x NH_2), 6.15 (2H, 2 x dd, 3H and 5H), 7.46 (1H, q, 4H); ^{19}F NMR ($CDCl_3$): δ 5.11 (s, F) ppm.

***N*-(2-(6-Fluoro)pyridyl)-2,2-dimethylpropionamide 6.6**

To a stirred solution of crude **6.5** (2.3 g, 20.6 mmol) in dry CH_2Cl_2 (20 ml) at 0 °C, trimethyl acetyl chloride (3.0 g, 24.7 mmol) followed by Et_3N (2.5 g, 24.7 mmol) were added. The reaction mixture was allowed to warm to rt and stirred overnight. Following the addition of water, the mixture was extracted with Et_2O. The combined Et_2O extracts were dried over anhydrous $MgSO_4$ filtered and the solvent evaporated to yield the crude product. Sublimation under high vacuum at 60 -70 °C gave the purified product **6.6** (3.64 g, 90%) as off-white crystals. TLC analysis (Et_2O-petroleum ether (40-60) 1:2) R_f 0.47; mp 98.5-100 °C; ^1H NMR ($CDCl_3$) δ 1.31 (9H, s, $C(CH_3)$), 6.65 (1H, dd, 5-H), 7.82 (1H, q, 4-H), 7.90 (1H, br s, NH), 8.11 ppm (1H, dd, 3-H).

***N*-(2-(6-Fluoro-3-trimethylsilyl)pyridyl)-2,2-dimethylpropionamide 6.7**

To stirred solution of compound **6.6** (1.1 g, 5.1 mmol) in dry Et_2O (50 ml) at -78 °C, under argon, was added Bu^tLi, 1.7 M in pentane (8.2 ml, 12.75 mmol). After stirring for 4 h Me_3SiCl (1.22 g, 10.2 mmol) was added and the reaction mixture allowed to warm to rt. After the addition of water, the mixture was extracted with Et_2O. The combined extracts were dried over anhydrous $MgSO_4$ and evaporated under reduced pressure.

Recrystallisation of the residue from petroleum ether (60-80) gave the product **6.7** (0.74 g, 54%) as off white crystals. TLC analysis (Et_2O-petroleum ether (40-60) 1:2) R_f 0.39; ^1H NMR ($CDCl_3$): δ 0.32 (9H, s, $Si(CH_3)_3$), 1.33 (9H, s, $C(CH_3)_3$), 6.79 (1H, dd, 5-H), 7.65 (1H, br s, NH), 7.94 ppm (1H, t, 4-H).

2,6-Difluoro-3-methylpyridine 6.10 and 2,6-difluoro-3,5-dimethylpyridine 6.9

To a stirred solution of diisopropylamine (0.24 g, 2.4 mmol) in dry THF cooled to -10 °C under argon, Bu^nLi, 1.5 M in hexane (1.6 ml, 2.4 mmol) was added. After 15 min the solution was cooled to -78 °C and **6.4** (0.25 g, 2.2 mmol) was added dropwise. Stirring was continued for 30 min before MeI (0.33 g, 2.3 mmol) was added dropwise. After a further 30 min the reaction mixture was allowed to warm to rt before the addition of water and Et_2O extraction with Et_2O. The Et_2O extract was dried over anhydrous $MgSO_4$, filtered and evaporated at a temperature upto 80 °C. Analysis of the crude reaction product (0.35 g) by ^1H and ^{19}F NMR showed it to be a mixture of **6.4, 6.10, 6.9,** THF and diisopropylamine, the molar ratio of **6.4, 6.10, 6.9** being 1.9:2.3:1. ^1H NMR ($CDCl_3$): δ (region 6.0 to 8.50), 6.74 (1H, dd, 5-H **6.10**), 6.84 (2H, d, 3,5-H **6.4**), 7.51 (1H, t, 4-H **6.9**), 7.72 (1H, q, 4-H **6.10**), 7.93 ppm (1H, qu, 4-H **6.4**); ^{19}F NMR ($CDCl_3$): δ -1.89 (2F, s, 2,6-F **6.9**), 2.46 (1F, s, 2-F **6.10**), 3.56 (1F, s, 6-F **6.10**), 7.78 ppm (2F, s, 2,6-F **6.4**).

7.5 Thermal melting experiments

7.5.1 Preparation of UV stock solutions for thermal analysis

The following buffer solution was prepared for UV thermal analysis:

$MgCl_2.6H_2O$ (100 mM), NaCl (1000 mM), Tris.HCl (250 mM) and spermine (5 mM) at pH 7.0.

7.5.2 Preparation of oligonucleotide solutions for UV thermal analysis

Appropriate aliquots of quantified oligonucleotide solutions in water were added to the cuvette followed by the stock buffer for thermal analysis. Water was then added to give a final concentration of 2.5 or 1.8 μM for each oligonucleotide in the sample (1600 μL final volume). A minature magnetic stirrer was added to the cuvette and the solution was stirred during 5 min and sonicated during 15 min before UV thermal analysis.

7.5.3 UV thermal analysis

Thermal UV analysis of antisense oligonucleotides was conducted using a Varian Cary 1E UV-Visible Spectrophotometer with a 12 sample heating block having a temperature range (-10 °C to >100 °C). All samples were stirred continuously during data acquisition. At low temperatures, condensation and frosting were prevented by passing a dry stream nitrogen over the UV cuvettes.

The 1 cm UV cuvette containing the oligonucleotide/buffer samples was placed in the heating block and heated at a rate of 0.5 °C per min from 20 °C to 80 °C. It was then cooled from 80 °C to 0 °C and re-heated to 80 °C. The last two ramps were repeated three times. Absorbance against temperature readings were recorded digitally at 0.5 °C intervals by Cary Thermal Analysis software and a Compaq personal computer.

References

Ali, H., Ouellet, R., DaSilva, J. N., Lier, J. E. (1993) Synthesis of steroidal nitroimidazoles as site-specific radiosensitizers. *J. Chem. Res (S)* 92-93.

Al-Shaar, A. H. M., Chambers, R. K., Gilmour, D. W., Lythgoe D. J., McClenaghan, I., Ramsden, C. A. (1992) The synthesis of heterocylces via addition elimination reactions of 4-aminoimidazoles and 5-aminoimidazoles. *J. Chem. Soc., Perkin Trans. 1* 2789-2811.

Anon (1994) Handling air-sensitive reagents. *Aldrich Technical Information Bulletin AL-134.*

Arcamone, F., Penco, S., Orezzi, P., Nicolella, V., Pirelli, A. (1964) Structure and synthesis of distamycin A. *Nature* **203**: 1064-1065.

Asensio, J. L., Lane, A. N., Dhesi, J., Bergqvist, S., Brown, T. (1998) The contribution of cytosine protonation to the stability of parallel DNA triple helices. *J. Mol. Biol.* **275**: 811-822.

Atkinson, T., Smith M. (1984) Solid phase synthesis of oligodeoxyribonucleotides by the the phosphite-triester method. In: Gait, M. J. (ed) *Oligonucleotide synthesis: a practical approach* Oxford: IRL Press, 35-81.

Azhayev, A. V., Antopolsky, M. L. (2001) Amide group assisted 3'-dephosphorylation of oligonucleotides on universal A-supports. *Tetrahedron* **57**: 4977-4986.

Balzarini, J., Herdewijn, P., De Clercq. E. (1989) Differential patterns of intracellular metabolism of 2',3'-didehydro-2',3'-dideoxythymidine and 3'-azido-2',3'-dideoxythymidine, 2 potent anti-human immunodeficiency virus compounds. *J. Biol. Chem.* **264**: 6127-6133.

Bansal, M. (2003) DNA structure: Revisiting the Watson-Crick double helix. *Current Science* **85**: 1556-1563.

Barresinoussi, F., Chermann, J. C., Rey, F., Nugeyre, M. T., Chamaret, S., Greust, J., Dauguet, C., Axlerblin, C., Vezinetbrun, F., Rouzioux, C., Rozenbaum, L., Montangnier, L. (1983) Isolation of a T-lymphotropic retrovirus from a patient at risk of aquired immune-deficiency syndrome (AIDS). *Science* **220**: 868-871.

Baxter, R. L. (2005) Nucleic acids. *University of Edinburgh* [online]
Available from:
http://www.chem.ed.ac.uk/teaching/undergrad/chemistry4/lectures/moduleN/NA/nalecture notes.pdf

Beckman Instruments Incorporated (1994) Oligo 1000 DNA syntheziser operating instructions 015-249129-D (USA).

Beaucage, S. L., Caruthers, M. H. (1981) Deoxynucleoside phosphoramidites-A new class of key intermediates for deoxypolynucleotide synthesis. *Tetrahedron Lett.* **22**: 1859-1862.

Beaucage, S. L., Iyer R. P. (1992) Advances in the synthesis of oligonucleotides by the phosphoramidite approach. *Tetrahedron* **48**: 2223-2311.

Beaucage, S. L., Iyer R. P. (1993a) The functionalisation of oligonucleotides via phsophoramidite derivatives. *Tetrahedron* **49**: 1925-1963.

Beaucage, S. L., Iyer R. P. (1993b) The synthesis of modified oligonucleotides by the phosphoramidite method and their applications. *Tetrahedron* **49**: 6123-6194.

Beaucage, S. L., Iyer R. P. (1993c) The synthesis of specific ribonucleotides and unrelated phosphorylated biomolecules by the phosphoramidite method. *Tetrahedron* **48**: 10441-10488.

Bhat C. C. (1968) *Synthetic Procedures in Nucleic Acid Chemistry* **1**: 521-522.

Bobbitt J. M., Doolittle, (1964) Copyrine and isoquinoline systems. *J. Org. Chem.* **29**: 2299-2302.

Bobbitt J. M., Scola D. A. (1960) Synthesis of isoquinoline alkaloids. II. *J. Org. Chem.* **25**: 560-564.

Bowater, R. P. (2003) DNA structure. *Encyclopedia of the Human Genome.* Nature Publishing Group:Macmillan Publishers Ltd, 1-9.

Breslauer, K. J. (1986) Methods for obtaining thermodynamic data on oligonucleotide transitions. In: Hinz, H. -J. (ed) *Thermodnamic data for biochemistry and biotechnology.* Berlin:Springer-Verlag, 402-427.

Brotschi, C., Mathis, G., Leumann, C. J. (2005) Bipyridyl- and biphenyl-DNA: a recognition motif based on interstrand aomatic stacking. *Chem. Eur. J.* **11**: 1911-1923.

Brown, T., Brown, D. J. S. (1991) Modern machine-aided methods of oligodeoxyribonucleotide synthesis. In Eckstein, F. (ed) *Oligonucleotides and analogues: a practical approach.* Oxford: IRL Press, 1-23.

Buchini, S., Leumann, C. J. (2003) Recent improvements in antigene technology. *Curr. Opin. Chem. Biol.* **7**: 717-726.

Chargaff, E., Vischer, E. (1948) Nucleoproteins, nucleic acids, and related substances. In Luck J. M. (ed) *Annual Review of Biochemistry* **17**: 201-226.

Chen, B. C., Chao, S. T., Sundeen J. E., Tellew J., Ahmad, S. (2002) Vicarious nucleophilic substitution of 1-benzyl-5-nitroimidazole, application to the synthesis of 6,7-dihydroimidazo[4,5-*d*][1,3]diazepin-8(3*H*)-one. *Tetrahedron Lett.* **43**: 1595-1596.

Chin, T. -M., Huang, L -K., Kan, L. -S. (1997) Improved synthesis of of halofuranose derivatives with the desired α configuration. *Chin. Chem. Soc. (Taipei)* **44**: 413-416.

Christensen, C., Eldrup, A. B., Haaima, G., Nielsen, P. E. (2002) 1,8-Naphthyridin-2,7-(1,8*H*)-dione is an effective mimic of protonated cytosine in peptide nucleic acid triplex recognition systems. *Bioorg. Med. Chem. Lett.* **12**: 3121-3124.

Clayton, R. (2001) The synthesis of nucleoside analogues from nitroimidazole precursors. PhD Thesis, Keele University.

Clayton, R., Davis, M. L., Fraser, W., Li, W., Ramsden, C. A. (2002) Synthesis of pyridine-stretched 2'-deoxynucleosides. *Synlett* 1483-1486.

Coldwell, M. C., Gadre, A., Jerman, J., King, F. D. Nash, D. (1995) The synthesis of dopamine D-2 and serotonin 5-HT_3 receptor affinity of 3-aza analogs (pyridyl) of 4-amino-5-chloro-2-methoxybenzamides. *Bioorg. Med. Chem. Lett.* **5**: 39-42.

Connor, T. H., Stoeckel, M., Evrard J., Legator M. S. (1977) The contribution of metronidazole and two metabolites to the mutagenic activity detected in urine of treated humans and mice. *Cancer Res.* **37**: 629-633.

Crozet, M. D., Perfetti, P., Kaafarani, M., Vanelle, P., Crozet, M. P. (2002) A new synthetic approach for novel 4-substituted-5-nitroimidazoles. *Tetrahedron Lett.* **43**: 4127-4129.

Dachs G. U., Abratt V. R., Woods, D. R. (1995) Mode of action of metronidazole and a *Bacteroides-fragilis* meta resistance gene in *E. coli. J. Antimicrob. Chemother.* **35**: 483-496.

Darby R. A. J., Sollogoub M., McKeen C., Brown L., Risitano A., Brown N., Barton C., Brown T., Fox K. R. (2002) High throughput measurement of duplex, triplex and quadruplex melting curves using molecular beacons and a LightCycler. *Nucleic Acids Res.* **30**, e39.

de Abreu, F. C., Ferraz P. A. D., Goulart, M. O. F. (2002) Some applications of electrochemistry in biomedical chemistry. Emphasis on the correlation of electrochemical and bioactive properties. *J. Braz. Chem. Soc.* **13**: 19-35.

Debin, A., Laboulais, C., Ouali, M., Malvy, C., Le Bret, M., Svinarchuk, F. (1999) Stability of G,A triple helices. *Nucleic Acids Res.* **27**: 2699-2707.

Dervan, P. B. (2001) Molecular recognition of DNA by small molecules. *Bioorg. Med. Chem.* **9** 2215-2235.

Devivar, R. V., Koontz, S. L., Peltier, W. J., Pearson, J. E. (1999) A new solid support for oligonucleotide synthesis. *Bioorg. Med. Chem. Lett.* **9**: 1239-1242.

Dhimitruka, I., SantaLucia, J. (2004) Efficient preparation of 2-deoxy-3,5-di-*O*-*p*-toluoyl-alpha-D-ribofuranosyl chloride. *Synlett* 335-337.

Doronina, S. O., Behr, J. P. (1997) Towards a general triple helix mediated DNA recognition scheme. *Chem. Soc. Rev.* **26**: 63-71.

Edwards, D. I. (1993) Nitroimidazole drugs-action and resistance mechanisms I. Mechanisms of action. *J. Antimicrob. Chemother.* **31**: 9-20

Egholm, M., Christensen, L., Dueholm, K. L., Buchardt, O., Coull, J., Nielsen, P. E. (1995) Efficient pH-independent sequence-specific DNA binding by pseudoisocytosine-containing bis-PNA. *Nucleic Acids Res.* **23**: 217-222.

Fearon, K. L., Hirschbein, B. L., Chiu, C. –Y., Quijano, M. R., Zon, G. (1997) Phosphorothioate oligodeoxynucleotides: large-scale synthesis, impurity characterization, and the effects of phosphorus stereochemistry. In: Chadwick D. J., Cardew, G. (eds) Oligonucleotides as therapeutic agents. Chichester: Wiley.

Felsenfeld, G., Davis, D. R., Rich, A. (1957) Formation of a three-stranded polynucleotide molecule. *J. Am. Chem. Soc.* **79**: 2023–2024.

Franklin, R. E., Gosling, R., (1953a) Evidence for 2-chain helix in crystalline structure of sodium deoxyribonucleate. *Nature* **172**: 156-157.

Franklin, R. E., Gosling, R. (1953b) Molecular configuration in sodium thymonucleate. *Nature* **171**: 740–741.

Fujitsu Corporation (2005) *CaChe Worksystem Pro Version 6.1.10.*

Gacy, A. M., Goellner, G. M., Spiro, C., Chen, X., Gupta, G., Bradbury, E. M., Dyer, R. B., Mikesell, M. J., Yao, J. Z., Johnson, A. J., Richter, A., Melancon, S.B., M^{c}Murry, C. T. (1998) GAA instability in Friedreich's Ataxia shares a common, DNA-directed and intraallelic mechanism with other trinucleotide diseases. *Molecular Cell* **1**: 583-593.

Gait, M., J., Pritchard C., Slim, G. (1991) Oligoribonucleotide synthesis. In: Eckstein, F. (ed) Oligonucleotides and analogues: a practical approach. Oxford: IRL Press.

Gao, J., Liu, H., Kool, E. T. (2004) Expanded-size bases in naturally sized DNA: evaluation of steric effects in Watson-Crick pairing. *J. Am. Chem. Soc.* **126**: 11826-11831.

Gao, J., Liu, H., Kool, E. T. (2005) Assembly of the complete eight-base artifical genetic helix, xDNA and its interaction with the natural genetic system. *Angew. Chem. Int. Ed. Engl.* **44**: 3118-3122.

Ghosh, A., Bansal, M. (2003) A glossary of DNA structures from A to Z. *Acta Crystallogr.* **D59**: 620–626.

Ghosh, S., Defrancq. E., Lhomme, J. H., Dumy, P., Bhattacharya, S. (2004) Efficient conjugation and characterization of distamycin-based peptides with selected oligonucleotide stretches. *Bioconjugate. Chem.* **15**: 520-529.

Glen Research (2006) Catalog: products for DNA research. Virginia. Available online: http://www.glenres.com/Catalog/Catalog06.pdf [Accessed September 2005]

Greig, M., Klopchin, P., Griffey, R., Hughes, J. (1996) Desalting of oligonucleotides for electrospray mass spectroscopy: application note. USA: Hewlett Packard, 1-6.

Groebke, K., Hunziker, J., Fraser, W., Peng, L., Diederichsen, U., Zimmermann, K., Holzner, A., Leumann, C., Eschenmoser, A. (1998) Why pentose- and not hexose-nucleic acids? Part V. (purine-purine)-base pairing in the homo-DNS-series: guanine, isoguanine, 2,6-diammopurine and xanthine. *Helvetica Chimica Acta* **81**: 375-474.

Hadd, H. E., Kokosa J. M. (2003) Purification of 1α-bromotriacetylglucuronate methyl ester. *Adrichchimica Acta* **36**: 2.

Haider, S., Parkinson, G. N., Neidle, S. (2002) Crystal structure of the potassium form of an oxytricha nova G-quadruplex. *J. Mol. Biol.* **320**: 189-200.

Harwood, L. M. (1985) "Dry column" flash chromatography. *Aldrichimica Acta* **18**: 25.

Hélène, C. (1994) Rational design of sequence-specific DNA ligands for artificial control of gene expression *Pure & Appl. Chem.* **66**: 663-669.

Herold, M., Hummel, M. (1991) Purification of synthetic oligonucleotides by HPLC: application note. USA: Hewlett Packard, 1-4.

Hirokawa, Y., Fujiwara, I., Suzuki, K., Harada, H., Yoshikawa, T., Yoshida, N., Kato, S. (2003) Synthesis and structure-affinity relationships of nNovel *N*-(1-ethyl-4-methylhexahydro-1,4-diazepin-6-yl)pyridine-3-carboxamides with potent serotonin 5-HT_3 and dopamine D_2 receptor antagonistic activity. *J. Med. Chem.* **46**: 702-715.

Hirokawa, Y., Horikawa, T., Kato, S. (2000) An efficient synthesis of 5-bromo-2-methoxy-6-methylaminopyridine-3-carboxylic acid. *Chem. Pharm. Bull.* **48**: 1847-1853.

Hoffer, M. (1960) α-Thymidin. *Chem. Ber.* **93**: 2777-2783.

Hoogsteen, K. (1963) The crystal and molecular structure of a hydrogen-bonded complex between 1-methylthymine and 9-methyladenine. *Acta Crystallogr.* **16**: 907–916.

Horwitz, J. P., Chua, J., Noel, M. (1964) Nucleosides.V. The monomesylates of 1-(2'-deoxy-beta-D-lyxofuranosyl) thymidine. *J. Org. Chem.* **29**: 2076-2078.

Huang, C. –Y., Miller, P. S. (1993) triplex formation by an oligodeoxynucleotide containing N^4-(6-aminopyridyl)-2'-deoxycytidine. *J. Am. Chem. Soc.* **115**: 10456-10457.

Huang, C. –Y., Bi, G., Miller, P. S. (1996) Triplex formation by oligonucleotides containing novel deoxycytidine derivatives. *Nucleic Acids Res.* **24**: 2606-2613.

Hubbard, A. J., Jones, A. S., Walker, R. T. (1984) An investigation by H-1-NMR spectroscopy into the factors determining the beta-alpha ratio of the product in 2'-deoxynuceloside synthesis. *Nucleic Acids Res.* **12**: 6827-6837.

Humphries, M. J., Ramsden, C. A. (1990) A Fresh AIR synthesis. *Synthesis* 985-992.

Humphries, M. J., Ramsden, C. A. (1995) A short synthesis and biomimetic transformation of 5-aminoimidazole ribonucleoside (AIRs). *Synlett* 203-204.

Hunter, C. A., Saunders, J. K. M. (1990) The nature of π -π interactions. *J. Am. Chem. Soc.* **112**: 5525-5534.

Hyrup, B., Nielsen, P. E. (1996) Peptide nucleic acids (PNA): synthesis, properties and potential applications. *Bioorg. Med. Chem.* **4**: 5-23.

Iwase, R., Murakami, A. (2002) Synthesis, properties and functions of peptide nucleic acids (PNA) and their derivatives. *J. Syn. Org. Chem. Jpn.* **60**: 1179-1189.

James, P. L., Brown, T., Fox, K. R. (2003) Thermodynamic and kinetic stability of intermolecular triple helices containing different proportions of C^+.GC and T.AT triplets. *Nucleic Acids Res.* **31**: 5598-5606.

Keppler, M. D., Fox, K. R. (1997) Relative stability of triplexes containing different numbers of T.AT and C^+.GC triplets. *Nucleic Acid Res.* **25**: 4644-4649.

Khorana, H. G. (1968) Nucleic acid synthesis. *Pure Appl. Chem.* **17**: 349-381.

Knauert, M. P., Glazer. P. M. (2001) Triplex forming oligonucleotides: sequence-specific tools for gene targeting. *Hum. Mol. Genet.* **10**: 2243-2251.

Koppelhus, U., Nielsen, P. (2003) Cellular delivery of peptide nucleic acid (PNA). *Advanced Drug Delivery Rev.* **55**: 267-280.

La-Scalea, M. A., Serrano, S. H., Ferreira, E. I., Oliveira Brett, A. M. (2002) Voltammetric behavior of benznidazole at a DNA-electrochemical biosensor. *J. Pharm. Biomed. Anal.* **29**: 561-568.

Le Doan, T. L., Perrouault, L., Praseuth, D., Habhoub, N., Decout, A., Thuong, N. T., Lhomme, J., Hélène, C. (1987) Sequence-specific recognition, photo-cross-linking and cleavage of the DNA double helix by an oligo-[alpha]-thymidylate covalently linked to an azidoproflavine derivative. *Nucleic Acids Res.* **15**: 7749-7760.

Lee, A. H. F., Gao, J., Kool, E. T. (2005) Novel benzopyrimidines as widened analogues of DNA bases. *J. Org. Chem.* **70**: 132-140.

Lee, A. H. F., Kool, E. T. (2005) A new four-base genetic helix, yDNA, composed of widened benzopyrimidine-purine pairs. *J. Am. Chem. Soc.* **127**: 3332-3338.

Lee, J. S., Woodsworth, M. L., Latimer, L. J., Morgan, A. R. (1984) Poly(pyrimidine).poly(purine) synthetic DNAs containing 5-methylisocytosine form stable triplexes at neutral pH. *Nucleic Acids Res.* **12**: 6603-6614.

Leonard, J., Lygo, B., Procter G. (1995), *Advanced Practical Organic Chemistry 2nd Edition* Blackie Academic and Professional, Chapman and Hall, Alden Press.

Leonard, N. J. (1982) Dimensional probes of enzyme-coenzyme binding-sites. *Acc. Chem. Res.* **15**: 128-135.

Leonard, N. J., Hiremath, S. P. (1986) Dimensional probes of binding and activity. *Tetrahedron* **42**: 1917-1961.

Leonard, N. J., Sprecker, M. A., Morrice, A. G. (1976) Defined dimensional changes in enzyme substrates and cofactors – synthesis of *lin*-benzoadenosine and enzymatic evaluation of derivatives of benzopurines. *J. Am. Chem. Soc.* **98**: 3987-3994.

Lessor, R. A., Leonard, N. J. (1981) Synthesis of 2'-deoxynucleosides by deoxygenation of ribonucleosides. *J. Org. Chem.* **46**: 4300-4301.

Letsinger, R. L., Finnan, J. L., Heavner, G. A., Lunsford, W. B. (1975) Nucleotide chemistry. XX. phosphite coupling procedure for generating internucleotide links *J. Am. Chem. Soc.* **97**: 3278-3279.

Lin, K. -Y., Jones, R. J., Matteucci, M. (1995) Tricyclic 2'-deoxycytidine analogs: syntheses and incorporation into oligodeoxynucleotides which have enhanced binding to complementary RNA. *J. Am. Chem. Soc.* **117**: 3873-3874.

Linkletter, B. A., Szabo, I. E., Bruice, T. C. (2001) Solid-phase synthesis of oligopurine deoxynucleic guanidine (DNG) and analysis of binding with DNA oligomers. *Nucleic Acids Res.* **29**: 270-2376.

Link Technologies (2005) Tools for molecular biology. Bellshill.
Available from:
http://www.linktech.co.uk/Downloads/2005%20Product%20Guide.pdf
[Accessed July 2005].

Liu, H., Gao, J., Kool, E. T. (2005a) Size-expanded analogues of dG and dC: synthesis and pairing properties in DNA. *J. Org. Chem.* **70**: 639-647.

Liu, H., Gao, J., Kool, E. T. (2005b) Helix-forming properties of size-expanded DNA, an alternative four-base genetic form. *J. Am. Chem. Soc.* **127**: 1396-1402.

Liu, H., Gao, J., Lynch, S. R.., Saito, Y. D., Maynard, L., Kool, E. T. (2003) A four-base paired genetic helix with expanded size. *Science* **302**: 868-871.

Liu, H., Gao, J., Maynard, L., Saito, Y. D., Kool, E. T. (2004a) Toward a new genetic system with expanded dimensions: size-expanded analogues of deoxyadenosine and thymidine. *J. Am. Chem. Soc.* **126**: 1102-1109.

Liu, H., He, K., Kool, E. T. (2004b) yDNA: A new geometry for size-expanded base pairs. *Angew. Chem. Int. Ed. Engl.* **43**: 5834-5836.

Liu, H., Lynch, S. R., Kool, E. T. (2004c) Solution structure of xDNA: a paired genetic helix with increased diameter. *J. Am. Chem. Soc* **126**: 6900-6905.

Liu, E., Song, F., Fan, J. (2005c) A novel fluorescent sensor for triplex DNA. *Bioorg. Med. Chem. Lett.* 15: 255-257.

Lyamichev, V. I., Mirkin, S. M., Frank-Kamenetskii, M. D. (1986) A pH-dependent structural transition in the homopurine-hompyrimidine tract in superhelical DNA. *J. Biomol. Struct. Dyn.* **3**: 327-338.

Makosza, M. (1997) Synthesis of heterocyclic compounds via vicarious nucleophilic substitution of hydrogen. *Pure Appl. Chem.* **69**: 559-564.

Makosza, M, Owczarczyk, Z. (1989) Dihalomethylation of nitro arenes via vicarious nucleophilic substitution of hydrogen with trihalomethyl carbanions. *J. Org. Chem.* **54**: 5094-5099.

Marx, A., Summerer, D. (2004) Bigger DNA: new double helix with expanded size. *Angew. Chem. Int. Ed. Engl.* **43**: 1625-1626.

Matteucci, M. D., Caruthers, M. H. (1981) Nucleotide chemistry. 4. Synthesis of deoxyoligonucleotides on a polymer support. *J. Am. Chem. Soc.* **103**: 3185-3191.

Matulic-Adamic, J., Beigelman, L. (2000) An improved synthesis of inosine 3'-phosphoramidite. *Synth. Commun.* **30**: 3963-3969.

M^{c}Bee, E. T., Wesseler, E. P., Hodgins, T. (1971) Reaction of trichloromethyllithium with 4-halonitrobenzenes *J. Org. Chem.* **36**: 2907-2909.

M^{c}Killop, A. (1983) 4- and 5-Nitroimidazoles: ^{13}C NMR assignment of structure *Tetrahedron* **39**: 3797-3799.

Menendez, D., Rojas, E., Herrera, L. A., Lopez, M. C., Sordo, M., Elizondo, G., Ostrosky-Wegman, P. (2001) DNA breakage due to metronidazole treatment. *Mutation Res.* **478**: 153-158.

Merrifield, B. (1963) Solid phase peptide synthesis. I. The synthesis of a tetrapeptide. *J. Am. Chem. Soc.* **85**: 2149-2154.

Michelson, A. M., Todd, A. R. (1955) Nucleotides part XXXII. Synthesis of a dithymidine dinucleotide containing a 3' : 5'-internucleotidic linkage. *J. Chem. Soc.* 2632-2638.

Mirkin, S. M. (1999) Structure and biology of H DNA. In: Malvy, C., Harel-Bellan, A., Pritchard, L. L. (eds) *Triple Helix Forming Oligonucleotides* London: Kluwer Academic Press, 193-222.

Mirkin, S. M., Frank-Kamenetskii, M. D. (1995) Triplex DNA structures. *Annu. Rev. Biochem.* **64**: 65-95.

Mirkin, S. M., Lyamichev, V. I., Drushlyak, K. N., Dobrynin, V. N., Filippov, S. A., Frank-Kamenetskii, M. D. (1987) DNA H-form requires a homopurine homopyrimidine mirror repeat. *Nature* **330**: 495-497.

Mohanty, D., Bansal, M. (1993) Conformational polymorphism in G-tetraplex structures: strand reversal by base flipover or sugar flipover. *Nucleic Acids Res.* **21**: 1767-1774

Montgomery, J. A. (1982) Studies on the biologic activity of purine and pyrimidine analogs. *Medicinal Research Rev.* **2**: 271-308

Moser, H. E., Dervan, P. B. (1987) Sequence-specific cleavage of double helical DNA by triple helix formation. *Science* **238**: 645-650.

Obika, S., Nakagawa, O., Hiroto, A., Hari, Y., Imanishi, T. (2003) Synthesis and properties of a novel bridged nucleic acid with a P3'→N5' phosphoramidate linkage, 5'-amino-2',4'-BNA. *Chem. Commun.* 2202-2203.

Oliveira, R. B., Passos, A. P. F., Alves, R. O., Romanha, A. J., Prado, M. A. F., de Souza Filho, J. D., Alves, R. J. (2003) *In vitro* evaluation of the activity of aromatic nitrocompounds against *Trypanosoma cruzi*. *Memorias-Inst. Oswaldo Cruz* **98**: 141-144.

Ostrowski, S. (1999) Synthesis of *N*-7-substituted purines from imidazole precursors. *Molecules* **4**: 287-309.

Parel, S. P., Leumann, C. J. (2001) Triple-helix formation in the antiparallel binding motif of oligodeoxynucleotides containing N^9- and N^7-2-aminopurine deoxynucleodides. *Nucleic Acids Res.* **29**: 2260-2267.

Parrick, J., Porssa, M. (1993) Synthesis of a nitro oligo-*N*-methylimidazole carboxamide derivative: a radiosensitiser targeted to DNA. *Tetrahedron Lett.* **34**: 5011-5014.

Parrick, J., Porssa, M. (1995) Synthesis of polyaminederivatives of 2-nitroimidazole as DNA-directed radiosensitisers. *J. Chem. Res. (S)* 186-187.

Parrick, J., Porssa, M., Davies, L. K., Dennis, M. F. (1993) Targeting radiosensitizers to DNA by minor groove binding: nitroarenes based on netropsin and distamycin. *Bioorg. Med. Chem. Lett.* **3**: 1697-1702.

Pauling, L., Corey, R. B. (1953) A proposed structure for the nucleic acids. *Proc. Nat. Acad. Sci., USA* **39**: 84–97.

Pedersen, D. S., Robenbohm, C. (2001) Dry column vacuum chromatography. *Synthesis* 2431-2434.

Pendland, S. L., Piscitelli, S. C., Schreckenberger, P. C., Danziger, L. H. (1994) *In vitro* activities of metronidazole and its hydroxy metabolite against *Bacteroides spp. Antimicrob. Agents Chemother.* **38**: 2106-2110.

Perrin, D. D., Armarego, W. L. F., Perrin. D. R. (1980) *Purification of Laboratory Chemicals 2nd Edition*. Oxford: Pergamon Press.

Petersson, B., Nielsen, B. B., Rasmussen, H., Larsen, I. K., Gajhede, M., Nielsen, P. E., Kastrup, J. S. (2005) Crystal structure of a partly self-complementary peptide nucleic acid (PNA) oligomer showing a duplex-triplex network. *J. Am. Chem. Soc.* **127**: 1424-1430.

Piccirilli, J. A., Krauch, T., Moroney, S. E., Benner, S. A. (1990) Enzymatic incorporation of a new base pair into DNA and RNA extends the genetic alphabet. *Nature* **343**: 33-37.

Pingoud, A, Fliess, A., Pingoud V. (1989) HPLC of oligonucleotides. In Oliver, R. W. A. (ed) *HPLC of macromolecules: a practical approach* Oxford: IRL Press.

Pon, R. T., Usman, N., Ogilvie, K. K. (1988) Derivatization of controlled pore glass beads for solid phase oligonucleotide synthesis. *Biotechniques* **8**: 768-775.

Pon, R. T., Yu, S. (1997) Hydroquinone-O,O' diacetic acid as a more labile replacement for succinic acid linkers in solid-phase oligonucleotide synthesis. *Tetrahedron Lett.* **38**: 3327-3330.

Portes-Sentis, S., Sergeant, A., Gruffat, H. (1997) A particular DNA structure is required for the function of a cis-acting component of the Epstein-Barr virus OriLyt origin of replication. *Nucleic Acid Res.* **25**: 1347-1354.

Queguiner, G., Marais, F. (1994) Directed metalation of pi-deficient azaaromatics: Strategies of functionalization of pyridines, quinolines and diazines. In Katritzky, AR (ed): *Ad. Heterocylic Chem.* **52**: 187-231.

Radhakrishnan, I., Patel D. J. (1993) Solution structure of a purine.purine.pyrimidine DNA triplex containing G.GC and T.AT triples. *Structure* **1**: 135-152.

Rajappan, V. P., Schneller, S. W. (2001) An 8-aminoimidazo[4,5-*g*]quinazoline carbocyclic nucleoside: a ring-extended analog of 5'-noraristeromycin. *Tetrahedron* **57**: 9049-9053.

Ranasinghe, R. T., Rusling, D. A., Powers, V. E. C, Fox, K. R., Brown, T. (2005) Recogntion of CG inversions in DNA triple helices by methylated 3*H*-pyrrolo[2,3-d]pyrimidin-2(7*H*)-one nucleoside analogues. *Chem. Commun.* 2555-2557.

Ray, A., Noerden, B. (2000) Peptide nucleic acid (PNA): its medical and biotechnical applications and promise for the future. *FASEB J.* **14**: 1041-1060.

Reysset, G. (1996) Genetics of 5-nitroimidazole resistance in bacteroides species. *Aearobe* **2**: 59-69.

Riether, S., Jeltsch, A. (2002) Specificity of DNA triple helix formation analyzed by FRET assay. *BMC Biochemistry* **3**: 27-35.

Risitano, A., Fox, K. R. (2003) The stability of intramolecular DNA quadruplexes with extended loops forming inter- and intra-loop duplexes. *Org. Biomo. Chem.* **1**: 1852-1855.

Rojanasakul, Y. (1996) Antisense oligonucleotide therapeutics: drug delivery and targeting *Advanced Drug Delivery Reviews* **18**:115-131.

Saenger, W. (1984) *Principles of nucleic acid structure* New York: Springer-Verlag, 116-158.

Seley, K. L., Januszczyk, P., Hagos, A., Zhang, L., Dransfield, D. T. (2000) Synthesis and antitumor activity of thieno-separated tricyclic purines. *J. Med. Chem.* **43**: 4877-4883.

Seltzman, H. H., Berrang B. D. (1993) Nickel boride reduction of aryl nitro compounds. *Tetrahedron Lett.* **34**: 3083-3086.

Siddiqui, S., Gustafson, B., Hosmane, R. S. (1999) A new synthetic approach toward ring-expanded ("fat") purine nucleobases: synthesis and use of 5-dichloromethyl-1-*p*-methoxybenzyl-4-nitroimidazole as a versatile intermediate. *Third International Electronic Conference on Synthetic Organic Chemistry (ECSOC-3)* [online]. www.mdpi.org/ecsoc-3.htm [accessed 2003]

Simmonds, R. J. (1992) *Chemistry of biomolecules: an introduction.* Cambridge: The Royal Society of Chemistry, 137-139.

Simon, H., Förtsch, I., Burckhardt, G., Gabrielyan, A., Birch-Hirschfeld, E. Stelzner, A., Prévot-Halter, I., Leumann, C., Zimmer, C. (1999) Triple Helix Formation Inhibits Gyrase Activity. *Antisense & Nucleic Acid Drug Development* **9**: 527-531.

Simons, C. (2001a) *Nucleoside Mimetics, their chemistry and biological properties* Gordon & Breach: Overseas Publishers Association, 20-22.

Simons, C. (2001b) *Nucleoside Mimetics, their chemistry and biological properties* Gordon & Breach: Overseas Publishers Association, 83-102.

Singleton, S. F., Dervan, P. B. (1994) Temperature dependence of the energetics of oligonucleotide-directed triple helix formation at single DNA site. *J. Am. Chem. Soc.* **116**: 10376-10382.

Sinha, N. D., Biernat, J., McManus, J., Köster, H. (1984) Polymer supported oligonucleotide synthesis 18. Use of a beta-cyanoethyl-*N*,*N*-dialkylamino-*N*-morpholino phosphoramidite of deoxynucleosides for the synthesis of DNA fragments simplifying deprotection and isolation of the final product. *Nucleic Acids Res.* **12**: 4536-4557.

Sørensen, J. J., Nielsen, J. T., Petersen, M. (2004) Solution structure of a dsDNA:LNA triplex. *Nucleic Acids Res.* **32**: 1-8.

Soyfer, V. N., Potaman, V. N. (1996) *Triple-helical nucleic acids* New York: Springer, 100-150.

Stewart, J. J. P. (1989) Optimization of parameters for semi-empirical methods. 1. Method. *J. Comp. Chem.* **10**: 209-220.

Still, W. C., Kahn, M., Mitra, A. (1978) Rapid chromatographic technique for preparative separations with moderate resolution. *J. Org. Chem.* **43**: 2923-2925.

Sullivan, C. (1982) Synthesis of 1-(2-hydroxyethyl)-2-methyl-5-aminoimidazole: a ring-intact reduction product of metronidazole. *Biochem. Pharm.* **31**: 2689-2691.

Tocher, J. H. (1997) Reductive activation of nitroheterocyclic compounds. *Gen. Pharmacol.* **28**: 485-487.

Townson, S. M., Boreham, P. F. L., Upcroft, P., Upcroft, J. A. (1994) Resistance to nitroheterocyclic drugs. *Acta Trop. (Basel)* **56**: 173-194.

Vlieghe, D., Van Meervelt, L., Dautant, A., Gallois, B., Precigoux, G., Kennard, O. (1996) Parallel and antiparallel (G GC)-2 triple helix fragments in a crystal structure. *Science* **273**: 1702-1705.

Vischer, Z., Chargaff, E. (1949) Microbial nucleic acids: the desoxypentose nucleic acids of avian *Tubercle bacilli* and yeast. *J. Biol. Chem.* **177**: 429-438.

Walsh, A. J. (1999) Synthesis of triplex-forming oligonucleotide conjugates of the anticancer drug temodal. PhD Thesis, Aston University.

Walsh, A. J., Clark, G. C., Fraser, W. (1997) A direct and efficient method for derivatisation of solid supports for oligonucleotide synthesis. *Tetrahedron Lett.* **38**:1651-1654.

Watson, J. D., Crick, F. H. C. (1953a) Molecular structure for nucleic acids: a structure for deoxyribose nucleic acid. *Nature* **171**: 737–738.

Watson, J. D., Crick, F. H. C. (1953b) Genetical Implications of the structure of Deoxyribonucleic Acid. *Nature* **171**: 964-967.

Wiberg, K. B. (1953) The mechanism of hydrogen peroxide reactions. I. The conversion of benzonitrile to benzamide. *J. Am. Chem. Soc.* **75**: 3961–3964.

Wilkins M. H. F., Stokes A.R., Wilson, H. R. (1953) Molecular Structure of Deoxypentose Nucleic Acids. *Nature* **171**: 738-740.

Willis, R. C. (2004). Boundless biotech: new technology fostered the biotechnology revolution. *Enterprise of the Chemical Science* 99-104. Occasional publication from ACS [online].
Available from:
http://pubs.acs.org/supplements/chemchronicles2/ [Accessed 2005]

Wright D. E., Podmore M. L., Chambers R. K., McKillop. A. (1983) 4- and 5-nitroimidazoles: ^{13}C NMR assignment of structure. *Tetrahedron* **39**: 3797-3800.

Appendix 1: ^{1}H nmr spectrum of nitroimidazole nucleoside **2.22**

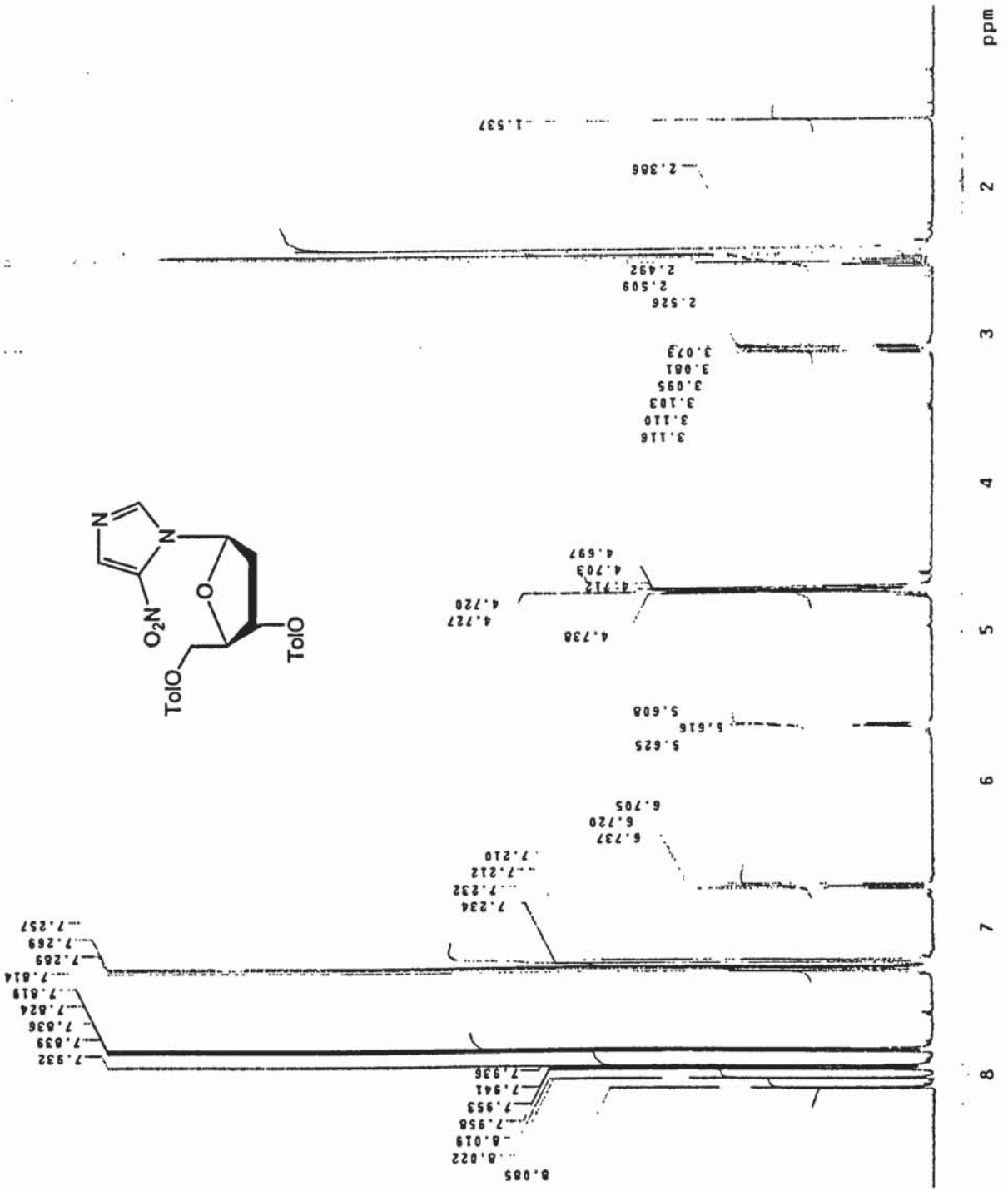

Appendix 1: NOESY spectrum of nitroimidazole nucleoside **2.22**

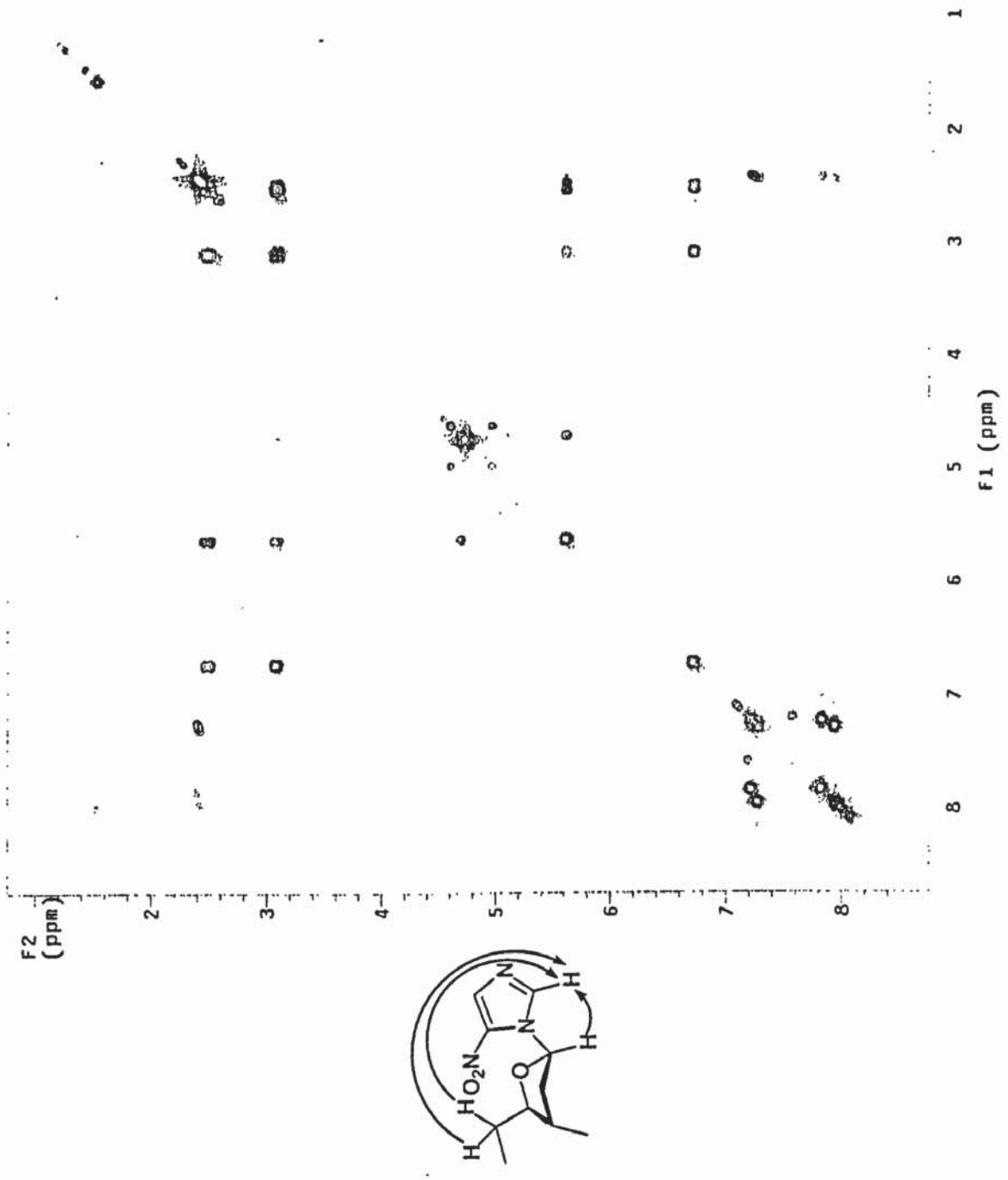

Appendix 1: ^{1}H nmr spectrum of nitroimidazole nucleoside **2.24**

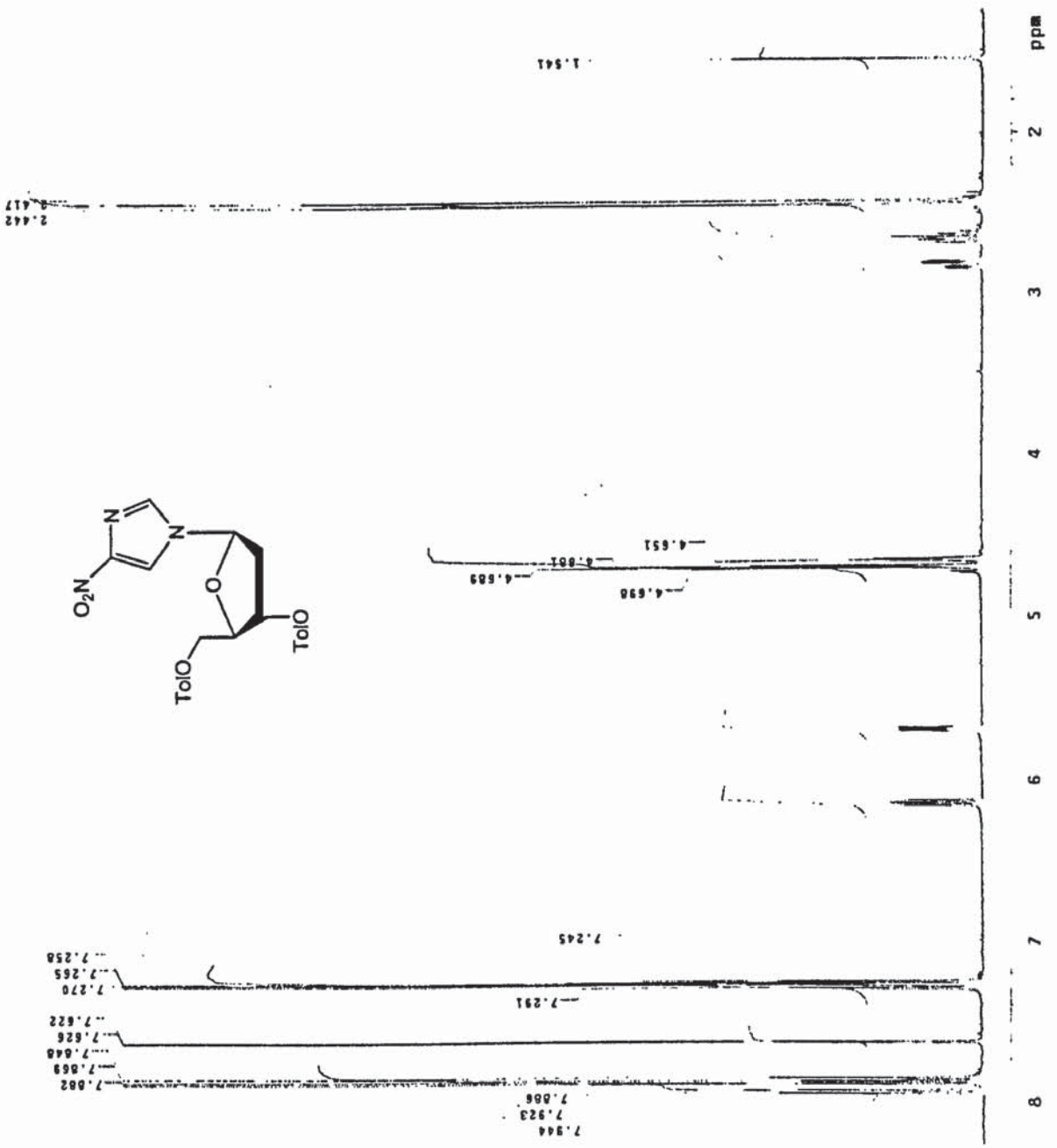

Appendix 1: NOESY spectrum of nitroimidazole nucleoside **2.24**

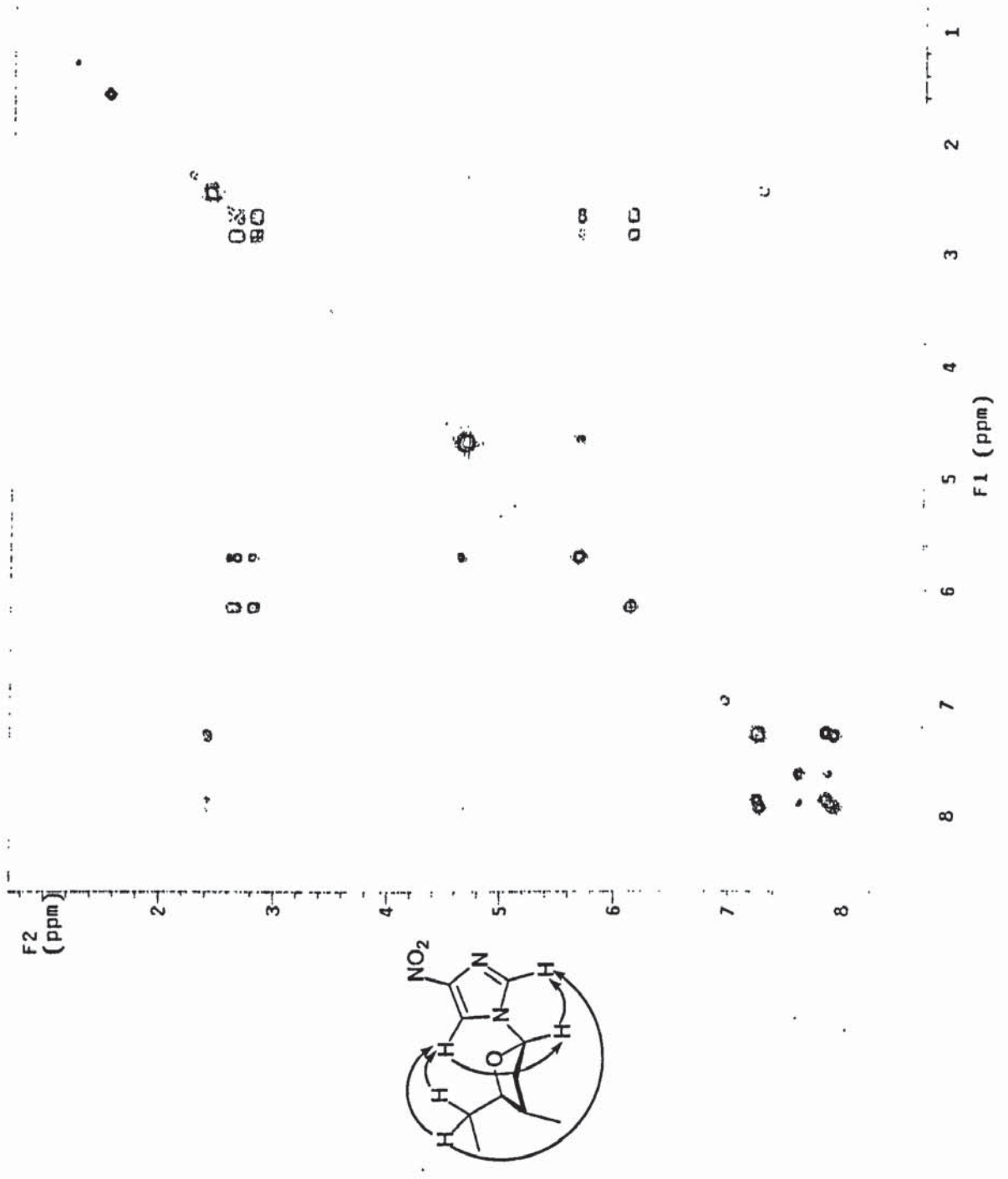

Appendix 1: ^{1}H nmr spectrum of nitroimidazole nucleoside **2.38**

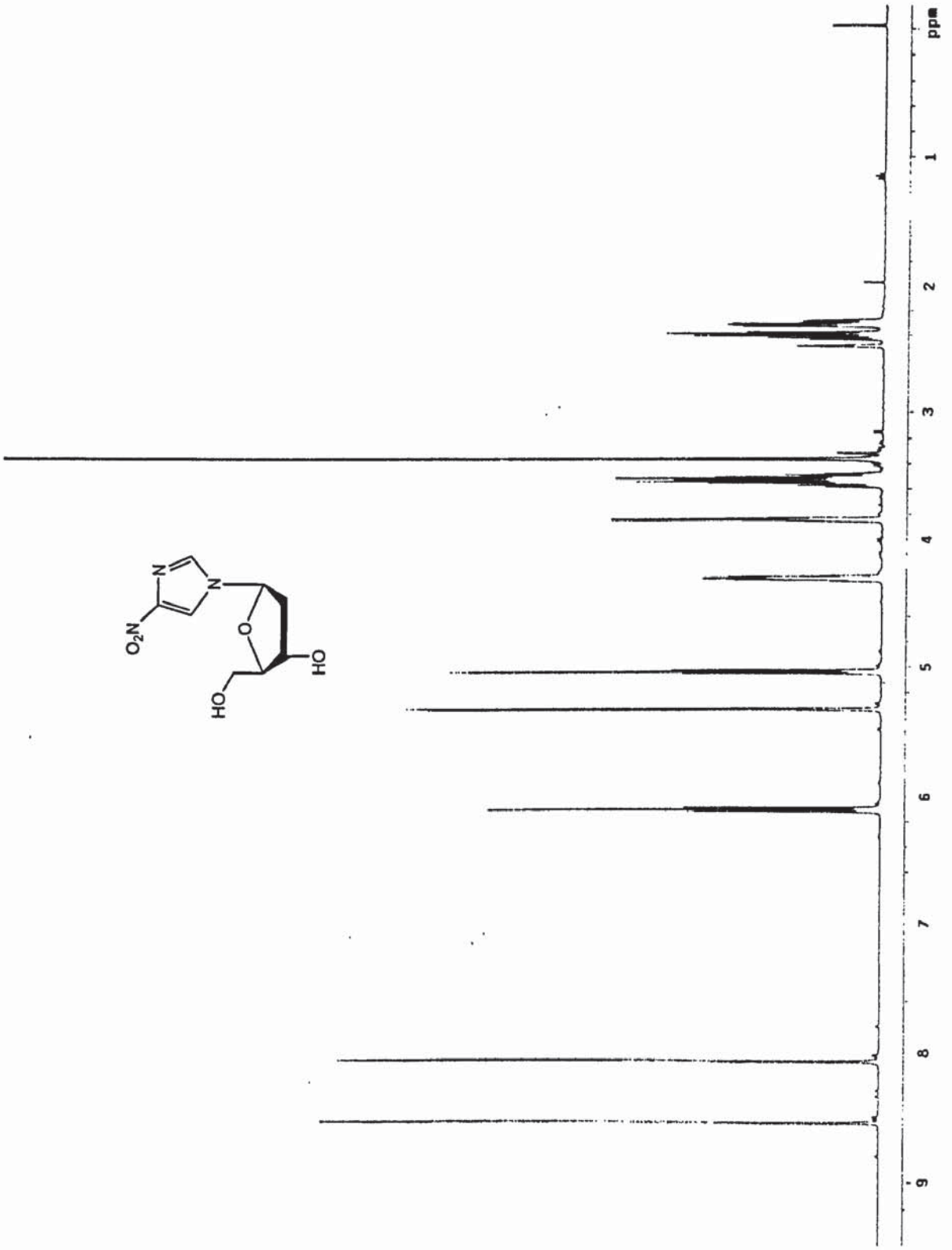

Appendix 1: NOESY spectrum of nitroimidazole nucleoside **2.38**

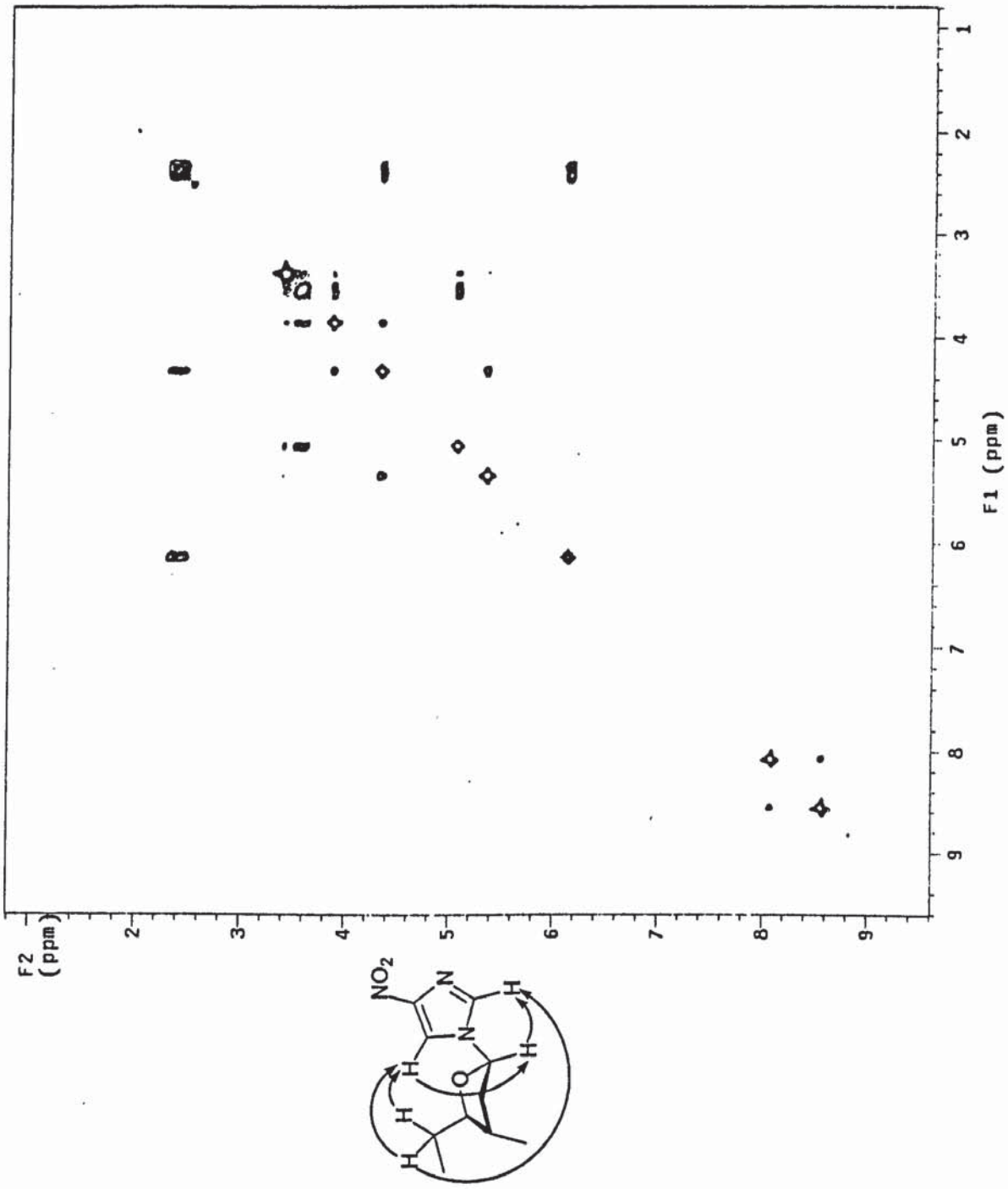

Appendix 1: ^{1}H nmr spectrum of nitroimidazole nucleoside **2.37**

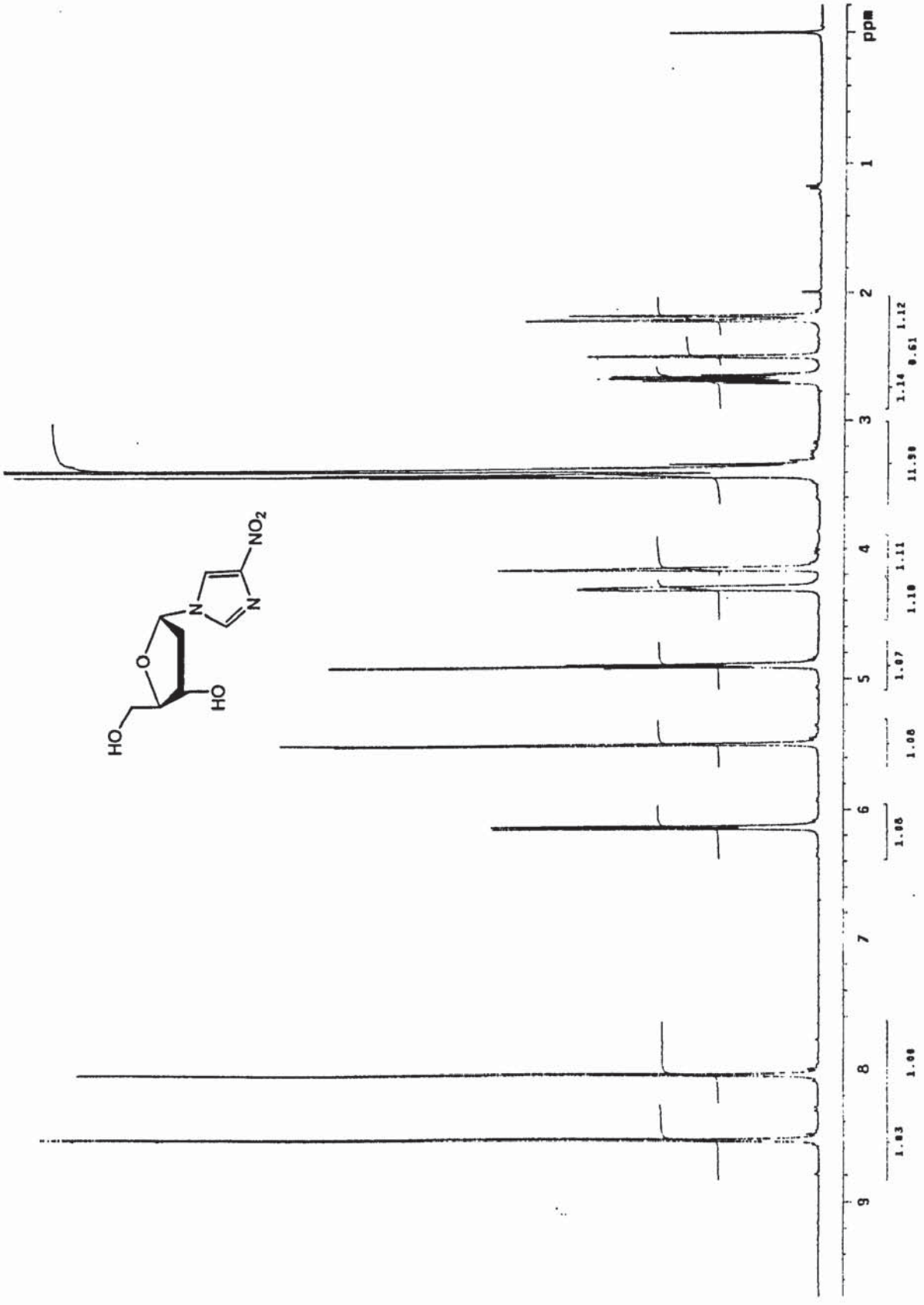

Appendix 1: NOESY spectrum of nitroimidazole nucleoside **2.37**